2014

The Rate And Process Of Mangrove Forest Expansion On Above- And Belowground Carbon Relations In Coastal Louisiana

Hai Thanh Pham
North Carolina Agricultural and Technical State University

The Rate and Process of Mangrove Forest Expansion on Above- and Belowground Carbon Relations in Coastal Louisiana

Hai Thanh Pham

North Carolina A&T State University

A dissertation submitted to the graduate faculty

in partial fulfillment of the requirements for the degree of

DOCTOR OF PHILOSOPHY

Department: Energy and Environmental Systems

Major: Energy and Environmental Systems

Co-Major Professor: Dr. Thomas W. Doyle

Co-Major Professor: Dr. Manuel R. Reyes

Greensboro, North Carolina

2014

The Graduate School
North Carolina Agricultural and Technical State University
This is to certify that the Doctoral Dissertation of

Hai Thanh Pham

has met the dissertation requirements of
North Carolina Agricultural and Technical State University

Greensboro, North Carolina
2014

Approved by:

Thomas W. Doyle, Ph.D.
Co-Major Professor

Manuel R. Reyes, Ph.D.
Co-Major Professor

Mucha R. Reddy, Ph.D.
Committee Member

Keith A. Schimmel, Ph.D.
Committee Member

Keith A. Schimmel, Ph.D.
Department Chair

John R. Meriwether, Ph.D.
Committee Member

Dr. Sanjiv Sarin
Dean, The Graduate School

Biographical Sketch

Hai Thanh Pham was born in Da Lat city, Lam Dong and grew up in Ho Chi Minh city, Vietnam. He graduated from HCMC Nong Lam University with a Bachelor of Science in Forestry in 2005. Hai has worked as a Faculty of Forestry, Nong Lam University as a junior lecturer since 2005. In 2007, he was awarded the Vietnam government scholarship to study for a Master's degree at Colorado State University, USA. He completed the Master of Natural Resource and Stewardship in 2009. He came back and worked at Nong Lam University as a lecturer since 2009. In 2011, Hai was awarded a full scholarship from the Vietnam International Education Development and North Carolina A&T State University for pursuing a Ph.D. degree in Energy & Environmental Systems. He has been studying in the Energy and Environmental Systems program since 2012. Hai will be a lecturer at HCMC Nong Lam University after he completes his Ph.D. degree.

Dedication

To all those who supported and motivated me during the past three years.

Acknowledgements

I would like to thank my primary research advisors Dr. Thomas Doyle and Dr. Manuel Reyes, who guided, inspired, and supported me during my Ph.D. journey. I am very grateful to my committee members: Dr. John Meriwether, Dr. Mucha Reddy, and Dr. Keith Schimmel for sharing their expertise with me and contributing to this research.

I would like to thank Dr. Tommy Michot for helping with housing and university access and giving good advice when I was a visiting scholar at the University of Louisiana at Lafayette. I would like to thank Mr. Todd Henry, secretary of UL Department of Physics for helping with liquid nitrogen delivery. I am especially grateful to Mr. Larry Allain, Mr. Ches Vervaeke, Mr. Jack Larriviere, Dr. Richard Day, Dr. Micheal Osland, Dr. Darren Johnson, Dr. Bogdan Chivoiu, and all staff at the National Wetland Research Center who helped me in the field, greenhouse, laboratory, and with data analysis.

I own many thanks to my parents, my family, and all friends who supported me during my doctoral studies. Lastly, I would like to thank the Vietnam International Education Development and North Carolina A&T State University for granting me a full scholarship to pursue my Ph.D. degree.

Table of Contents

List of Figures

List of Tables

List of Abbreviations

RTK GPS	Real Time Kinematic Global Positioning System
NWRC	National Wetlands Research Center
SET	Surface Elevation Table
UNEP	United Nations Environment Programme
UN	United Nations
LSD	Least Significant Difference
ANOVA	Analysis of variance
MANOVA	Multivariate analysis of variance
PAR	Photosynthetically Active Radiation
NAVD	North American Vertical Datum

Abstract

Global climate change is a major environmental threat to natural and cultural resources in low-lying coastal zones and deltas worldwide. It is expected to have a significant effect on the development of coastal wetlands by changing species range expansion. In fact, recent studies have shown that there has been an increasing mangrove encroachment poleward in the Southern and Northern Hemispheres into temperate saltmarsh zones due to the lack of freeze events. This phenomenon could have a critical impact on the structure and function of tidal wetlands at critical latitudes, especially in carbon sequestration, since mangroves are thought to sequester more carbon than marshes due to their extensive roots, leaves, and branches. To understand this likely outcome of climate warming better, a study site was established in Port Fourchon, Louisiana, where mangroves are expanding into formerly saltmarsh-dominated habitat. The aim of this study was to estimate the rate and process of the conversion of marsh to mangrove and associated carbon sequestration of soils of historically saltmarsh or mangrove dominated cover in this locale. A chronosequence approach was used to compare carbon stores between mangrove and saltmarsh at different states of mangrove cover. Moreover, greenhouse experiments were conducted to understand the effects of different biotic properties and abiotic factors on propagule regeneration success and seedling growth.

Results showed that tall *Avicennia* have higher aboveground biomass than *Spartina* and mixed mangrove/marsh zone. Tall *Avicennia* by habitat type also contributed the greater carbon storage and elevation compared to *Spartina* over the past 50 years based on ^{137}Cs dating method. Propagule size, floating time, and temperature thresholds had significant effects on mangrove regeneration, while elevated CO_2 and sunlight had no effect on propagule regeneration success.

CHAPTER 1

Introduction

Climate change is one of the effects of potential ecosystem crisis due to the negative impact of human activities such as increasing population, deforestation, and fossil-fuels consumption and associated greenhouse gas releases to the atmosphere (see Figure 1). Climate change factors of concern for coastal ecosystems include increasing storm frequency/intensity, warming surface air and sea temperature, and rising sea level (Intergovernmental Panel on Climate Change, 2013). Coastal areas may be seriously affected by climate change due to their low elevation (< 0.5 m). Therefore, coastal management and protection is a critical task in the 21st century.

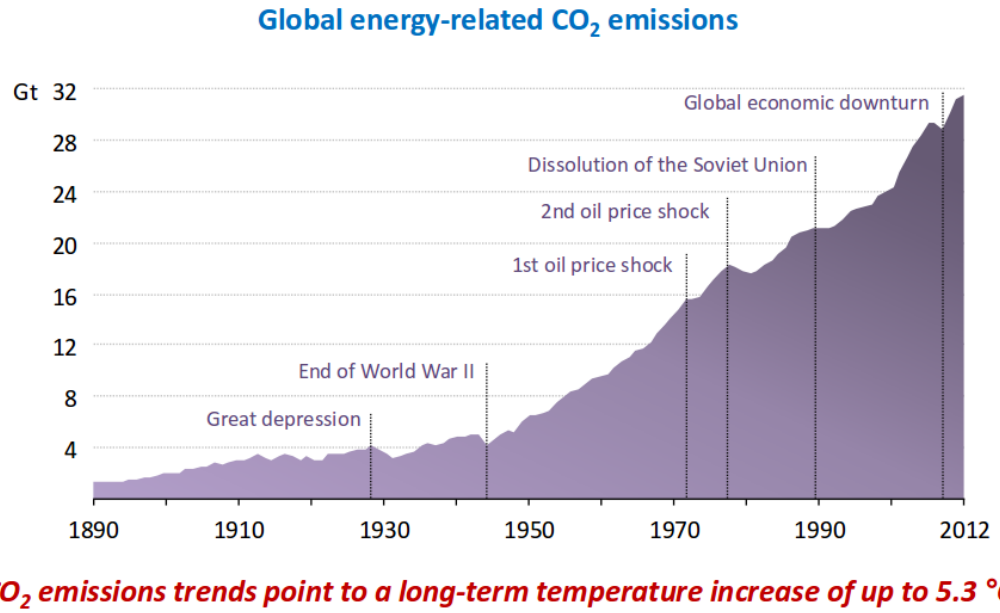

Figure 1. Global energy-related CO_2 emission. (Source: International Energy Agency)

The present climate change debate focuses on the concentration and regulation of black carbon, which is a greenhouse gas released from burning fossil fuels. There is less information about blue carbon, which is carbon sequestered by oceanic- and estuarine-associated ecosystems such as sea grass meadows, salt marshes, and mangroves. Although covering less than 0.5% of

the sea bed, these coastal ecosystems are thought to capture more than 55% of all carbon in the world (Nellemann et al., 2009). According to Dr. Achim Striner, UN Under-Secretary General and Executive Director of UNEP, they are disappearing faster than anything on land and may be lost in a few decades if we do not act immediately to protect them (Nellemann et al., 2009).

Mangroves are predicted to expand poleward under warming air and sea-surface temperature from climate change. Moreover, they are thought to increase carbon storage due to their extensive branch and root systems (Bianchi et al., 2013; Comeaux, Allison, & Bianchi, 2012; Perry & Mendelssohn, 2009). Thus, research on the role and process of carbon sequestration in mangrove ecosystems and with their potential expansion poleward and replacement of saltmarsh-dominated systems is an important research need and task.

The primary research objective of this study is to estimate the rate and process of the conversion of marsh to mangrove and carbon sequestration of historically saltmarsh-dominated systems of coastal Louisiana. The central hypothesis to be tested is that mangrove expansion into saltmarsh zones increases carbon gain and storage (i.e., sequestration), helping to mitigate the carbon balance aspect of climate change. There are many technological means to sequester carbon, but the ecosystem process provides a natural feedback and accounting that may not be fully understood or incorporated in global climate models. A chronosequence approach will be used to compare carbon sequestration between mangrove and saltmarsh at different stages of mangrove cover and forest development. The study objectives were achieved by conducting three specific tasks, as outlined below.

Task 1. Forest Attributes and Aboveground Carbon Stores of Saltmarsh/Mangrove Stage

The working hypothesis was that there is no difference in forest attributes and aboveground carbon stores between saltmarsh/mangrove stages: tall mangrove, short mangrove,

marsh only, and a mix of mangrove and marsh. A gradient of sites from marsh only to different cover stages of mangrove encroachment and structure were established. Differences in tree architecture and stem growth were measured by internode lengths of lateral branches from select trees and seedlings in each of the saltmarsh/mangrove cover classes. Differences in internode variation of node count, length, and diameter were related to tree and forest age corresponding with imagery showing mangrove presence and closure as a function of calendar date.

Task 2. Soil Accretion, Elevation, and Carbon Stores of Saltmarsh/Mangrove Stage

The primary hypothesis was that mangrove presence and abundance would account for higher soil elevation, accretion rates, and carbon stores than saltmarsh concomitant with degree of aboveground structure and associated root systems. Sediment cores were extracted along transects of representative sites of saltmarsh/mangrove stage and cover to account for carbon content and accretion. The ^{137}Cs dating method was used to measure the decadal accretion from 1963 peak radioactive fallout to present, a span of 50 years. Other wetland studies have indicated that mangrove reside on higher elevations than adjoining marsh. It is not known whether pre-existing conditions of higher elevation facilitates mangrove regeneration or mangrove ingrowth thereafter promotes higher deposition and increased elevation with vegetation complexity or stand age. All sites were surveyed with real-time kinematic (RTK) global positioning system (GPS) to determine absolute surface elevation of all sites to relate with water level history from nearby tide gages and site-specific water level recorders.

Task 3. Propagule Regeneration Success for Restoration

Propagule spread and establishment are the main sources for mangrove expansion into saltmarsh-dominated zones. Their life history includes three stages: floating stage (the mature propagule drops from the parent trees floating on the ocean water), stranded stage (the

propagules stranded on shore or soil surface), and established seedling stage (successful propagules established with new true leaf and upright stem). It is unclear what factors control propagule regeneration success or canopy height and closure in the transition stages from marsh to mangrove forest. The height, density, and condition of saltmarsh and mangrove may restrict light attenuation to sustain propagule regeneration success. Additionally, propagule size, air and soil water temperature, and the floating period may affect regeneration success. Mangrove shrub and tree forms above marsh height with and without neighboring shrubs/trees are expected to create altered light conditions and growth potential on underlying marsh and mangrove. High and low sea-level anomalies, wet/dry periods, or winter severity are climate conditions that may contribute to either marsh or mangrove stress sufficient to promote or inhibit regeneration success or stage change. The working hypothesis was that regeneration success, seedling establishment, and growth are influenced by associated cover characteristics and tidal relations of inundation and hydroperiod. To explore this, greenhouse experiments were conducted to understand the different biotic properties and abiotic factors controlling propagule regeneration and seedling growth as follows:

- Propagule weight and floating time,
- Soil heat treatments,
- Elevated atmospheric CO_2, and
- Sunlight level.

Knowledge of how mangroves expand landward and poleward during warming periods and under sea level rise is in its infancy, but paramount along the northern Gulf Coast, particularly Louisiana, where new mangrove range extensions have been noted in recent years. The potential for wholesale conversion of temperate saltmarsh and further mangrove spread

along the Gulf Coast and South Atlantic is even more likely under climate change where the periodicity of hard freeze events may lessen with projected climate warming. Self-reproducing populations of black mangrove may speed expansion based on the abundance of propagule and opportunities for mangrove ingrowth into marsh settings of coastal Louisiana that has only been documented with limited mapping studies and little or no accounting of field investigations of forest age and structure.

This dissertation was designed to address the rate and process of mangrove encroachment and cover change with specific field and experimental tasks to account for carbon gain and sequestration, aboveground and belowground, in relation to surface elevation, tidal range, and recent climate. Results from this investigation are expected to guide coastal restoration when considering the choice to plant mangrove for the benefit of blue carbon credits and qualities of holding or building shoreline.

Study Site

The study was conducted in a mangrove/saltmarsh community in Port Fourchon, LA (see Figure 2). It is located on the southern tip of Lafourche Parish, Louisiana, on the Gulf of Mexico and is the state's southernmost port. Port Fourchon has significant petroleum industry traffic and serves over 90% of the Gulf of Mexico's deepwater oil production ("Port Fourchon, Louisiana," n.d.). *Avicennia germinans* and *Spartina alterniflora* are the two dominant species found in the area. Black mangrove (*Avicennia germinans*) is a subtropical shrub growing with saltmarsh near high tide elevation. The highest recorded individual plant height in the area is 4.0 m, and up to 2.5 m at the study site. Black mangrove can be found in pure stands or growing intermixed with smooth cordgrass (*S. alterniflora*). Over the last few decades, mangroves have been expanding into temperate saltmarshes Gulfwide due to the lack of freezing events (Comeaux et al., 2012;

Doyle, Krauss, Conner, & From, 2010; Henry & Twilley, 2013; Perry & Mendelssohn, 2009). There are four distinctive habitat zones in the study area: tall *Avicennia*, short *Avicennia, Spartina*, and mixed zone of *Avicennia and Spartina.* Tall *Avicennia* dominated zone across study transects was about 5 m in width starting at the edge of the tidal channel grading to short *Avicennia* at the interface or ecotone with interior *Spartina* marsh. The highest recorded individual tall mangrove was about 2.5 m in height. The short *Avicennia* zone was about 3 m wide and the highest recorded individual short *Avicennia* was about 0.7 m tall. The marsh zone is about 21 m wide, but varies by location as to wide or narrow depending on landform characteristics. The mix zone of mangrove and marsh was about 4 m wide starting from the marsh zone to the backside tidal creek. Black mangrove plays an important role in the coastal ecosystem; it serves as sediment stabilizer, shore protection, and provides habitat for many species including the Louisiana state bird, the brown pelican (Visser, Vermillion, Evers, Linscombe, & Sasser , 2005).

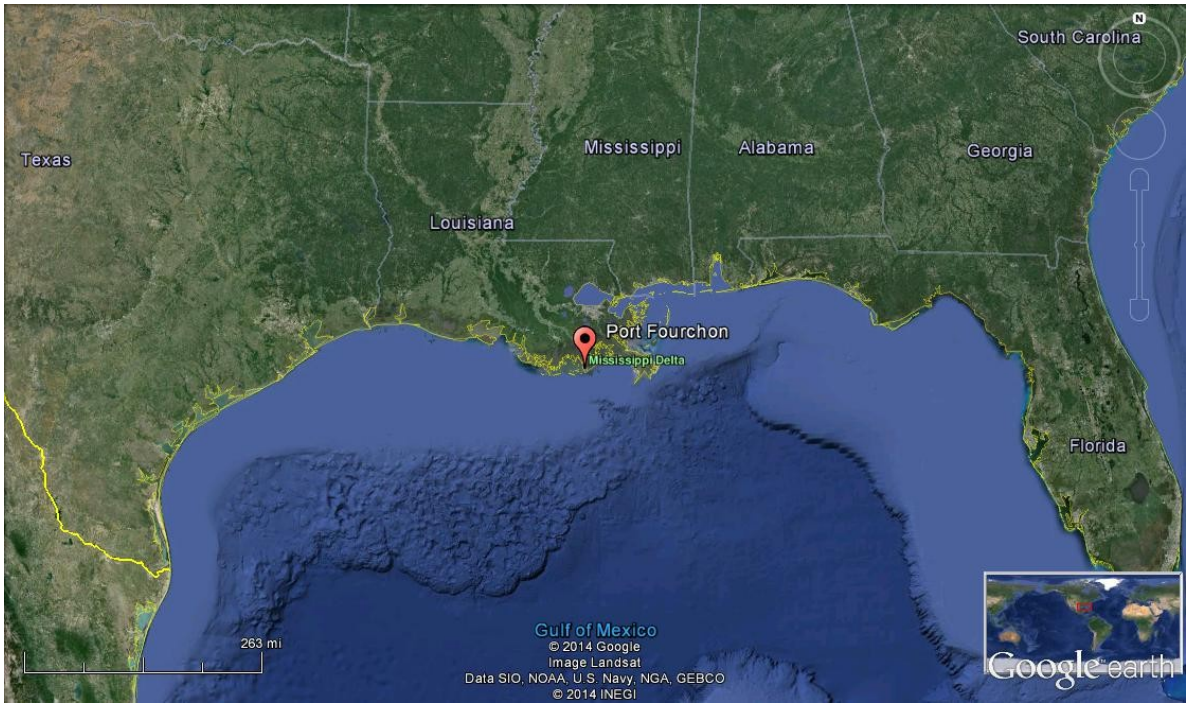

Figure 2. Study site - Port Fourchon, LA.

CHAPTER 2

Literature Review

The Ecosystem

Scientists have raised the potential for environmental crises, such as resource depletion, pollution, and lack of clean water and air; biodiversity loss; ozone holes; dangerous diseases, rich-poverty polarization, and war; chemical, biological, and nuclear weapons; and the greenhouse effect and sea level rise, to name just a few. It all leads to a local crisis and the entire ecosystem recession risk can occur if humanity does not act promptly to "save the earth," our friendly environment!

An ecosystem includes all of the mutual relations, dependencies, and interactions as a combination of factors having the same function in a united system of society and nature. Striking features of the ecosystem are metabolic processes, information, energy, and self-correcting dynamic balance. Ecosystems are not only different in scale and nature, but also intertwined and interlocking. Except for close ecosystem, the universe, all ecosystems are open systems, receiving the material, energy, and information through metabolic processes, self-adjusting, creating dynamic balance status, food chains; process of genetic variation, adaptive process; competitive survival; process of birth, aging, sickness, and death, etc.

Since the existence of humans, the elements of the ecosystem include producing organisms (autotrophic), consuming organisms (heterotrophic), biological saprophytes (decompose), people and society, and the inorganic and organic substances necessary for life. With the development of science and technology, people have an increasingly strong impact on the ecosystem: People—Society and Nature.

Louisiana Ecosystem

Louisiana is located in the southern United States, bordered on the west by Texas; to the north by Arkansas; to the east by the state of Mississippi; and to the south by the Gulf of Mexico. It has a humid subtropical climate with long, hot, humid summers and short, mild winters. The average temperature is 27.3°C in summer and 10.5°C in winter. Sometimes snow and ice storms happen in northern parts of the state due to cold fronts from the north. Tropical storms and major hurricanes occur once every decade or less affecting coastal areas in the most southern extent of the state. The topography of the state can be split in two parts: the uplands of the north, and the alluvial along the coast and Mississippi River. A large amount of the state's land was created by sediment from the Mississippi River over 7,000 years, making huge deltas and immense areas of coastal marsh and swamp. These deltas can be divided into two parts: the Deltaic Plain in the central and southeastern portion of the coast, and the Chenier Plain in the southwestern part of the state (see Figure 3). The Deltaic Plain is a vast expanse of marshland with an area of approximately 38,850 km^2 (Fisk, 1944). The research site is located in the Deltaic Plain. The Chenier Plain is a Holocene strand plain composed of wooded beach ridges (cheniers) and intervening mudflat grassy wetlands with an area of 26,304 km^2 (Esslinger & Wilson, 2001; Owen 2008). These wetlands act as an environmental filter and protection. They help mitigate storm and wave impact. Wetland plants help remove heavy metals, sewage, and pesticides from polluted water. In addition, wetlands provide a habitat of rich and diverse fauna and flora. The fauna include fish and shellfish, migratory birds, the American alligator, and some endangered species such as the Louisiana black bear, piping plover, and green sea turtles. The common floras contain cattails, swamp rose, spider lilies, and cypress trees. Wetlands also play an important role in culture and the economy of the state. According to Wikipedia,

commercial fishing accounts for more than $300 million of the state's economy, and more than 70% of major species such as shrimp, oysters, and blue crabs rely on coastal wetlands as a nursery for their young. There are more than 330,000 hunting licenses and 900,000 fishing licenses sold every year ("Wetlands of Louisiana," n.d.). Other recreational activities in the wetlands include boating, swimming, camping, hiking, and photography. In addition, these wetlands provide an ideal environment for scientific research.

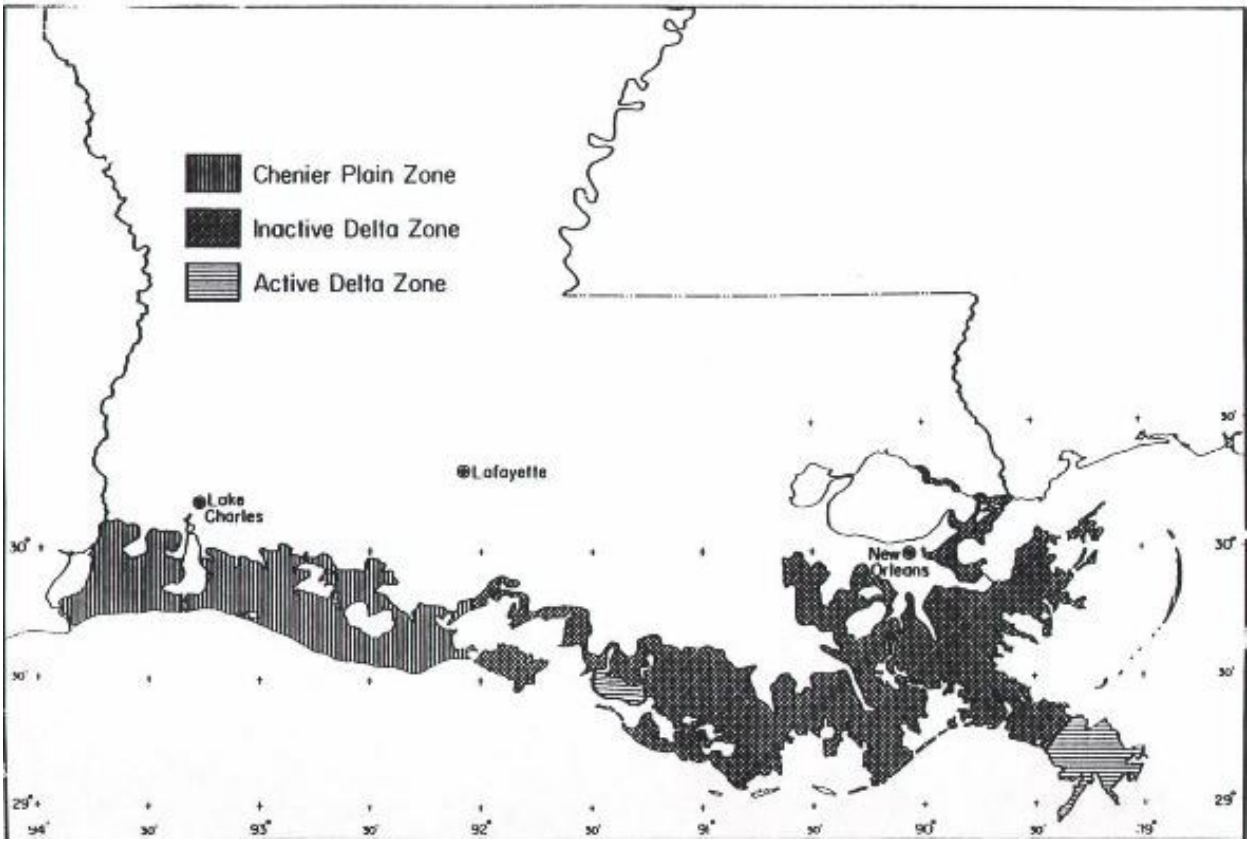

Figure 3. Marsh zones of the Louisiana coastal marshes. Source: (Foret, 1997), Figure 1.

However, wetland loss is currently a major concern. According to the National Wildlife Federation, coastal Louisiana is losing 24 square miles of wetlands each year—roughly equivalent to a football field every 30 minutes due to subsidence, wave erosion, and human causes ("Mississippi River Delta," n.d.). The subsidence rate in Deltaic region approaches 1.1 cm/yr compared to 0.57 cm/yr in Chenier Plain (Penland & Suter, 1989). Human activities such

as building levees, channels, canals, dams, and agriculture disrupt the natural balance of the wetland and worsen wetland loss. Therefore, protecting the wetlands has become a significant task today.

Status and Major Characteristics of the Coastal Louisiana Ecosystem

Louisiana's emergent saltwater wetlands include saltmarsh, mangrove, and mixed zonation between the two species. The common mangrove species in Louisiana is black mangrove (*Avicennia germinans*), and the most common species found in saltmarsh is smooth cord grass (*Spartina alterniflora*). Both species are salt tolerant plants that trap mineral sediment and coexist in tropical latitudes globally (Comeaux et al., 2012). Mangroves are more structurally complex and productive than saltmarsh due to their extensive branch and root systems. However, mangrove are freeze intolerant because of xylem embolism and loss of hydraulic conductivity occurring under freezing conditions (Comeaux et al., 2012). Therefore, their populations are limited to tropical climates and shorelines of the Gulf Coast with periodic and sparse encroachment in Louisiana marshes. In fact, saltmarshes are the historically dominant ecosystem along the subtropical northern Gulf Coast. Based on historical aerial photos, mangrove distribution was very restricted until the early 1990s (Perry & Mendelssohn, 2009). Severe freezes of 1983 and 1989 were responsible for eliminating all mangroves statewide.

The major effects of climate change to coastal ecosystems of Louisiana include expansion of species' range, displacement of species, and disruption of community dynamics (Walther et al., 2002). In recent decades, mangrove regrowth and expansion into saltmarsh along the northern Gulf Coast, and Louisiana in particular, has been substantial due to relatively mild winters and lack of freeze events (Bianchi et al., 2013; Comeaux et al., 2012; Osland et al., 2012;

Perry & Mendelssohn, 2009). As a result, mangrove has made some significant changes to the regional ecosystem in recent decades.

Perry and Mendelssohn (2009) investigated the ecological effect of mangrove expansion on salt marshes in Louisiana. Their results indicated that mangrove expansion had no major effects on the ecosystem in process or degree of sediment accretion, carbon sequestration, and carbon stores. However, they found that where mangroves expanded to marshes, soil moisture and porewater salinity were slightly lower, while elevation, redox potential, bulk density, and soil ammonium were slightly higher. Over the long term, they speculated that marsh to mangrove conversion might have a measurable impact on wetland structure and function in the future. Two other similar studies were carried out along the Texas coast, where mangrove is expanding to temperate saltmarsh. Comeaux et al. (2012) investigated the change in resistance to sea level rise and wave attack during large storms, on organic carbon sequestration, and soil geochemistry. They found that mangrove exhibited higher resistant to sea level rise and wave attack because they have a capacity for higher sediment accumulation and higher root volume. However, the carbon sequestration and storage aspect of mangrove expansion remained unclear. Bianchi et al. (2013), on the other hand, studied the change in the ecosytem with a focus on carbon sequestration. They hypothesized that mangroves increase the storage and carbon sequestration in the coastal zone. Their results indicated that mangrove enhanced the carbon sequestration and lignin storage rates compared to saltmarsh. They also recommended conducting more research on alterations in the overall carbon storages on a regional scale to better verify that such coastal margin alterations are influencing local carbon fluxes. Therefore, further investigation on how marsh to mangrove conversion changes carbon sequestration and storage on a regional scale is an important task.

Mangrove Forest Ecosystems

The term "mangrove" refers to a tidally influenced wetland ecosystem within the intertidal zone of tropical and subtropical latitudes. Mangroves are marine tidal forests that include trees, shrubs, palms, epiphytes, and ferns (Tomlinson, 1986). Mangrove ecosystems are heterogeneous habitats with an unusual variety of animals and plants adapted to the environmental conditions typified by highly saline, frequently inundated, and soft-bottomed anaerobic mud (Macintosh & Ashton, 2002).

Mangroves cover a total of 152,000 square kilometers in 123 countries and territories worldwide (Spalding, Kainuma, & Collins, 2010). They generate some of the highest primary production rates among the world forest ecosystems. Recent research showed that total aboveground biomass of the world mangrove forest may be over 3700 Tg of carbon and that mangroves could sequester 14-17 Tg of carbon per year (Spalding et al., 2010). Moreover, mangroves provide many ecosystem services including forestry value, fisheries value, hurricane protection, and carbon cycling that benefits the local, national, and international community. In fact, tropical mangrove forest ecosystems play an important role in coastal zone protection. They are thought to lessen wave impact caused by tropical storms and tsunamis (Tran, 2011). In addition, they provide breeding and nursing grounds for marine and pelagic species, food, medicine, fuel, and building materials for local communities (Giri et al., 2011). Despite covering only 0.1% of the earth's continental surface, mangrove forests have the potential to capture approximately 22.8 million metric tons of carbon every year (Giri et al., 2011). In addition, they contribute about 11% of the total input of terrestrial carbon into the ocean (Jennerjahn & Ittekkot, 2002) and 10% of the terrestrial dissolved organic carbon (DOC) exported to the ocean (Dittmar, Hertkorn, Kattner, & Lara, 2006). Mangroves play an important role in the economic

life of local people through activities such as aquaculture and fishing. The total economic value of mangrove ecosystems per square kilometer has estimated values as much as US$200,000 to US$900,000 (Wells, Ravilious, & Corcoran, 2006). The indirect value of mangroves, including hurricane protection, water quality, pollutant uptake, and sediment retention provide valuable ecosystem services and cost savings, but do not directly generate income for the management of the area. Since people favor only their direct goods and services, which hold only a very small part of the total mangroves' value, mangrove ecosystems have consistently been undervalued. The undervaluing of mangrove conservation compared to alternative uses leads to unwise decisions and policies.

The international community benefits from the subsistence of mangroves. Nevertheless, the management of mangrove conservation depends on national and local implementation. Hence, free riding on global public good, such as carbon sequestration and storage, will remain unless international payment is provided for local people to encourage them to preserve mangroves.

Carbon Sequestration in Wetland Ecosystems

Green carbon or biological carbon is a major portion of the global carbon. It is carbon removed by photosynthesis and stored in the plants and soil of natural ecosystems (Nellemann et al., 2009). Over half (55%) of green carbon captured in the world is from marine living organisms such as mangroves, marshes and sea grasses (Nellemann et al., 2009). They capture and store carbon in the marine sediment. Hence, it is called "blue carbon" as related to ocean sources.

Mangroves and saltmarshes play a vital role in the global blue carbon cycle. They remove CO_2 from the atmosphere and store it as carbon in plant structure and soil in the process

called carbon sequestration (Suratman, 2008). Several studies estimated the carbon sequestrated by mangrove and marsh habitat. According to Bridgham, Megonigal, Keller, Bliss, and Trettin (2006), tidal marshes with a global area of nearly 22,000 km^2 could sequester 4.6 Tg of carbon per year. This carbon can be divided into soil and plant pools, which are 0.43 and 0.007 Pg (430 and 7 Tg) of carbon, respectively. Mangroves are thought to sequester more carbon than marshes with their extensive root system that better enables them to hold and store carbon. Since about half of the biomass of mangroves is composed of carbon, they represent the largest stock of carbon source in coastal zones. With an area of approximately 152,000 square kilometers, mangroves could sequester 14-17 Tg of carbon per year (Spalding et al., 2010). In contrast, using an indirect approach for wood production component and assuming a global coverage of 160,000 square kilometers, Bouillon et al. (2008) estimated that net primary production of mangroves was 218 ± 72 Tg of carbon per year. In addition, Bridgham et al. (2006) thought that mangroves with an global area of 181,000 square kilometers could seize 38 Tg of carbon per year, which can be divided into soil (4.9 Pg C or 4900 Tg C) and plant (4.0 Pg C or 4000 Tg C) pools. According to Kristensen, Bouillon, Dittmar, and Marchand (2008), the total net primary production (leaf litter, wood, and root production) were roughly 149 mol C m^{-2} $year^{-1}$ ($1.788x10^{-3}$ Tg C km^{-2} $year^{-1}$).

One of the important aspects of the mangrove carbon storage is their deposition and decomposition with respects to quality and longevity. McKee, Cahoon, and Feller (2007) reported that C-rich deposits of *Rhizophora mangle* forest in Belize was 10 m deep and over 6,000 years old. In contrast, rain forest carbon stores are thought to sequester carbon for decades, or even centuries (Chambers, Higuchi, Tribuzy, & Trumbore, 2001). Over decades and centuries, mangroves accumulate carbon in various forms of primary production, which is the

process of converting solar energy, CO_2, and water to glucose and eventually plant tissue through photosynthesis. Primary production includes aboveground and belowground production. Aboveground pools contain the primary production of leaves, stem, and wood. Belowground production, containing coarse and fine roots, builds up and increases the biomass standing stock. Litter from trees (dead leaves, propagules, and twigs) fall to the forest floor where they are consumed by local fauna, remineralized into the atmosphere, exported to adjacent coastal environments, or buried in mangrove sediment (Yee, 2010).

Mangrove aboveground (leaf and wood) production. Leaf production is a commonly measured functional aspect of mangrove forest. It is a major component of carbon cycling and nutrients in the mangrove ecosystem (Röderstein, Hertel, & Leuschner, 2005). Litter fall production may represent 31% of total productivity (Alongi, Clough, & Robertson, 2005; Bouillon et al., 2008). As latitude increases, leaf fall biomass tends to decline because of changes in solar radiation, temperature, and precipitation (Saenger & Snedaker, 1993). The global average of litter fall rate was estimated to be ~38 mol C m^{-2} $year^{-1}$ (16.73 tCO_2/ha $year^{-1}$) (Jennerjahn & Ittekkot, 2002; Twilley, Chen, & Hargis, 1992).

Wood production accounts for 31% of mangrove productivity (Bouillon et al., 2008). It decreases with increasing latitude. Twilley et al. (1992) estimated that global average wood production was 67 mol C m^{-2} $year^{-1}$ (29.50 tCO_2/ha $year^{-1}$). Global aboveground wood production rate was estimated to be 66.4±37.3 Tg C $year^{-1}$(243.688 x 10^6 ± 136.891 x 10^6 tCO_2 $year^{-1}$) (Bouillon et al., 2008). Khan, Suwa, and Hagihara (2007) found that average aboveground wood production of a mangrove stand of *Kandelia obavata* was 67.1 Mg/ha (246.27 tCO_2/ha).

Mangrove belowground production (roots). Belowground production is an important part of mangrove carbon sequestration. Roots can hold up to 50% of total biomass of a

mangrove forest (Alongi & Dixon, 2000). Mangroves store about 50% of C in soil (Khan et al., 2007). They have unique physiological and structural adaptations to tidal environments with complex aerial root systems (Tomlinson, 1986). These systems account for 38% of primary production (Bouillon et al., 2008).

Carbon accumulation in belowground biomass for *Kandelia obovata* was estimated to be 67 Mg/ha (245.89 tCO_2/ha) (Khan et al., 2007). Belowground production for *Rhizophora stylosa* and *Avicennia marina* ranged from 23.9 to 48.8 t DW/ha (43.85 to 89.54 tCO_2/ha) and 12.8 to 19.4 t DW/ha (23.48 to 35.59 tCO_2/ha), respectively (Alongi et al., 2005). On global scale, Kristensen et al. (2008) found rate of belowground root productivity equal to 44 mol C m^{-2} $year^{-1}$ (19.37 tCO_2/ha $year^{-1}$) while Bouillon et al. (2008) estimated belowground production to be 82.8 ± 57.7 Tg C $year^{-1}$ (30094 x 10^4 ± 21175.9 x 10^4 tCO_2 $year^{-1}$)

CHAPTER 3

Methodology

The main objective of this research was to estimate the rate and process of carbon sequestration of saltmarsh-mangrove ecotone of coastal Louisiana with the increasing expansion of black mangrove into adjoining saltmarsh. The primary hypothesis was that mangrove would increase the carbon storage with their extensive aboveground biomass and root systems compared to marsh. The following three specific tasks were carried out:

- Forest Attributes and Aboveground Carbon Stores of Saltmarsh/Mangrove Stage.
- Soil Accretion, Elevation, and Carbon Stores of Saltmarsh/Mangrove Stage.
- Propagule Regeneration Success for Restoration

Aboveground Biomass

A gradient of sites were established from marsh only to different cover stages of mangrove encroachment and structure. Site location was focused on state and private lands near Port Fourchon, Louisiana using historic maps and aerial photography to locate potential marsh/mangrove stages of age and development for field survey. Mangrove structure and complexity were quantified with quadrant survey 1 m^2 plots on a grid network (2 m x 30 m) to measure vegetation type, plant canopy cover, tree density, diameter, height, pneumatophore density and height, and propagule density and development. Two random plots from representative cover types of tall mangrove, short mangrove, marsh, and mixed habitat were harvested for determining plant biomass. After getting the fresh weights for each plot, samples were put in the oven at 60°C for two weeks to obtain dry weight. Statistical comparison of fresh and dry weight biomass was achieved by an analysis of ANOVA where the type 3 error was used to test the fixed effect.

Tree Architecture

Tree internodes reflect the successive growth of mangrove trees. In Louisiana, mangroves are thought to grow faster in spring and summer, and slower in fall and winter. In fact, mangrove leaves and stem cells can embolize when exposed to freezing temperatures below 0°C leading to tree mortality or partial dieback.

Differences in internode patterns by count, length, diameter, and leaf sets present were evaluated to predict tree and forest age and to correspond with imagery showing mangrove presence and closure by calendar date. Simple ruler and micrometer measurements of internode length and diameter from terminal leaf sets to branch inserts were taken to capture sequential growth of branch and stem. Flags were placed on measured branch and stem structures to allow re-measurement every month thereafter to determine growth rate patterns as a function of tree architecture, intertree competition, and site conditions.

Soil Accretion and Carbon Stores of Saltmarsh/Mangrove Stage

Soil accretion was identified from the distribution of ^{137}Cs in the sediment profile (Delaune et al., 1978). As shown in Figure 4, the atmospheric fallout from nuclear weapons testing peaked sharply in 1963. The ^{137}Cs portion of that fallout chemically attaches to the clays in the soil or sediment surface. The ^{137}Cs remains with the clays of that surface as new accretion covers that surface (Tamura and Jacobs, 1960). A modern core finds the peak ^{137}Cs activity at a depth corresponding to the 1963 surface.

Cores were taken to depths of 50 cm or more (Meriwether, Sheu, Hardaway, & Beck, 1996) and subdivided into 2- cm thick, vertical sections. Each section was dried at 60 ^{0}C and ground to a coarse powder (to insure uniform counting geometry) and weighed. The ^{137}Cs specific activity in each section was determined using gamma ray spectroscopy. The high purity

germanium detectors (HPGe) were calibrated for energy and intensity with a standard ^{137}Cs source traceable to NIST (National Institute of Standards and Technology). The sections were counted for at least 11 hours to have reasonable statistical error. Assuming no mechanical mixing of the sediment, the accretion rate is the ratio of the ^{137}Cs peak depth divided by the time interval between the current year and 1963. Soil bulk density was determined as a simple dry weight to volume ratio (Blake & Hartge, 1986). Soil organic matter (SOM) were determined via loss on ignition (Wang, Li, & Wang, 2011).

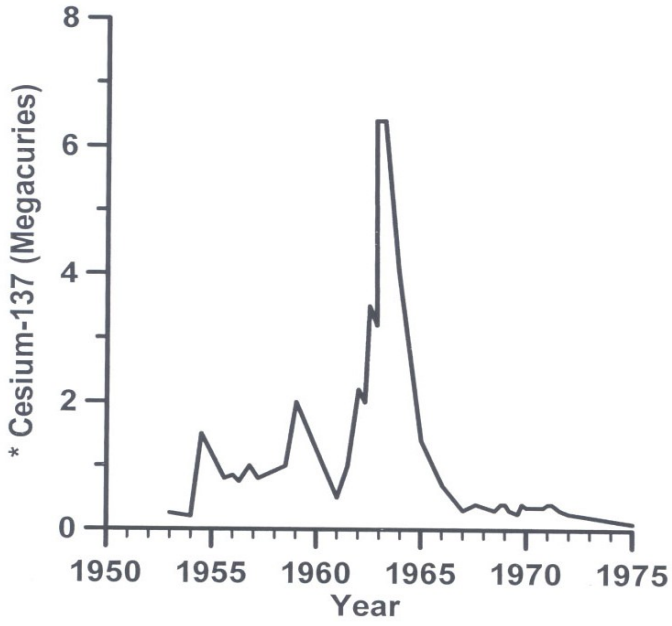

Figure 4. Atmospheric fallout of ^{137}Cs, with respect to time (Meriwether et al., n.d.).

Elevation

Other wetland studies have indicated that mangroves reside on higher elevations in some wetland settings. It is not known whether pre-existing conditions of higher elevation facilitates mangrove regeneration or mangrove ingrowth thereafter promotes higher deposition and increased elevation with vegetation complexity or stand age. All sites were surveyed with RTK GPS to determine absolute surface elevation of all sites to relate with water level history from nearby tide gages and site-specific water level recorders.

Propagule Regeneration Success for Restoration

Greenhouse experiments were conducted to understand the different biotic properties and abiotic factors influencing propagule regeneration and seedling growth as follows:

Propagule weight and floating time for regeneration success.

Soil preparation. Soils were prepared from commercial products of peat moss and sand to achieve uniformity among all treatments and a proven medium for regeneration studies of woody species. The soil was a tumbled mix of 50% peat moss and 50% sand saturated in fresh well water. All watering thereafter for all experimental treatments used fresh well water; no salinity or nutrient amendments were used to prevent any confounding factors for seedling success or the lack thereof.

Propagule preparation. Propagule length, width, and weight were measured after they were removed from parent trees by hand on November 21 and December 21, 2013. Collected propagules were sorted and counted by size and weight class determined from fresh weight. The most available quantity of propagules was chosen by weight class for experimental purposes as follows:

- Three treatments by weight:

- Size 1 (weight from 1 g to 1.99 g),
- Size 2 (weight from 2 g to 2.99 g)
- Size 3 (weigh from 3 g to 3.99 g).

All propagules were put in fresh water and Captan 50 Wettable Powder solution for 48 hours in the NWRC greenhouse to promote shredding of pericarp and prevent fungus infection. The working hypothesis is that the longer individual propagules float on water, the less chance they

have for regeneration success due to expending their maternal reserves and energy, larger propagules lasting longer and being more successful over time.

Experimental design. The experiment was designed by random complete design with 14 propagules for each size class per week (see Figure 5). The propagules were measured at least three times per week for radical extension, establishment, first leaf emergence, and nodal development. Propagules were randomly selected by size class for each of 11 successive weeks and tray sets.

Week 1 (tray 1)			**Week 1 (tray 2)**			...	**Week 11 (tray 1)**			**Week 11 (tray 2)**		
S1	S2	S3	S1	S2	S3	...	S1	S2	S3	S1	S2	S3
S1	S2	S3	S1	S2	S3	...	S1	S2	S3	S1	S2	S3
S1	S2	S3	S1	S2	S3	...	S1	S2	S3	S1	S2	S3
S1	S2	S3	S1	S2	S3	...	S1	S2	S3	S1	S2	S3
S1	S2	S3	S1	S2	S3	...	S1	S2	S3	S1	S2	S3
S1	S2	S3	S1	S2	S3	...	S1	S2	S3	S1	S2	S3
S1	S2	S3	S1	S2	S3	...	S1	S2	S3	S1	S2	S3

Figure 5. Experimental design for size class and floating time.

Heat treatments for regeneration success. Because black mangrove propagule development peaks in late fall/early winter in Louisiana and due to mangrove sensitivity to freezing temperatures, the effect of soil temperature on regeneration timing and success were tested. In addition to using propagules collected from parent trees, a random grab sample of dispersed propagules resting at low and high tide positions was collected at the Port Fourchon boat launch site, referred to as LO and HI propagule sets, respectively. LO propagules were collected below low tide level in a submerged condition resting on the tidal basin mud bottom

just beyond mangrove shrub cover (see Figure 6). The date of propagule collection was Dec 21, 2013. After washing the collective group of propagules back at NWRC, nearly all floated to the surface as opposed to staying submerged. The condition of lying submerged in the field could be the effect of drag and capture of suspended mud accounting for lack of buoyancy. It is uncertain why the cleaned propagules floated after washing whether by reduction of removed mud weight or other reason.

Tray 1: CL, 80 S1 & S2	**Tray 2:** HI, 80 Root	**Tray 3:** HI, 80, CL	**Tray 4:** LO, 80, CL	**Tray 5:** LO, 80 CL & OP	**Tray 6:** HI, 80 OP
Tray 7: CL, 60, S1 & S2	**Tray 8:** HI, 60, CL	**Tray 9:** LO, 60, OP & CL	**Tray 10:** LO, 60, OP & CL	**Tray 11:** HI, 60, OP	

Figure 6. Experimental design for heat treatment.

HI propagules were collected at the highest stranded elevation at the upper edge of mangrove cover. It is presumed that these are composed of propagules dropped from parent trees on the high end of the elevation gradient or floated on high tide and stranded from parent trees anywhere. After washing, these HI propagules sank in the water bath rather than floated. Both groups were sorted by size and growth stage (cotyledon closed, open, radical extension, and presence of dangling roots). None of these propagules showed any advanced stage of true leaf or stem development. More than half of all propagules in the LO and HI collection showed signs of fungal blemishes demonstrating widespread infection in the wild.

Propagule selection for out-planting into the soil heat treatment experiment included those without apparent blemish of fungal infection and developmental stages possibly indicative of exposure time since drop from parent plant:

CL: closed condition

OP: slightly open cotyledon

S1: size 1: 1 g to 1.99 g (Dec, 1)

S2: size 2: 2 g to 2.99 g (Dec, 2)

Root: radical extension to fully open and long radical with and without root extension.

Two soil-heating treatments were applied at 60° F and 80°F.

Elevated CO_2 for regeneration success. The working hypothesis is that elevated CO_2 will increase regeneration success. Four trays, each with 12 propagules of size class 2 after 1 week floating time, were put in four CO_2 greenhouses: greenhouse 1 and 3 with 720 ppm CO_2, and greenhouse 2 and 4 with 320 ppm CO_2 (ambient). Propagule condition and response was monitored at least three times a week for radical extension, establishment, first leaf emergence, and survival rate.

Sunlight level for regeneration success. The working hypothesis is that sunlight will increase the regeneration success. Three trays, each with 18 propagules of size class 2 were put in three different light levels from magnified sunlight level, normal ambient sunlight, and shaded condition (50% ambient sunlight). Propagule condition and response was monitored at least three times a week for radical extension, establishment, first leaf emergence, and survival rate.

Statistical Analysis

Propagule regeneration and biomass data were processed in SAS 9.3 and Microsoft Excel 2010. Simple ANOVAs were applied for test of differences. Fixed effect was used to compare the effect of vegetation to the aboveground biomass and to compare mean difference between floating time and propagule weight. The fixed effects model is robust to normality. The univariate fixed effects model provided the lsmeans table from SAS output (Montgomery, 1991).

In addition, the propagule data were calibrated using an algorithm to fill in missing values for floating time and propagule weight. Then MANOVA was applied ($p < 0.05$) for analysis.

CHAPTER 4

Results

Aboveground Biomass

Results showed that mean biomass (dry wt) by treatment class was significant. 'Mix' and 'Marsh' are less than 'Tall'. Model error was normal and constant variance. All comparisons were evaluated at $\alpha = 0.05$ (see Table 1).

Table 1

Effect of Vegetation on Aboveground Biomass

Type 3 Tests of Fixed Effects				
Effect	**Num DF**	**Den DF**	**F Value**	**Pr > F**
Veg	3	4	9.15	0.0290

Least Squares Means						
Effect	**Veg**	**Estimate**	**Standard Error**	**DF**	**t Value**	**Pr > |t|**
Veg	MR	1082.85	523.47	4	2.07	0.1074
Veg	MX	616.97	523.47	4	1.18	0.3039
Veg	SM	2018.07	523.47	4	3.86	0.0182
Veg	TM	4184.25	523.47	4	7.99	0.0013

Differences of Least Squares Means									
Effect	**Veg**	**_Veg**	**Estimate**	**Standard Error**	**DF**	**t Value**	**Pr > |t|**	**Adjustment**	**Adj P**
Veg	MR	MX	465.87	740.30	4	0.63	0.5633	Tukey	0.9175
Veg	MR	SM	-935.22	740.30	4	-1.26	0.2751	Tukey	0.6264
Veg	MR	TM	-3101.41	740.30	4	-4.19	0.0138	Tukey	0.0456
Veg	MX	SM	-1401.09	740.30	4	-1.89	0.1314	Tukey	0.3568
Veg	MX	TM	-3567.28	740.30	4	-4.82	0.0085	Tukey	0.0286
Veg	SM	TM	-2166.19	740.30	4	-2.93	0.0430	Tukey	0.1332

Tall mangroves on these transects were near 2.5 m in height and more or less typical of mature scrub along tidal creeks in this area. The cumulative stemwood structure and size of this tall mangrove habitat accounts for anywhere from 2x to 4x greater standing biomass than adjoining "short" mangrove and "healthy" marsh near 1 m in height. The mixed marsh/mangrove zone supports the lowest standing biomass among the habitat classes existing in a ponded condition due to its low elevation and having a less than healthy stature and growth allowing sufficient light to reach surface to support a surface of algal growth.

Mangroves are dominant on the tidal creek berm with the tall form on the highest ground and short form on the backside. In this setting, the ecotone between pure mangrove and marsh appears rather distinct and persistent based on poles marking the same boundary a decade earlier. However, mangrove ingrowth is evident throughout the open marsh mostly of first year seedlings. Nearly every square quadrat across the landscape gradient from main tidal creek to backside tidal inlet contain mangrove seedlings or shrubs indicative of widespread propagule dispersal and regeneration, but limiting conditions for mangrove persistence (see Figure 7). The presence of isolated and scattered mangrove shrubs throughout the marsh zone suggests that periodic anomalies of climate or sea level and recruit hardiness can advance mangrove encroachment at lower elevations and more flooded and unconsolidated soil conditions. Elevation surveys were more difficult to hold rods at surface due to the saturated soil conditions insufficient to hold a person's weight and feet at surface or the rod bottom without using boards for support. The more prominent the area coverage of algal mat was indicative of degree and duration of tidal flooding above surface and likelihood of loose, unconsolidated soil.

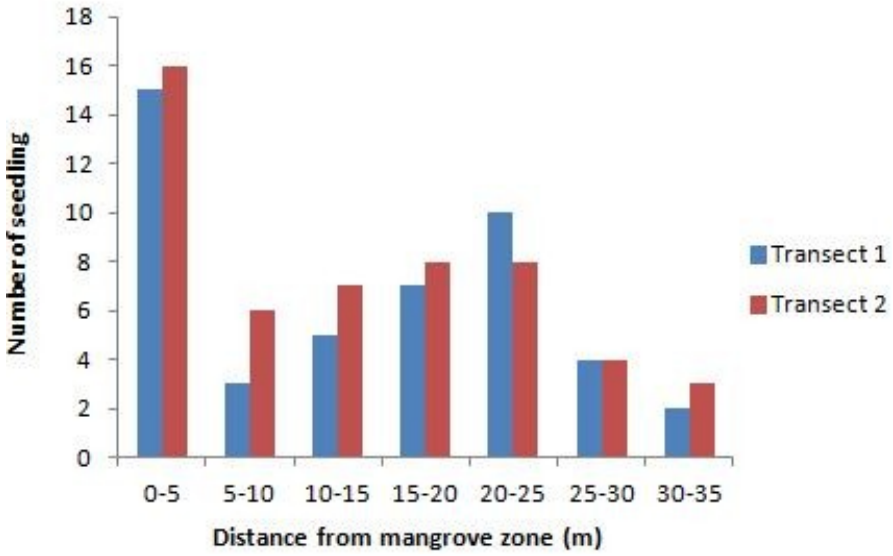

Figure 7. Number of mangrove seedlings along transect in open marsh zone.

Tree Growth, Architecture, and Internode Measurement

To determine differences in mangrove growth and form from different habitat zones and stages, tree samples were collected and measured from different areas from open sunlight to shaded condition and different stem forms, seedling, saplings, and re-sprouts to contrast leaf morphology and to predict age or disturbance history. In addition, some trees were tagged to track their growth over time to determine how seasonal conditions control growth habits and performance by re-measurement once every month.

The following are examples of growth measurements and differences from the same plant or in different settings. Figure 8 shows successive internode measurements for four mangrove seedlings/saplings collected from the open marsh. They demonstrate a similar growth pattern and internode count. These four seedlings grew very fast from beginning by using the nutrient and energy reserves from the cotyledon and thereafter slower at levels depending on soil and site condition. They appeared to be 2-3 years old based on node count and cyclic growth pattern that is thought to be driven by seasonality. These seedlings had about 4-5 sets of green leaves of

smaller size and shorter internode lengths presumably due to marsh substrate condition since vegetation cover is low with exposure to full sunlight.

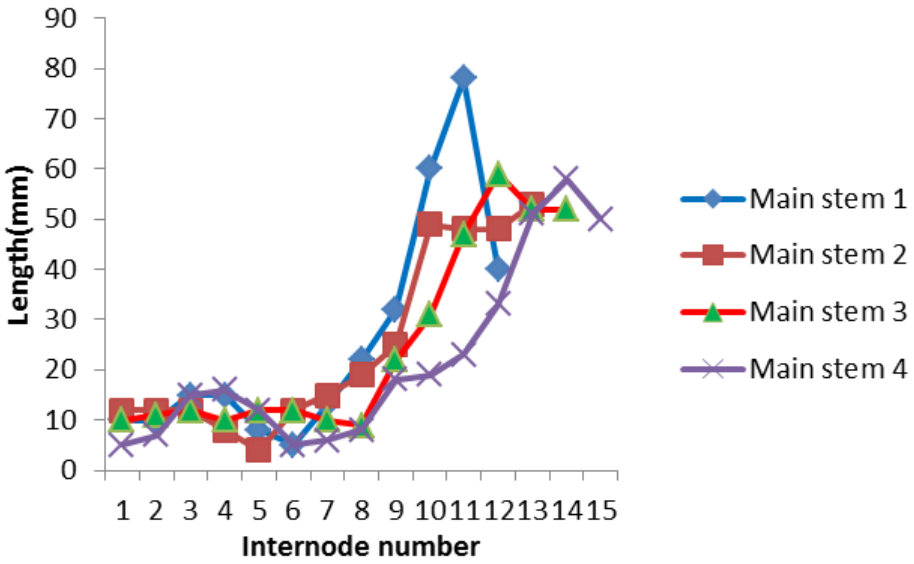

Figure 8. Internode lengths of four mangrove saplings growing in open marsh.

Re-sprout growth varied considerably within and between select trees perhaps related to plant allocation strategies and possible belowground differences in root size and health. Growth rate within a tree among different branches exhibited a highly variable response that can be greater than 2x or even become suppressed as a function of resource allocation change or self-shading (see Figure 9). Re-sprouts can be of the same age based on node count or subsequent year growth start based on the offset. Saplings with robust growth behavior indicate active growth whereas near zero nodal measurements if repeated indicate suppressed growth and the likelihood of abandonment if at the branch terminus. The first or second node at the terminus is often in active growth mode and can be small or short simply from recent initiation from the meristem. In many cases, re-sprouts can demonstrate a greater growth rate per node than main stem growth or other branch leads benefitting from a developed root system (see Figure 10).

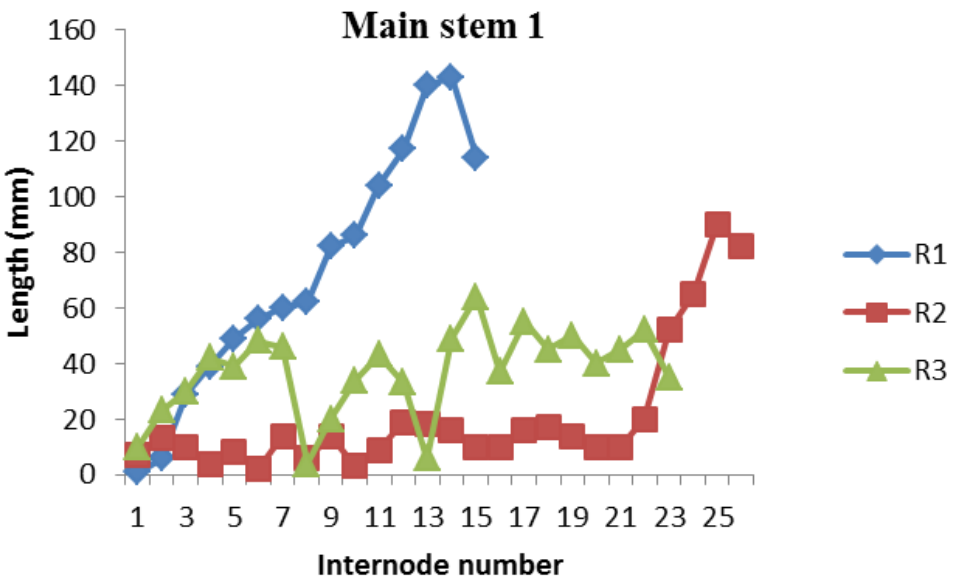

Figure 9. Internode measurements of three re-sprout stems from the same root base (main stem 1).

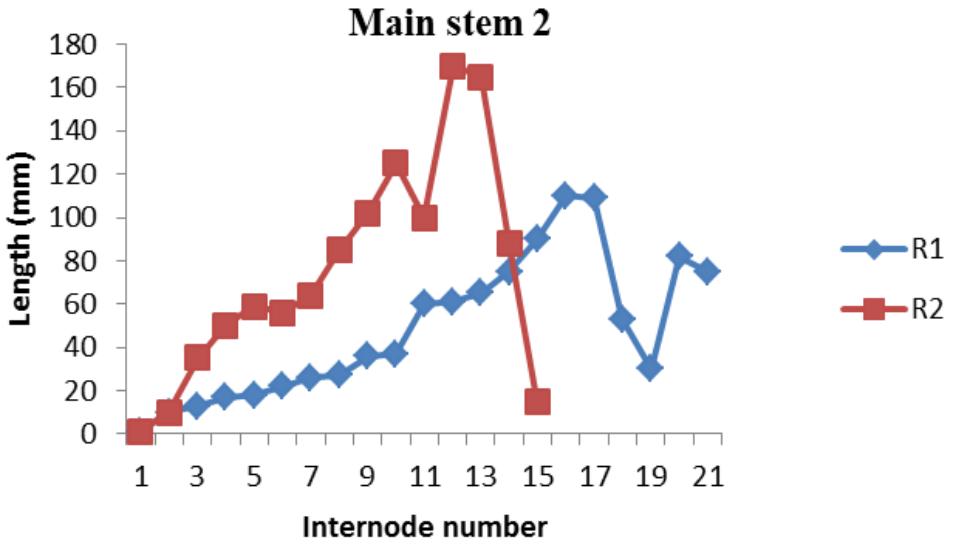

Figure 10. Internode measurements of two re-sprout stems from the same root base (main stem 2).

Figures 11 and 12 show 4 re-sprouts having a corresponding growth patterns. They were collected from the marsh. They are estimated to be 4 to 5 years old based on node count of 4-5

nodes per year. Initial growth from propagule reserves are characteristically robust but does not sustained effected by soil condition in the marsh and shading in the mangrove zone.

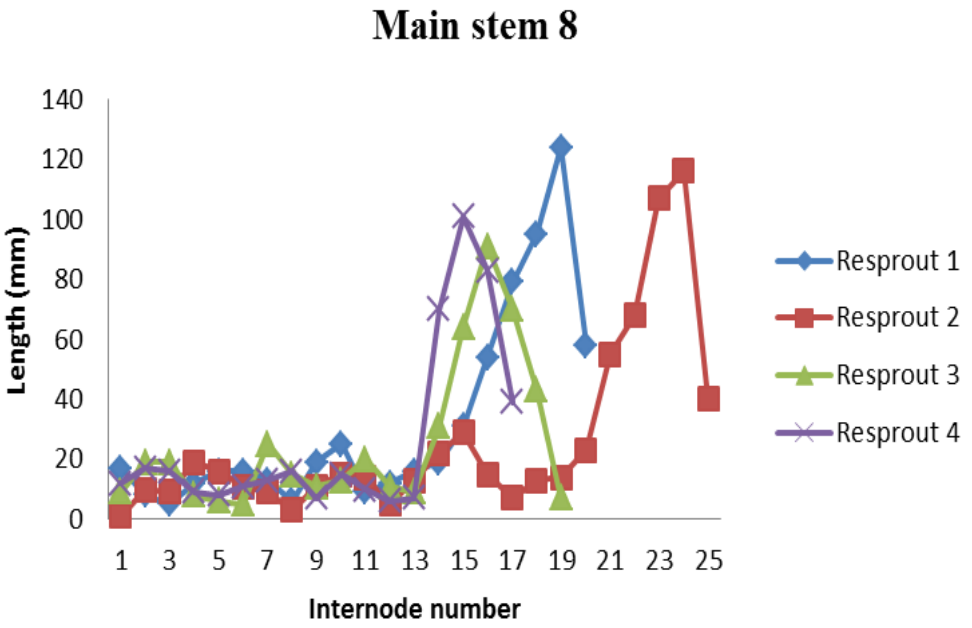

Figure 11. Internode count and lengths for four re-sprouts of main stem 8 with similar growth pattern and age.

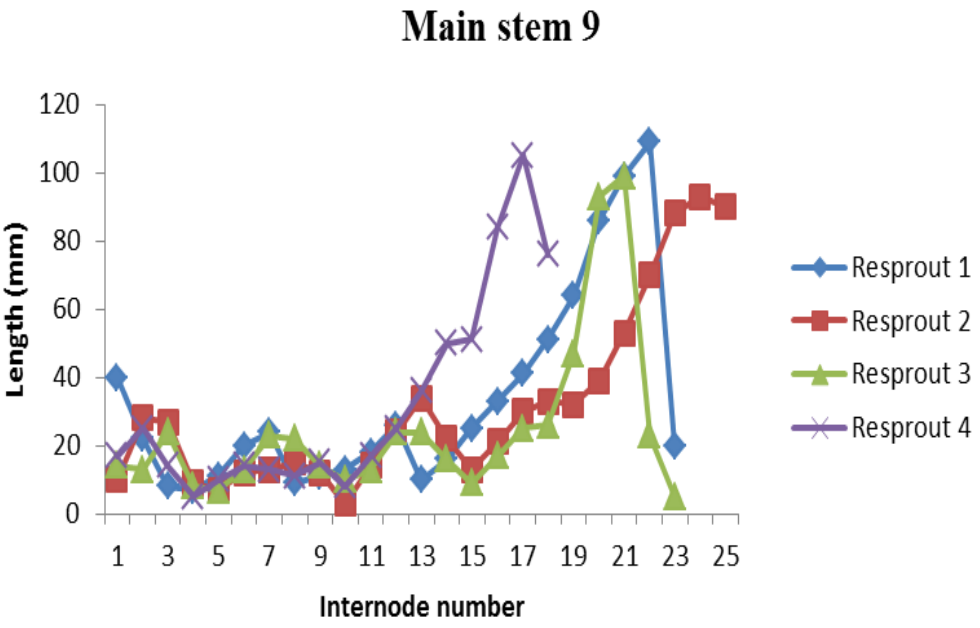

Figure 12. Internode count and lengths for four re-sprouts of main stem 9 with similar growth pattern and age.

Leaf size measurements of ten trees from open and shaded areas showed that there was a significant difference in the length and width between leaves with exposure to sunlight and/or soil conditions ($p = 0.001 < 0.05$, see Figure 13). The results showed that the leaves in the shaded area were longer and wider than those in open areas. Moreover, they appeared to be thinner.

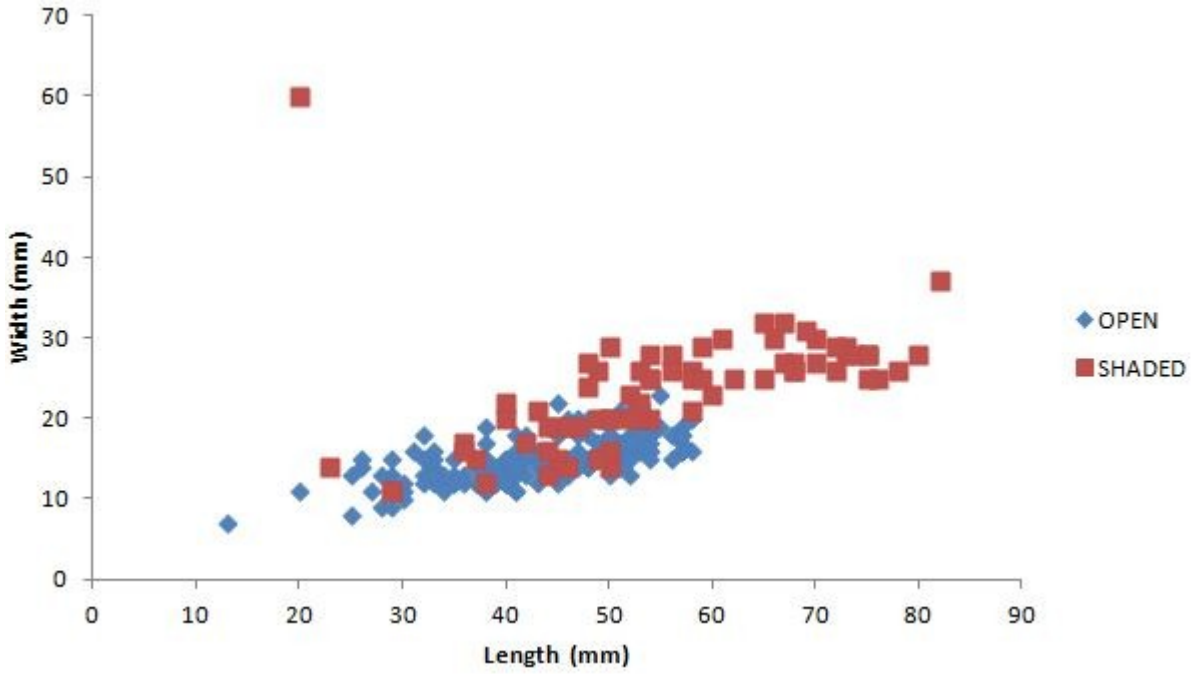

Figure 13. Comparison of leaf sets, width and length, between stems from open and shaded areas.

Ten stems representative of open and shaded areas at transect 1 and 2 were measured for differences in node count and size. Shaded trees had more internodes, and they were very short. As a result, they might be older than those in open areas, persisting under lesser conditions. It is thought that they grew slower than those in the open sunlight for lack of sunlight and growing space (see Figure 14 and 15).

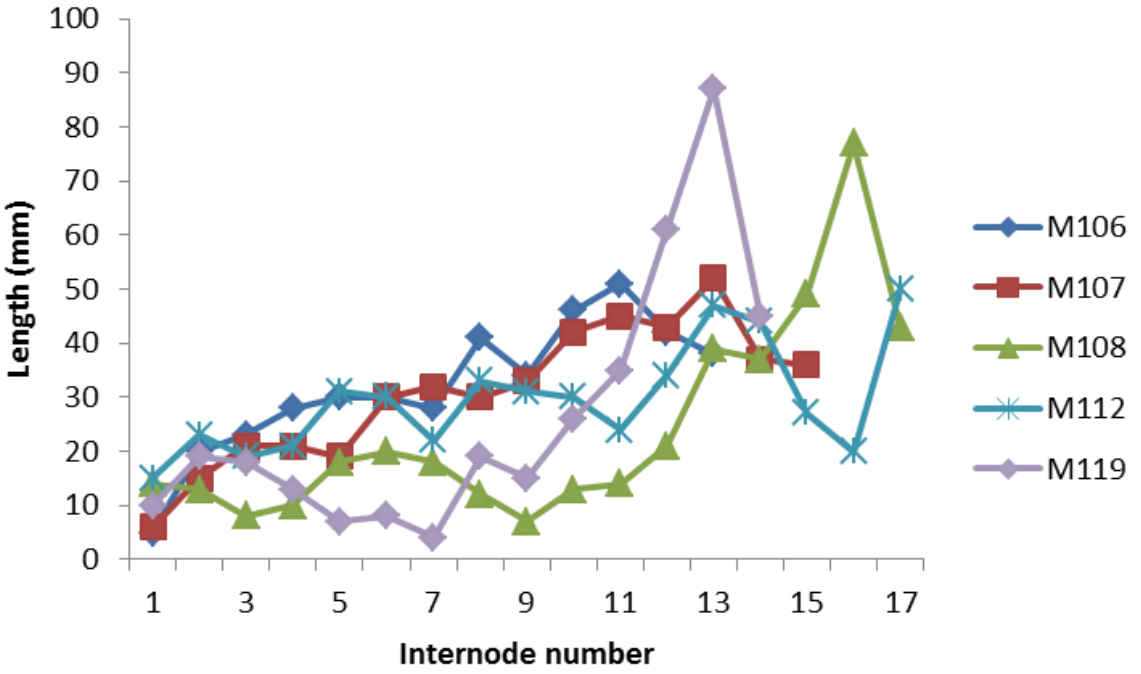

Figure 14. Internode count and lengths from single stems in open area.

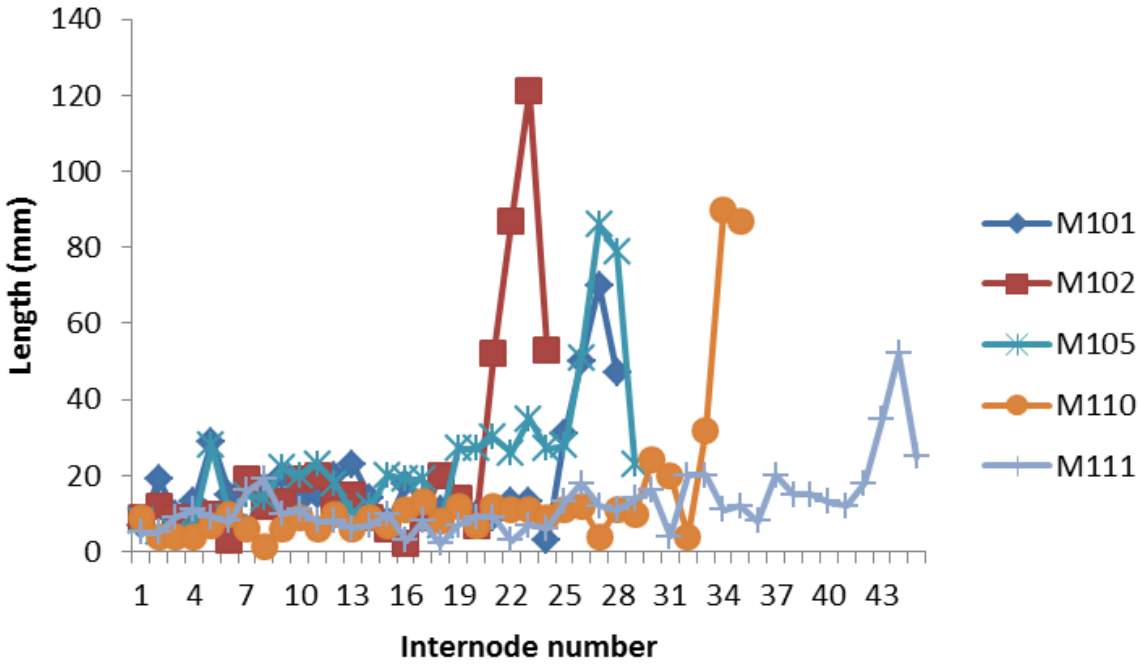

Figure 15. Internode count and lengths from single stems under shade.

To track seasonal growth of mangrove, about 100 single stems and branches near the Port Fourchon boat launch area were tagged on 16 Jan 2014. They were visited again about 6 weeks later on 8 March to determine the degree of internode growth and additions. Observations showed that most of them did not add any internodes. This might indicate that temperatures were not warm enough yet to stimulate cell growth since it was winter.

All tagged trees were re-measured on 22 May to determine any change in internode initiation or growth. Most trees grew at least two internodes as shown by example for 4 trees in Figure 16. This might be because from March to May, the temperature got warmer and there was more sunlight (see Figure 17).

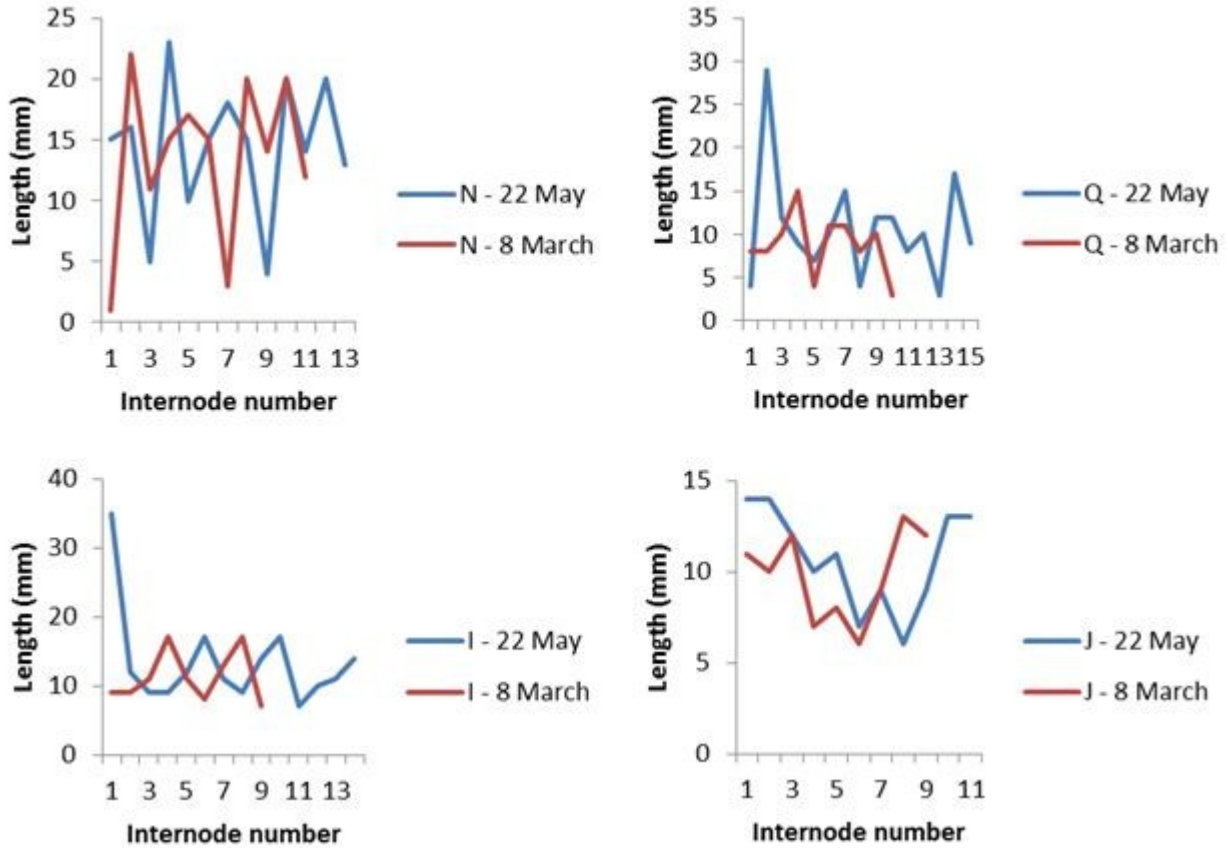

Figure 16. Internode growth and remeasurement of select tagged trees and branches.

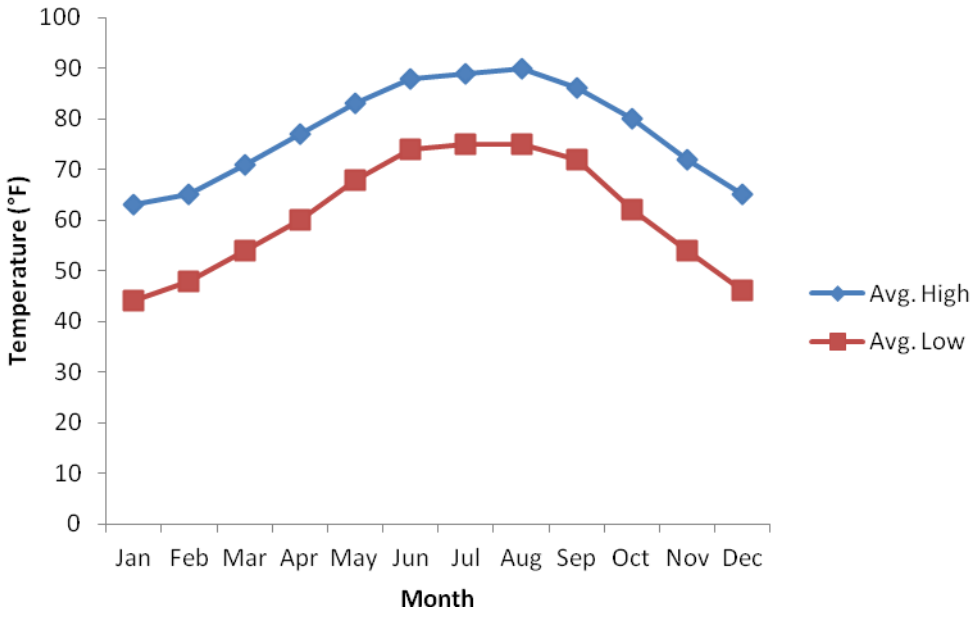

Figure 17. Mean monthly temperature of Port Fourchon, Louisiana (source: http://www.weather.com)

Soil Accretion

The ^{137} Cs dating method is an established technique to estimate the soil accretion rate from 1963-peak radioactivity fallout to present. Along the first transect, vegetation cover graded over 30 m from tall *Avicennia*, short *Avicennia*, *Spartina* marsh only, to a mixed zone of *Avicennia* and *Spartina*. Peak ^{137}Cs activity in each vegetation zone occurred at a depth of 47 cm in the tall *Avicennia* core, 39 cm in the short *Avicennia* and mixed *Avicennia* and *Spartina* core, and at 31 cm in *Spartina* only core. Therefore, tall *Avicennia* recorded the highest soil accretion rate of 0.94 ± 0.37 cm/year. Short *Avicennia* and the mixed zone exhibited an intermediate soil accretion rate of 0.78 ± 0.36 cm/year. The *Spartina* marsh core had the lowest accretion rate of 0.62 ± 0.34 cm/year. See Appendix C for ^{137}Cs profiles for transect 1. On the 2nd transect, peak ^{137}Cs activity was found at a depth of 37 cm in tall *Avicennia*, 29 cm in the short *Avicennia*, and 25 cm in *Spartina* and mixed *Avicennia* and *Spartina*. Therefore, tall *Avicennia* along this

transect also recorded the highest soil accretion rate of 0.74 ± 0.37 cm/year. Short *Avicennia* exhibited an intermediate soil accretion rate of 0.58 ± 0.35 cm/year. The *Spartina* marsh core and mixed zone had the lowest accretion rate 0.50 ± 0.36 cm/year and 0.50 ± 0.31 cm/year, respectively. See Appendix C for ^{137}Cs profiles for transect 2.

Carbon Stores of Saltmarsh/Mangrove

Carbon loss on ignition results are shown in Appendix C based on soil depth and by cover type along transect 1 from tall mangrove to short mangrove to marsh to a mixed marsh/mangrove zone. Results show an inverse relationship between percent organic matter and bulk density (see Appendix C-5). The bulk density generally increased with depth from the top to the bottom of the cores. In contrast, the organic matter decreased with depth from the top to the bottom of the core. End samples at the top and bottom of core often do not slice uniformly due to soil condition and composition affecting an accurate bulk density calculation at these depths.

Percent of organic matter was converted to carbon concentration in gram relative to overall soil weight by depth by multiplying organic matter percent to soil weight by depth. Organic matter from the soil surface to the 1963/1963 depth in each core was sum up to get a cumulative organic matter from 1963. The results showed that tall *Avicennia* recorded the highest organic matter of 180.44 g. Short *Avicennia* had an intermediate level organic matter of 170.88 g. *Spartina* and mixed zone exhibited the lowest organic matter level of 131.15 g and 130.60 g, respectively (see Figure 18).

Figure 18. Accumulative carbon stores of organic matter by cover type and zone from 1963 to present along transect 1.

In transect 2, the results demonstrated a similar pattern as transect 1. Tall *Avicennia* recorded the highest organic matter of 134.90 g. Short *Avicennia* exhibited an intermediate level organic matter of 122.66 g. *Spartina* and mixed zone had the lowest organic matter level of 78.72 g and 77.78 g, respectively (see Figure 19). In both transects, tall *Avicennia* have much higher carbon stores of organic matter than *Spartina*. Thus, *Avicennia* helped increase the organic matter to the soil.

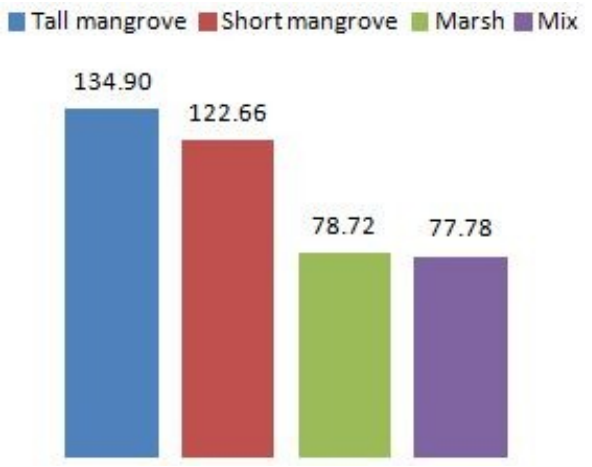

Figure 19. Accumulative carbon stores of organic matter by cover type and zone from 1963 to present along transect 2.

Surface Elevation Data Obtained from RTK GPS Surveys of Field Sites

Water elevation of the Port Fourchon tide gage was related to a site-specific water level record sensor and surface elevation surveys. A temporary water level recorded was installed in the tidal channel at the field site for a period of days to track high and low tide levels corresponding to the long-standing tide gage. The results showed that max water level were at 1.16 m, lowest were at – 0.5 m and mean range were at 0.369 m.

RTK GPS surveys including Dini Laser Survey and MR8 GPS were used to obtain the elevation for both transect. The MR8 GPS gave us the absolute elevation while the Dini Laser Survey gave us the relative elevation. In transect 1, the reference points were set up at SET sites that were available in the field. From these points, elevation for each soil core was calculated. The elevations of every meter from the canal edge to soil core in the mixed zone were also calculated (see Figure 20).

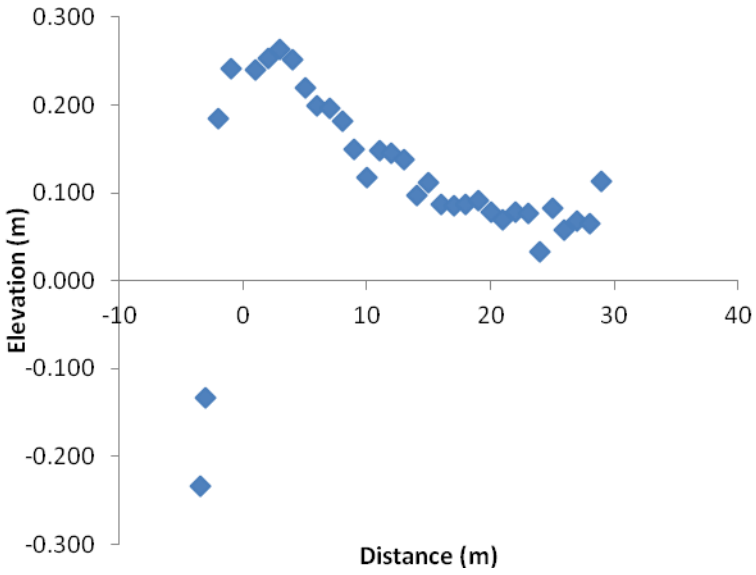

Figure 20. Elevations for every meter in transect 1.

The results showed that the elevation went up from the canal edge to the tall mangrove. It reached the highest peak at tall mangrove zone at 0.26 m. Then, it declined across the short

mangrove and marsh zone and slightly up again at the mix zone. Marsh soils were noticeably more saturated or ponded toward the mix zone. Moreover, algae appeared at this point and there was less mangrove regeneration.

The current surface elevation decreased with cover type and zone from 0.38 m in tall mangrove, 0.24 m in short mangrove, 0.14 m in marsh, and 0.11 m in mix zone. The 1963 elevation were obtained by subtracting the current elevation to the 1963 depth at each zone as 47 cm in tall mangrove zone, 39 cm at marsh zone and 31 cm at short mangrove and marsh zone. As a result, the elevations were -0.08 m at tall mangrove, -0.14 m at short mangrove, -0.16 m at marsh and -0.27 m at mixed zone (see Figures 21 and 22).

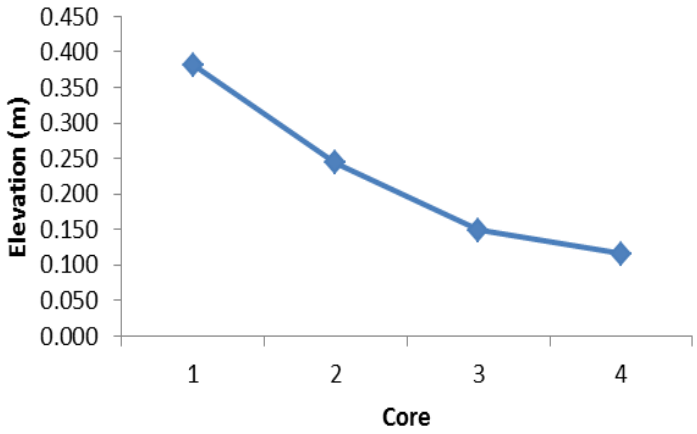

Figure 21. Surface elevation at core sites across cover type and zones of transect 1.

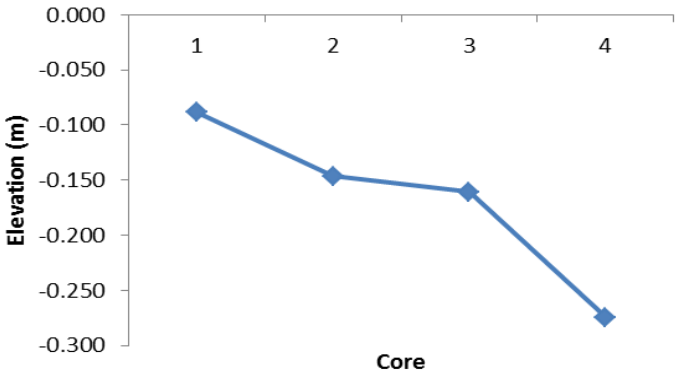

Figure 22. Reconstructed 1963 surface elevation at core sites of transect 1.

In transect 2, elevation for 4 cores sites at tall mangrove, short mangrove, marsh and mix zone were taken for replication purpose. The results showed that the current surface elevation decreased from 0.23 m in tall mangrove, 0.14 m in short mangrove, 0.03 m in marsh and - 0.001 m in mix zone. The 1963 elevations were obtained by subtracting the current elevation to the 1963 depth at each zone as 37 cm in tall mangrove zone, 29 cm at short mangrove and 31 cm at marsh zone and marsh zone. As a result, the elevations were -0.13 m at tall mangrove, -0.14 m at short mangrove, -0.21 m at marsh and -0.25 m at mix zone (see Figures 23 and 24).

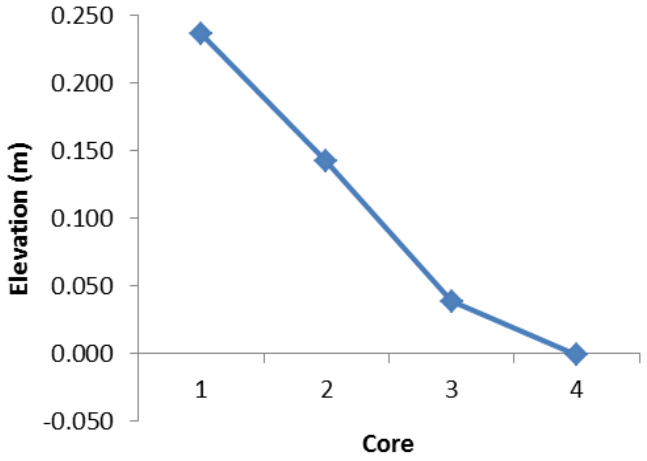

Figure 23. Surface elevation at core sites across transect 2.

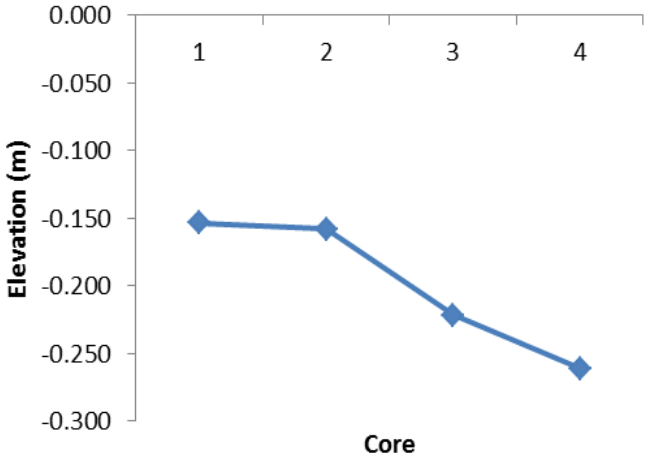

Figure 24. Reconstructed 1963 surface elevation at core sites of transect 2.

Propagule Regeneration for Restoration

Propagule collection. Differences were observed in the propagule size and frequency data from the Nov. 21 2013 and Dec. 21 2013 collections. The Nov. 21 propagule data were collected when there was an abundance of propagules of larger size. Unfortunately, a fungus infection killed most of our size 4 (4-5 g) propagules within a month affecting the integrity of the planned experiment. One month later, the Dec. 21 collection showed a shift in size class density from larger to smaller propagules (see Figure 25). We hypothesized that larger, more mature, propagules from 3g to 6g had dispersed or dropped to the ground between the two collection dates. There was no significant difference or form change between the weight and length of collected propagules from the November and December collections (see Figures 25 and 26).

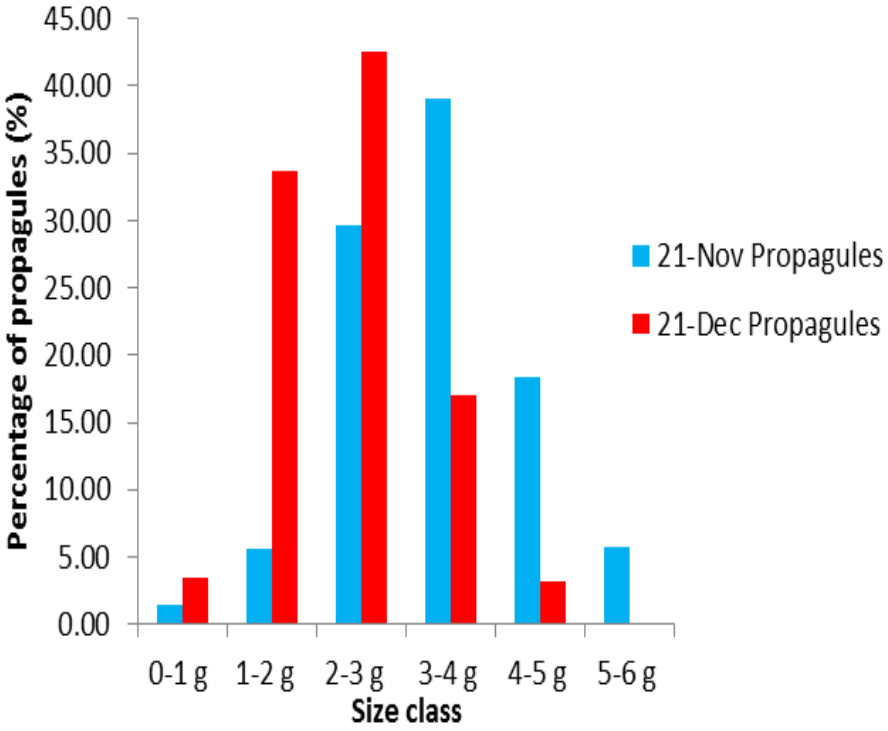

Figure 25. Distribution of collected propagule by sizes (weight).

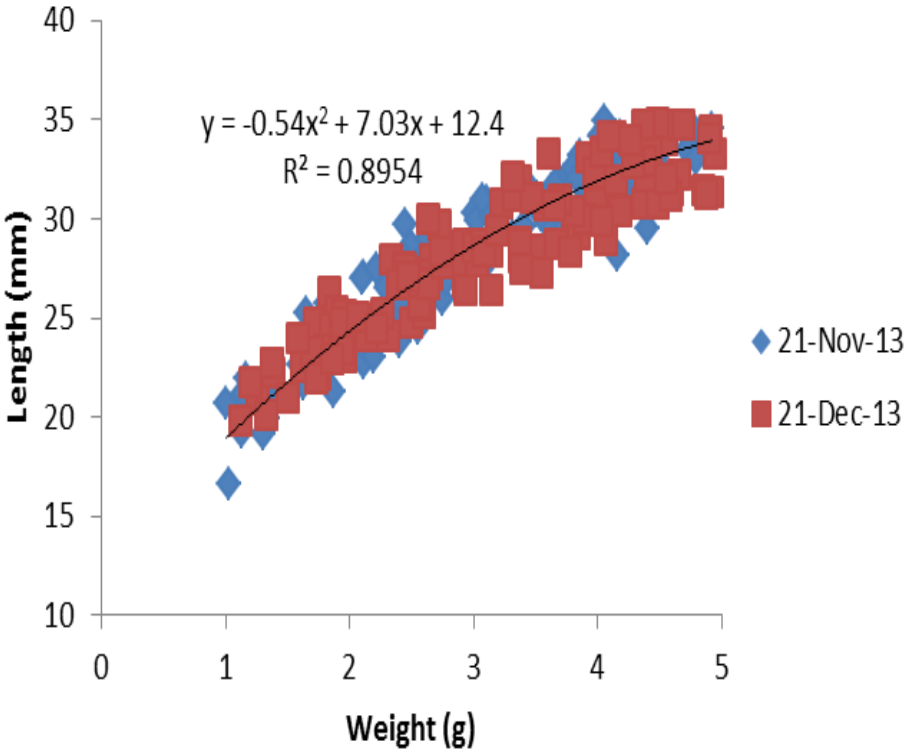

Figure 26. Estimated linear relationship between length (Y) and width (X) of collected propagules.

Propagule weight and floating time for regeneration success. Survival rates were generally high for all size classes and float times of propagules indicating the hardiness and propensity for regeneration success. Results showed that there was no significant difference in survival rate for both week and size ($p = 0.7643$ and $0.068 > 0.05$, respectively) based on float time and strand date (see Figure 27 and 28). The lowest survival rates were above 75% and most notably low for the smallest propagule class less than 2 g per individual that might be expected for least mature and lowest energy reserves.

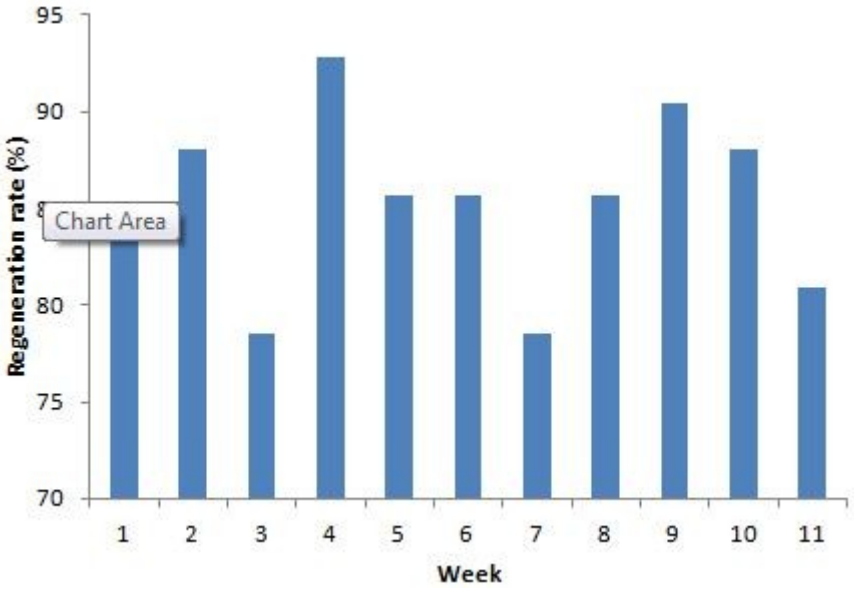

Figure 27. Regeneration rate by week.

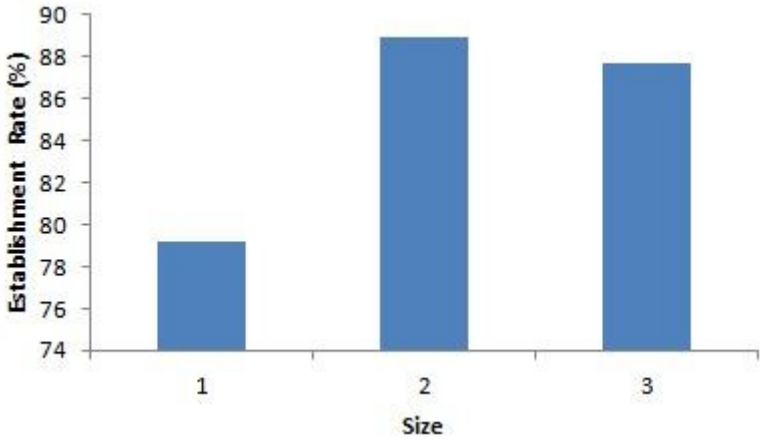

Figure 28. Propagule establishment rate by size.

There were seven response variables (hypocotyl growth, rooting day, lifting day, standing day, true leaf day, number of nodes and sum nodes) and two independent variables (size and float time). To increase the sample size for the MANOVA, missing values were estimated to the data.

The means were estimated from all of the known values of 'lifting day - rooting day' & 'true leaf day - standing day.' As a result, if rooting day was missing, it was estimated with

lifting day -19.43. Likewise, if true leaf day was missing, it was estimated with standing day +15.67 (see Table 2).

Table 2

SAS Output for Estimation of Missing Values

Variable	*M*	Standard Error	*N*
lift - root	19.43	1.06	175
TL - stand	15.67	1.104	379

For lifting day, the average of root and standing day were taken when both existed. For standing day the average of lifting and true leaf day were taken when both existed. As a result, sample size increased from 166 to 356 points with all seven responses (9% of the missing data was estimated to increase the sample size by 124%).

Because the MANOVA for the seven variables didn't follow normality, a nonparametric MANOVA ("L test," n.d.) was used. To do this, the seven variables were ranked from highest to lowest and adjusted the Pillai Trace statistic or (n - 1) * (Pillai trace). This follows a chi-square with p * (nd - 1) degrees of freedom ($p = 7$ or the number of responses & nd is the degrees of freedom of either size, float time, or the interaction). The results are shown in Table 3.

Table 3

SAS output for nonparametric MANOVA (L Test) (N = 356)

L stat variable	P * (nd - 1)	*p*-value
232.931 size	7 * (3 - 1) = 14	< 0.0001
435.566 float	7 * (11 - 1) = 70	< 0.0001
204.664 size*float	7 * (3 - 1) * (11 - 1) = 140	0.0003

To check for pairwise comparisons, the lsmeans of the two way ANOVA were taken by each response variable. Since both float time and size class are fixed effects (we are comparing

the means), the two-way ANOVA is robust to normality. If the interaction effect was not significant, the main effect was considered. The alpha level (0.05) for the mean comparisons were Bonferonni adjusted (size used .05/3, float time used .05/55 and the interaction used .05/1980). The results were as follows (note that only significant comparisons are given; others are not significant).

Number of nodes had a size effect. True leaf day had a float effect. Sum of nodes had a size effect and float effect. The size*float interaction was significant for hypocotyl growth, rooting, lifting, and standing day.

Mean comparisons.

For number of nodes, size class 3 > size class 2 > size class 1.

For sum of nodes or the height of seedling, size class3 > size class 2 > size class 1. Week 1 smaller than week 4, week 3, week 2, week 6, and week 8.

For number of true leaf day, week 9 is smaller than week 3. Week 9, week 8, week 5, and week 2 are smaller than week 11.

For hypocotyl growth of week 1 and week 2, size class 1 is smaller than size class 2.

In hypocotyl growth of size class 1, week 3 and week 4 are less than week 7, week 6, week 8, week 9, week 10, and week 11. Week 5, week 1, and week 2 are less than week 6, week 8, week 9, week 10, and week 11.

In hypocotyl growth of size class 2, week 1 and week 2 are less than week 5, week 6, week 7, week 8, week 9, week 10, and week 11. Week 4 and week 3 are less than week 6, week 7, week 8, week 9, week 10, and week 11. Week 5, week 6, and week 7 are less than week 8, week 9, week 10, and week 11.

In hypocotyl growth of size class 3, week 1, week 2, and week 3 are less than week 6, week 7, week 8, week 9, week 10, and week 11. Week 4 is less than week 7, week 8, week 9, week 10, and week 11. Week 5, week 6, and week 7 are less than week 8, week 9, week 10, and week 11.

For number of root day of size class 2, week 5 and week 1 are less than week 10 and week 11. For number of root day of week 5, size class 2 is less than size class 1.

For number of lift day of size class 2, week 5 is less than week 7, week 3, week 11 and week 10.

For number of stand day of size class 2, week 5 is less than week 3, week 10, and week 11.

Heat treatments for regeneration success. Because fungus infection was deemed a likely factor to inhibit propagule viability, the timing of propagule lift and root implant of any propagules was more important to observe when comparing any effect of soil temperature on regeneration success. Within 30 days of placement on soil surface (January 21), propagules under soil heating at 80°F were stimulated to initiate root extension and implant for all treatments compared to 60°F treatment and for all other regeneration experiments (see Figure 29 and 30). This suggests that temperature plays an important role in the start and progression of propagule regeneration months in advance of those on field sites and in other greenhouse experiments.

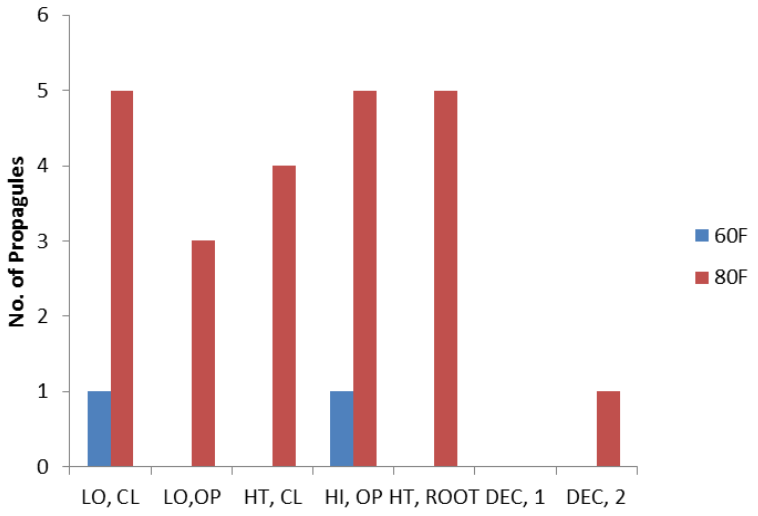

Figure 29. Number of established propagules after 30 days.

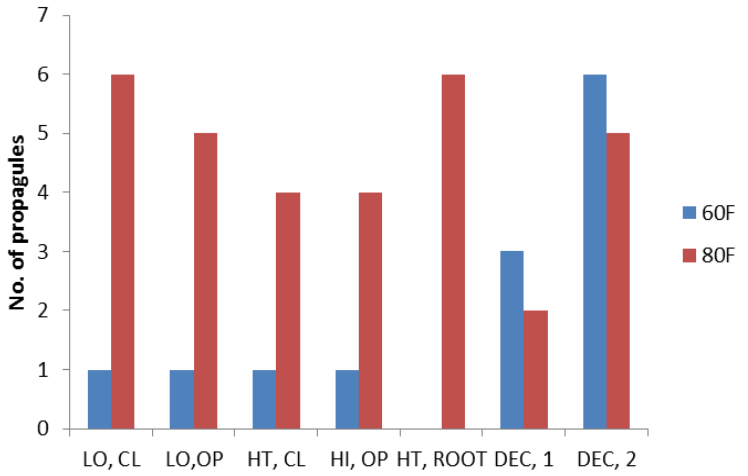

Figure 30. Number of established propagules after 80 days.

Elevated CO_2 for regeneration success. Regeneration success was equally high at over 97% under both ambient (400 ppm) and elevated (720 ppm) atmospheric CO_2 concentrations. There were four response variables (hypocotyl extension, lifting day, standing day, true leaf day). ANOVA was applied to compare the mean differences of four response variables of the different stages of regeneration. Results showed that the elevated CO_2 had no effect on radicle extension, lifting day, standing day, or true leaf day, respectively (p = 0.2365, 0.2038, 0.2245 and 0.6488 > 0.05).

Sunlight level for regeneration success. Propagule establishment rates were 22.22%, 44.44% and 61.11% for control, open and shaded treatments from 26 January to 15 May 2014, respectively. Results showed that sunlight had no effect on propagule regeneration success; lift-up, standing, or true leaf emergence ($p > 0.05$). More importantly, the date and timing of successful propagule establishment was similar for all sunlight levels and the float experiment within the same greenhouse space. Evidence suggests that neither sunlight advanced regeneration nor shade (less than 50% PAR) retarded the timing of regeneration (see Figure 31). Actual lift up, standing, and true leaf emergence dates were coincident with all other unshaded propagules in the greenhouse reinforcing the role of temperature as the primary factor for propagule growth and establishment.

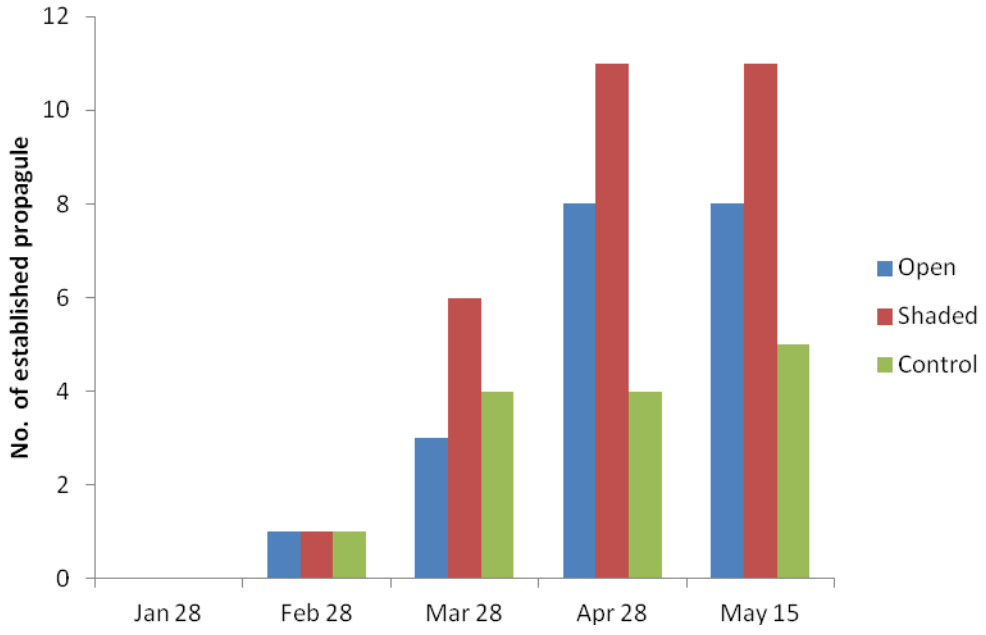

Figure 31. Number of established propagules under different sunlight levels.

CHAPTER 5

Discussion and Future Research

Aboveground Biomass

Aboveground biomass and carbon stores for the different stages of marsh/mangrove habitat and mixing varied greatly, and was highest for pure mangrove scrub, tall and short, due to their extensive leaves, branches, and root systems. Tall mangrove was significantly greater than pure marsh or mixed marsh/mangrove zone by more than double the standing biomass.

Biomass values corresponded with elevation grade such that the higher elevations supported dense vegetation of mangrove and marsh (see Figure 32). The greater height and vertical profile of woody stem growth of tall mangrove accounted for biomass values that were 2x or greater on average for short mangrove and healthy marsh, and even more so for ponded marsh and marsh/mangrove mix at the lowest elevations. As elevation decreased across the grade from tidal creek berm to backside inlets, surface flooding from tides was greater in extent and frequency while vegetation height and density was less for either marsh or mangrove. Algal mats are prominent in this lower zone for the added flood conditions and sunlight for lack of canopy cover.

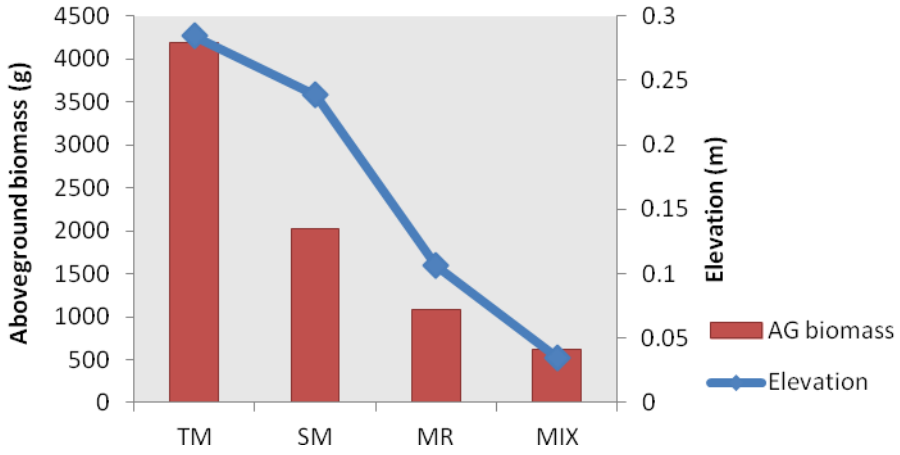

Figure 32. Correlation between elevation and aboveground biomass.

Tree Growth, Architecture, and Internode Measurement

Growth behavior and cyclic internode patterns support the study hypothesis that mangrove in Louisiana grow faster in spring and slower, if at all, in winter. By measuring the internode development in different settings of open area, shaded area, re-sprouts, seedlings, and tagging trees, it was shown that mangrove grew very little or might stop growing in winter. It was evaluated by comparing the growth pattern of the remeasured tagged branch and stems and seedlings in the same setting environment. They grew very long internodes in summer and very short internodes in winter. In extreme weather when the temperature drops below 0°C, mangrove leaves, and stem cells can embolize leading to tree mortality or partial dieback. In fact, in this study, most of tagged mangrove did not grow any internodes from January to March when the temperature was seasonably cool. In contrast, tagged branches and stems added from two to five internodes from March to May when the air temperature got warmer and daylength was greater. Temperature appears to be a critical factor in mangrove regeneration in the field and greenhouse experiments and for stem elongation and growth in the field. Near freezing conditions can cause plant tissue damage and death, and relatively modest seasonal temperatures less than 20°C appear to limit growth and regeneration.

Leaf size and internode length of seedlings and saplings varied from open and shaded positions in marsh and mangrove zones. Black mangrove is a shade intolerant species growing best under full sunlight, but can survive under shade with modification to leaf form, wider, longer, and overall larger leaf area. In contrast, leaf size and internode length between comparable open-grown seedlings and saplings of similar internode count and age were much shorter in marsh soils than those on higher elevation mangrove zones. A number of factors may account for slower growth between these settings primarily due to the difference in flooding

frequency as affected by elevation and likely difference in available soil oxygen. It was observed that mangrove seedlings at lower elevations were coated with sediment and algal growth from overtopping by tidal flood that may affect leaf function efficiency and reduce photosynthesis.

Tree internode measurement and tree architecture are very simple and efficient methods of tracking mangrove growth and estimating carbon stores. Osland, Day, Larriviere and From (2014) developed aboveground allometric equations which can be used to quantify mangrove total aboveground biomass, leaf biomass, stem plus branch biomass, and leaf area. In this study, instead of using such allometric equations, the 1 m^2 quadrat survey was applied to estimate the aboveground biomass for mangrove and marsh because it is simpler and more accurate. Understanding cyclic patterns of annual growth can also help determine how old the mangrove are and what causes them to grow slow or fast. Therefore, tree architecture could provide the history of establishment of mangrove in a specific area when analyzed or confirmed with aerial photography or other personal account or documentation.

Soil Accretion

The yearly increase or addition of soil material and elevation, known as accretion, involves a combination of processes including positive contributions of mineral sedimentation, organic matter deposition, and negative components of decomposition and erosion (Foret, 2001). These processes connect soil formation to the sustainability of a wetland ecosystem. The conversion of marsh to mangrove in the Gulf of Mexico by some is thought to promote sediment trapping and shoreline stability and thereby possibly increase the soil accretion rate (Comeaux et al., 2012; Perry & Mendelssohn, 2009).

The results from ^{137}Cs dating of soils fully supported the hypothesis that mangrove has higher soil accretion rate and carbon stores than marsh in this setting due to their extensive leaves, branches and root systems. In both transects, tall mangrove exhibited the higher accretion rates of 0.94 ± 0.37 cm/year and 0.74 ± 0.37 cm/year compared to the marsh zone at 0.62 ± 0.34 cm/year and 0.50 ± 0.31 cm/year, respectively. Short mangrove and the mixed zone demonstrated an intermediate accretion rate of 0.78 ± 0.36 cm/year on transect 1. On transect 2, short mangrove exhibited an intermediate accretion rate of 0.58 ± 0.35 cm/year. The mixed zone had the lowest accretion rate of 0.50 ± 0.36 cm/year. These are long-term estimates of net accretion over 5 decades showing mangrove, tall and short form, occupied the highest elevations, and accumulated the greater soil accretion.

Landscape position may prove to be the more important factor of natural berm development at tidal creek edge where deposition of mineral and organic debris from marine and estuarine tidal circulation falls out or traps most readily, accounting for higher elevation. Marsh and mangrove persist on these berms and both cover types are sufficiently healthy and dense to strand floating propagules of mangrove from parent trees local and regional. Raft lines from high tides can often comply with organic debris from marine seagrass, marsh and mangrove leaf and stem parts, and mangrove propagules. The success of mangrove regeneration thereafter is not well understood, but likely depends on a number of climate, soil, and biotic interactions. Because mangroves are generally found at the highest elevations, it has long been questioned as to whether they require or create the higher elevation. The results of this study demonstrate that mangrove regenerate at all elevations, high and low, but succeed more readily at higher elevations and contribute higher organic production above- and belowground after establishment.

Bulk Density and Carbon Storage

Bulk density generally increased with soil depth and inversely in relationship to percent organic matter. When the bulk density was high, there was more clay in the samples. The bulk density often reached near its highest value at the depth of peak ^{137}Cs specific activity for nearly all sediment cores regardless of cover type.

Soil formation is manipulated by both the contribution of biomass production and the loss of organic matter through decomposition (Foret, 2001). Mangroves are thought to increase both belowground plant production and deposition rate through their large leaves, branches, and root systems. Therefore, they are thought to have a higher carbon sequestration rate than marshes (Bianchi et al., 2013).

Study results demonstrated that mangrove accumulate higher soil carbon and storage than marsh. Carbon gain or accumulation from 1963 in both transects confirmed that tall mangrove soils sequestered the highest carbon at 180.44 g in transect 1 and 134.90 g in transect 2, Short mangrove exhibited an intermediate level of 170.88 g in transect 1 and 122.66 g in transect 2. Marsh and mixed zone had the lowest carbon at 131.15 g and 130.60 g in transect 1 and 78.72 g and 77.78 g in transect 2, respectively.

Elevation

Mangroves are known to establish on higher elevations than marsh in some wetland settings. Thom (1967) indicated that the primary elements responsible for mangrove species zonation are geomorphic features of an area combined with subtle elevational variations. In addition, mangrove is usually found at higher elevations where duration and frequency of flooding are relatively low (Chapman, 1976). Similarly, Patterson (1992) found that the elevation was highest in the *Avicennia* zone, intermediate in transition zone, and lowest in

Spartina zone. In this study, the working hypothesis was that mangrove ingrowth thereafter promoted higher deposition and increased elevation with vegetation complexity or stand age. The results supported this hypothesis. In both site transects, tall mangrove surveyed at higher elevations of 0.38 m and 0.23 m (NAVD) compared to 0.14 m and 0.03 m (NAVD) of marsh, respectively. The surface elevation in 1963 based on accretion rate by ^{137}Cs dating of soils showed little difference of -0.08 m and -0.13 m (NAVD) in tall mangrove sites and -0.16 m and - 0.21 m (NAVD) in marsh, respectively. As a result, in transect 1, the elevation increased 0.46 m in tall mangrove zone compared to 0.30 m in marsh zone. In transect 2, the elevation increased 0.36 m in tall mangrove zone compared to 0.24 m in marsh zone. Elevation clearly plays an important role of interaction with tidal flooding that influences the import of allocthonous material and generation of greater autocthonous deposition from less flooded and healthy marsh or mangrove.

Propagule Regeneration for Restoration Success

Propagule weight and floating time for regeneration success. The results showed that propagule size and floating time have a significant effect on regeneration success and growth of seedlings. Larger propagules by size class accounted for greater height growth after establishment, which may be important for survival and persistence in the field where subsequent, flooding or submersion can slow growth or cause death.

The condition and capacity of propagules to successfully establish after floating in tidal waters for different lengths of weeks before becoming stranded was investigated to test whether floating time had an effect on both regeneration success and seedling growth. Overall, floating time for a period up to 11 weeks did not inhibit regeneration success showing that greater than 80% of propagules in all treatments became established under controlled conditions. Regardless

of floating time prior to becoming stranded, propagules of small or large mass have the propensity to regenerate.

Temperature effect on regeneration success. More than any factor, temperature was the common factor in the field, greenhouse, or by heat treatment sustained above 20°C that stimulated metabolic activity and regeneration start of propagules. In Louisiana, black mangrove propagules usually mature and drop in late fall, November and December. In the field, propagules lay dormant on the ground or float in warm Gulf waters exposed to cold air masses and temperatures during winter months, January and February. Pickens and Hester (2010) investigated the effect of low temperature on propagule viability in early life state. They found that duration and temperature of exposure decreased propagule survivorship, specifically 24 hours exposure at -6.5°C. In addition, propagules exposed to −6.5°C were most vulnerable to fungal infection (Pickens & Hester, 2010). In this study, soil heating at 80°F advanced regeneration success 2 months ahead of constant heating at 60°F or other experiments in same greenhouse space.

Sunlight for regeneration success. All propagules remained relatively dormant from December planting though February, but suddenly and synchronously stood up in March when air temperature was warmer and there was greater daylength. Neither amplified sunlight nor shading at 50% PAR advanced or retarded regeneration start different from the control group or other treatments sharing the same greenhouse space.

Elevated CO_2 for regeneration success. Elevated atmospheric CO_2 is known to increase the nutrient and water use efficiency in many plant species. McKee and Rooth (2008) investigated the effect of elevated atmospheric CO_2 concentration (720 ppm) on mangrove and marsh species demonstrating above- and belowground production increases above ambient (385

ppm). Similarly, Adam Langley, Mozdzer, Shepard, Hagerty, and Patrick Megonigal (2013) found that elevated CO_2 and nitrogen addition directly affected belowground production and soil accretion of marsh species to increase surface elevation. In this study, we exposed mangrove propagules to elevated CO_2 (720 ppm) to detect any acceleration on regeneration start. There was no difference in regeneration start or establishment between ambient or elevated CO_2 environment. Propagules under both CO_2 treatments synchronously began regeneration activity in late March along with other greenhouse and field propagules. Except soil heating at 80°F where regeneration start was advanced by a month or more, all other treatments of float time, soil heating at 60°F, amplified sunlight, deep shade, or elevated atmospheric CO_2 significantly advanced or retarded regeneration start or establishment. These collective treatments suggest that there is a critical temperature constant that must be reached or sustained to stimulate metabolic activity toward seedling establishment.

References

Adam Langley, J., Mozdzer, T. J., Shepard, K. A., Hagerty, S. B., & Patrick Megonigal, J. (2013). Tidal marsh plant responses to elevated CO_2 , nitrogen fertilization, and sea level rise. *Glob Chang Biol, 19*(5), 1495–1503. doi: 10.1111/gcb.12147

Alongi, D. M., Clough, B. F., & Robertson, A. I. (2005). Nutrient-use efficiency in arid-zone forests of the mangroves Rhizophora stylosa and Avicennia marina. *Aquatic Botany, 82*, 121–131. doi: 10.1016/j.aquabot.2005.04.005

Alongi, D. M., & Dixon, P. (2000). Mangrove primary production and above- and below-ground biomass in Sawi Bay, southern Thailand. *Phuket Marine Biology Center Special Publication, 22*, 31–38.

Bianchi, T. S., Allison, M. A., Zhao, J., Li, X., Comeaux, R. S., Feagin, R. A., & Kulawardhana, R. W. (2013). Historical reconstruction of mangrove expansion in the Gulf of Mexico: Linking climate change with carbon sequestration in coastal wetlands. *Estuarine, Coastal and Shelf Science, 119*, 7–16. doi: 10.1016/j.ecss.2012.12.007

Bouillon, S., Borges, A. V., Castañeda-Moya, E., Diele, K., Dittmar, T., Duke, N. C., . . . Twilley, R. R. (2008). Mangrove production and carbon sinks: A revision of global budget estimates. *Global Biogeochemical Cycles, 22*(2), n/a–n/a. doi: 10.1029/2007gb003052

Bridgham, S. D., Megonigal, J. P., Keller, J. K., Bliss, N. B., & Trettin, C. (2006). The carbon balance of north american wetlands. *The Society of Wetland Scientists, 26*(4), 889–916. doi: 10.1672/0277-5212(2006)26[889:TCBONA]2.0.CO;2

Chambers, J. Q., Higuchi, N., Tribuzy, E. S., & Trumbore, S. E. (2001). Carbon sink for a century. *Nature, 410*(22), 429–429.

Chapman, V. J. (1976). *Mangrove Vegetation*. Vaduz, Liechtenstein: J. Cramer.

Comeaux, R. S., Allison, M. A., & Bianchi, T. S. (2012). Mangrove expansion in the Gulf of Mexico with climate change: Implications for wetland health and resistance to rising sea levels. *Estuarine, Coastal and Shelf Science, 96*, 81–95. doi: 10.1016/j.ecss.2011.10.003

Delaune, R. D., Patrick, W. H., & Buresh, R. J. (1978). Sedimentation rates determined by ^{137}Cs dating in a rapidly accreting salt marsh. *Nature, 275*(5680), 532–533.

Dittmar, T., Hertkorn, N., Kattner, G., & Lara, R. J. (2006). Mangroves, a major source of dissolved organic carbon to the oceans. *Global Biogeochemical Cycles, 20*(GB1012). doi: 10.1029/2005GB002570

Doyle, T. W., Krauss, K. W., Conner, W. H., & From, A. S. (2010). Predicting the retreat and migration of tidal forests along the northern Gulf of Mexico under sea-level rise. *Forest Ecology and Management, 259*(4), 770–777. doi: 10.1016/j.foreco.2009.10.023

Esslinger, C. G., & Wilson, B. C. (2001). *North American Waterfowl Management Plan, Gulf Coast Joint Venture: Chenier Plain Initiative.* Albuquerque, NM: North American Waterfowl Management Plan.

Fisk, H. N. (1944). *Geological investigation of the Alluvial Valley of the Lower Mississippi River conducted for the Mississippi River Commission, Vicksburg, MS.*

Foret, D. J. (1997). *Accretion, sedimentation, and nutrient accumulation rates as influenced by manipulations in marsh hydrology in the Chenier plain, Louisiana* (Master's thesis), the University of Southwestern Louisiana.

Foret, D. J. (2001). *Nutrient limitation of tidal marshes on the Chenier plain, Louisiana.* (Doctoral dissertation). University of Louisina at Lafayette, University of Louisina at Lafayette.

Giri, C., Ochieng, E., Tieszen, L. L., Zhu, Z., Singh, A., Loveland, T., . . . Duke, N. (2011). Status and distribution of mangrove forests of the world using earth observation satellite data. *Global Ecology and Biogeography, 20*(1), 154–159. doi: 10.1111/j.1466-8238.2010.00584.x

Henry, K. M., & Twilley, R. R. (2013). Soil development in a coastal Louisiana wetland during a climate-induced vegetation shift from salt marsh to mangrove. *Journal of Coastal Research*. doi: 10.2112/jcoastres-d-12-00184.1

Intergovernmental Panel on Climate Change. (2013). *Climate Change 2013: The Physical Science Basis. Contribution of Working Group I to the Fifth Assessment Report of the Intergovernmental Panel on Climate Change*. [Stocker, T.F., D. Qin, G.-K. Plattner, M. Tignor, S.K. Allen, J. Boschung, A. Nauels, Y. Xia, V. Bex and P.M. Midgley (eds.)]. Cambridge University Press, Cambridge, United Kingdom and New York, NY, USA, 1535 pp.

Jennerjahn, T., & Ittekkot, V. (2002). Relevance of mangroves for the production and deposition of organic matter along tropical continental margins. *Naturwissenschaften, 89*(1), 23–30. doi: 10.1007/s00114-001-0283-x

Khan, M. N. I., Suwa, R., & Hagihara, A. (2007). Carbon and nitrogen pools in a mangrove stand of Kandelia obovata (S., L.) Yong: vertical distribution in the soil–vegetation system. *Wetlands Ecol Manage, 15,* 141–153. doi: 10.1007/s11273-006-9020-8

Kristensen, E., Bouillon, S., Dittmar, T., & Marchand, C. (2008). Organic carbon dynamics in mangrove ecosystems: A review. *Aquatic Botany, 89*(2), 201–219. doi: 10.1016/j.aquabot.2007.12.005

L test. (n.d.). Retrieved September 4, 2014, from http://www.lexjansen.com/nesug/nesug07/sa/sa22.pdf

Macintosh, D. J., & Ashton, E. C. (2002). *A review of mangrove biodiversity conservation and management.* Centre for Tropical Ecosystems Research, University of Aarhus, Denmark (pdf file).

McKee, K. L., Cahoon, D. R., & Feller, I. C. (2007). Caribbean mangroves adjust to rising sea level through biotic controls on change in soil elevation. *Global Ecology and Biogeography, 16*(5), 545–556. doi: 10.1111/j.1466-8238.2007.00317.x

McKee, K. L., & Rooth, J. E. (2008). Where temperate meets tropical: multi-factorial effects of elevated CO_2, nitrogen enrichment, and competition on a mangrove-salt marsh community. *Global Change Biology, 14*(5), 971–984. doi: 10.1111/j.1365-2486.2008.01547.x

Meriwether, J. R., Sharp, A. L., Zaunbrecher, K., Williams, M., Ledet, K., & Steyer, G. (n.d.). *Mapping the sediment deposition of Hurricane Rita's storm surge.*

Meriwether, J. R., Sheu, W.-J., Hardaway, C., & Beck, J. N. (1996). Coring sampler for chemical analyses of soft sediments. *Microchemical Journal, 53*(2), 201–206. doi: http://dx.doi.org/10.1006/mchj.1996.0029

Mississippi River Delta. (n.d.). Retrieved September 3, 2014, from http://www.nwf.org/wildlife/wild-places/mississippi-river-delta.aspx

Montgomery, D. C. (1991). *Design and analysis of experiments* (3rd ed.). New York, NY: Wiley.

Nellemann, C., Corcoran, E., Duarte, C. M., Valdés, L., De Young, C., Fonseca, L., & Grimsditch, G. (2009). *Blue carbon: A rapid response assessment*. United Nations Environment Programme, GRID-Arendal.

Osland, M. J., Day, R. H., Larriviere, J. C., & From, A. S. (2014). Aboveground Allometric Models for Freeze-Affected Black Mangroves (Avicennia germinans): Equations for a Climate Sensitive Mangrove-Marsh Ecotone. *PLoS One, 9*(6), e99604. doi: 10.1371/journal.pone.0099604.g001

Osland, M. J., Spivak, A. C., Nestlerode, J. A., Lessmann, J. M., Almario, A. E., Heitmuller, P. T., . . . Stagg, C. L. (2012). Ecosystem development after mangrove wetland creation: Plant-soil change across a 20-year chronosequence. *Ecosystems, 15*(5), 848–866. doi: 10.1007/s10021-012-9551-1

Owen , D. E. (2008). Geology of the Chenier Plain of Cameron Parish, southwestern Louisiana. In G. Moore (Ed.), Geological Society of America Field Guide 14, 2008 Joint Annual Meeting, Houston, Texas, 5–9 October 2008. 27–38. doi: 10.1130/2008.fld014(02)

Patterson, C. S. (1992). *Factors controlling the distribution of the black mangrove, Avicennia germinans L., in a Louisiana mangal/salt marsh community.* (Doctoral dissertation), Louisiana State University and Agricultural and Mechanical College, Louisiana State University and Agricultural and Mechanical College.

Penland, S., & Suter, J. R. (1989). The geomorphology of the Mississippi River chenier plain. *Marine Geology, 90*(4), 231–258. doi: http://dx.doi.org/10.1016/0025-3227(89)90127-8

Perry, C. L., & Mendelssohn, I. A. (2009). Ecosystem effects of expanding populations of avicennia germinans in a louisiana salt marsh. *Wetlands Ecology and Management, 29*(1), 396–406.

Pickens, C. N., & Hester, M. W. (2010). Temperature tolerance of early life history stages of black mangrove Avicennia germinans: Implications for range expansion. *Estuaries and Coasts, 34*(4), 824–830. doi: 10.1007/s12237-010-9358-2

Port Fourchon, Louisiana. (n.d.). In *Wikipedia, The Free Encyclopedia.* Retrieved September 12, 2014, from http://en.wikipedia.org/w/index.php?title=Port_Fourchon,_Louisiana&oldid=621065621

Röderstein, M., Hertel, D., & Leuschner, C. (2005). Above- and below-ground litter production in three tropical montane forests in southern Ecuador. *Journal of Tropical Ecology, 21*(5), 483–492. doi: 10.1017/S026646740500249X

Saenger, P., & Snedaker, S. C. (1993). Pantropieal trends in mangrove above-ground biomass and annual litterfall. *Oecologia, 96,* 293 299.

Spalding, M., Kainuma, M., & Collins, L. (2010). *World atlas of mangroves.* Earthan.

Suratman, M. N. (2008). Carbon sequestration potential of mangroves in Southeast Asia. In F. Bravo, V. LeMay, R. Jandl, & K. von Gadow (Eds.), *Managing forest ecosystems: The challenge of climate change*. Springer Science.

Tamura, T., and D.G. Jacobs. 1960. Structural implications in cesium sorption. Health Phys. 2:391-398

Thom, B. G. (1967). Mangrove Ecology and Deltaic Geomorphology: Tabasco, Mexico. *Journal of Ecology, 55*(2), 301-343.

Tomlinson, P. B. (1986). *The Botany of mangroves*. Cambridge, UK: Cambridge University Press.

Tran, B. Q. (2011). Effect of mangrove forest structures on wave attenuation in coastal Vietnam. *Oceanologia, 53*(3), 807–818. doi: 10.5697/oc.53-3.807

Twilley, R. T., Chen, R. I., & Hargis, T. (1992). Carbon sinks in mangroves and their implications to carbon budget of tropical coastal ecosystems. *Water, Air, and Soil Pollution, 64,* 265–288.

Visser, J. M., Vermillion, W. G., Evers, D. E., Linscombe, R. G., & Sasser, C. E. (2005). Nesting habitat requirements of the brown pelican and their management implications. *Journal of Coastal Research, 212*, e27–e35. doi: 10.2112/04-0176.1

Walther, G. R., Post, E., Convey, P., Menzel, A., Parmesan, C., Beebee, T. J. C., . . . Bairlein, F. (2002). Ecological responses to recent climate change. *Nature, 416,* 389–395.

Wang, Q., Li, Y., & Wang, Y. (2011). Optimizing the weight loss-on-ignition methodology to quantify organic and carbonate carbon of sediments from diverse sources. *Environmental Monitoring and Assessment, 174*(1-4), 241–257. doi: 10.1007/s10661-010-1454-z

Wells, S., Ravilious, C., & Corcoran, E. (2006). *In the front line: Shoreline protection and other ecosystem services from mangroves and coral reefs* (p. 33). Cambridge, UK: UNEP-WCMC.

Wetlands of Louisiana. (n.d.). In *Wikipedia, The Free Encyclopedia.* Retrieved September 3, 2014, from http://en.wikipedia.org/wiki/Wetlands_of_Louisiana

Yee, S. M. (2010). *REDD and BLUE Carbon Carbon Payments for Mangrove Conservation.* MAS Marine Biodiversity and Conservation Capstone Project.

Appendix A

Tall Avicennia

Short *Avicennia*

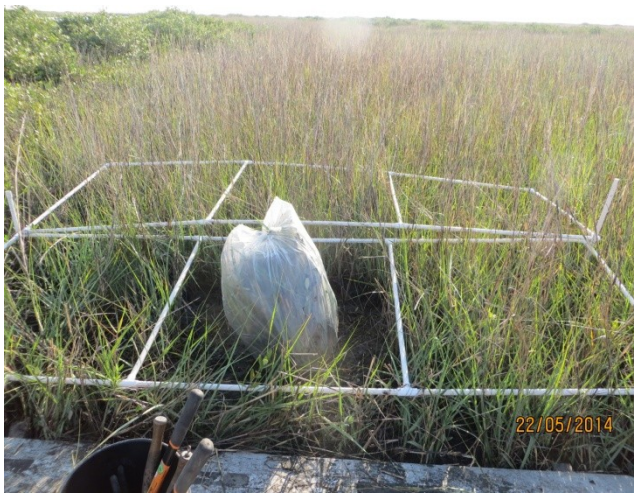

Spartina - Marsh

Mixed zone

Study site Mangrove and marsh ecotone

Extract soil core

Slice the core

Dry samples

Grinding the soil

Soil in the bottles

^{137}Cs analysis

Soil preparation 1

Soil preparation 2

Soil preparation 3

Soil preparation 4

Propagule classification

Pre-treat for fungus

Compare 3 size classes

Float time and size treatment 1

Float time and size treatment 2

Sunlight treatment

Heat treatment

Elevated CO_2 treatment

Elevation survey

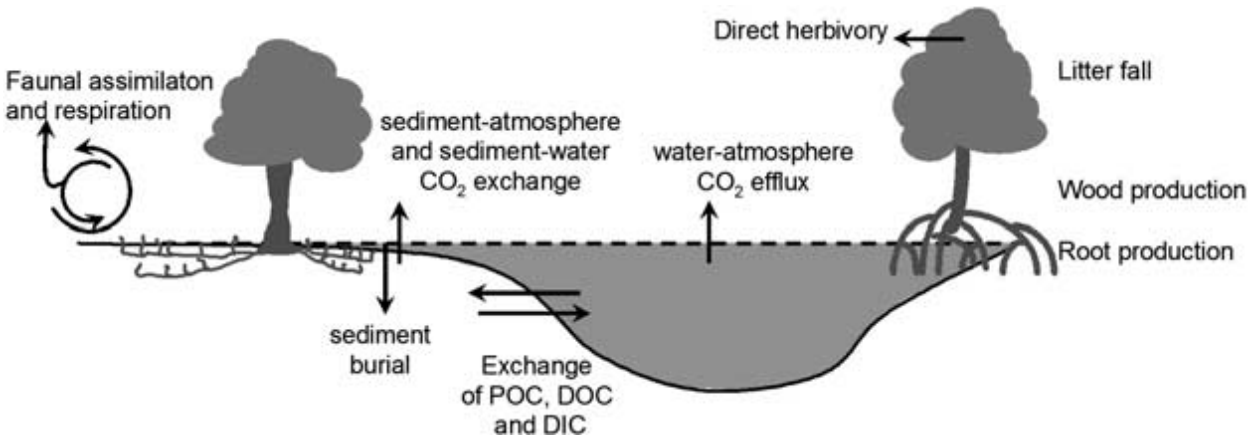

Figure A-1. Primary production (litter fall, wood, and root production) and various sink terms. (From Bouillon et al., 2008)

Table A-1

Regeneration Data from Floating Time and Size Treatment

Propagules	float_time	hrad_grow	size	nnodes	sum_nodes	root_day	lift_day	stand_day	TL_day
1	1	43	1	2	60	.	69	73	93
2	1	27	1	2	46	57	77	81	113
3	1	43	1	2	63	72	.	93	103
4	1	43	1	1	10	72	.	95	107
5	1	5	1	none	.	none	none	none	none
6	1	19	1	2	37	.	93	95	107
7	1	7	1	sick	.	69	sick	sick	sick
8	1	5	2	2	69	69	.	97	111
9	1	13	2	2	50	72	85	87	111
10	1	9	2	3	93	57	95	97	107
11	1	9	2	2	55	57	79	87	105
12	1	15	2	2	75	72	87	89	105
13	1	5	2	2	65	.	65	73	95
14	1	29	2	3	80	.	69	73	93
15	1	5	3	3	112	72	89	91	97
16	1	7	3	4	116	.	61	63	83
17	1	23	3	3	83	69	85	91	105
18	1	17	3	3	105	72	87	91	103
19	1	5	3	3	106	69	87	91	105
20	1	43	3	die	.	die			
21	1	43	3	sick	.				
22	1	5	1	2	63	.	69	77	93
23	1	43	1	2	51	72	87	91	105
24	1	7	1	2	42	57	59	63	79

25	1	5	1	3	82	.	61	63	81
26	1	5	1	none	.	69			
27	1	5	1	0	0	72		130	
28	1	37	1	1	20	72	113	117	130
29	1	7	2	3	59	57		97	109
30	1	5	2	3	89	.	61	63	93
31	1	41	2	none	.				
32	1	9	2	3	84	.	57	59	80
33	1	7	2	2	42	69	75	97	115
34	1	5	2	2	62	.	67	73	109
35	1	5	2	1	15	72	79	85	105
36	1	43	3	2	55	72	99	113	119
37	1	5	3	0	0	133			
38	1	27	3	2	78	.	69	73	99
39	1	5	3	2	75	72	91	95	109
40	1	9	3	3	73	.	65	93	103
41	1	5	3	2	78	72	99	103	107
42	1	15	3	4	57	.	63	83	91
43	2	31	1	0	0	72	125	130	
44	2	27	1	sick	.				
45	2	25	1	3	75	.	65	67	87
46	2	7	1	none	.				
47	2	7	1	none	.				
48	2	13	1	3	92	.	57	59	74
49	2	43	1	none	.				
50	2	7	2	3	138	57	63	65	87
51	2	7	2	3	79	.	59	63	81
52	2	7	2	1	15	72	117	119	133
53	2	7	2	2	38	72	117	119	123
54	2	9	2	3	104	69	.	81	104
55	2	7	2	2	100	72	101	103	115
56	2	7	2	3	104	72	87	91	103
57	2	17	3	3	169		69	79	89
58	2	35	3	4	129	72	81	83	101
59	2	43	3	3	89	72		97	107
60	2	7	3	1	50	115		117	130
61	2	13	3	4	172		57	59	77
62	2	21	3	3	80	72	77	81	101
63	2	15	3	4	174	72		97	101
64	2	43	1	2	67		63	65	87
65	2	43	1	2	98	72	87	89	105
66	2	7	1	1	55	72	99	101	116
67	2	43	1	2	47	72		97	111
68	2	35	1	2	47		69	75	101
69	2	17	1	2	58		61	63	93
70	2	27	1	2	53		69	75	97
71	2	7	2	3	103	57	59	61	77
72	2	7	2	3	79	57	75	77	97

73	2	27	2	3	87	57	87	91	99
74	2	7	2	3	86	69	87	91	101
75	2	35	2	3	112		67	69	87
76	2	7	2	1	25	72	117	119	130
77	2	35	2	3	109			95	105
78	2	35	3	3	131	69	77	81	93
79	2	21	3	3	121			95	105
80	2	7	3	2	117	72	77	81	95
81	2	35	3	none	.				
82	2	17	3	2	80	72		97	107
83	2	19	3	3	104	72	87	91	105
84	2	7	3	4	140	57	61	63	81
85	3	21	1	0	0				
86	3	15	1	2	115	72	77	79	101
87	3	15	1	sick	.				
88	3	15	1	2	55	72	91	93	107
89	3	15	1	3	101	72	77	81	97
90	3	15	1	3	75	72	79	81	97
91	3	27	1	1	20	72	105	107	130
92	3	15	2	3	118	72	95	97	109
93	3	15	2	3	111		61	63	91
94	3	15	2	2	75	72	91	93	111
95	3	43	2	3	93	72	93	95	109
96	3	17	2	2	63	72	83	85	107
97	3	15	2	3	104			61	83
98	3	35	2	1	45	72		113	123
99	3	15	3	3	111	72		87	97
100	3	15	3	2	22	72	117	119	130
101	3	17	3	2	65	72	97	99	113
102	3	27	3	0	0	138			
103	3	21	3	0	0	138			
104	3	35	3	none	.				
105	3	43	3	3	110	72	83	87	103
106	3	25	1	1	5	72	125	130	138
107	3	15	1	none	.				
108	3	21	1	none	.				
109	3	15	1	2	63	72	97	99	111
110	3	15	1	3	83	72		91	104
111	3	43	1	2	55	72		97	111
112	3	15	1	2	49	72		97	117
113	3	23	2	3	102	72	85	87	101
114	3	29	2	3	111	72	85	87	103
115	3	21	2	1	25	72	111	117	130
116	3	27	2	3	74		69	75	99
117	3	15	2	none	.				
118	3	15	2	2	71	72	99	103	117
119	3	15	2	2	92	72	81	83	101
120	3	21	3	3	106	72	97	99	111

121	3	17	3	3	137	72	81	83	97
122	3	15	3	3	159	72	87	91	101
123	3	15	3	0	0				
124	3	17	3	3	108	72	85	87	101
125	3	19	3	3	137	72	77	81	95
126	3	15	3	3	125	72	77	81	95
127	4	23	1	0	0				
128	4	43	1	2	46	72	111	113	122
129	4	35	1	3	71	72	85	87	101
130	4	21	1	0	0	72		123	138
131	4	21	1	0	0	72	125	130	
132	4	21	1	2	73	72		87	96
133	4	21	1	3	51	72	77	81	97
134	4	21	2	none	.				
135	4	21	2	3	95		57	59	79
136	4	23	2	3	96	72		81	103
137	4	23	2	2	85	72		105	113
138	4	21	2	2	98	72	77	81	105
139	4	35	2	2	85		57	61	83
140	4	21	2	2	70	72	93	93	103
141	4	21	3	4	145		63	65	85
142	4	21	3	4	113		61	65	81
143	4	21	3	3	133		59	63	83
144	4	21	3	3	144		59	61	79
145	4	21	3	3	141			65	81
146	4	21	3	3	128	72		91	101
147	4	21	3	3	130	72	77	79	93
148	4	35	1	2	54	72	95	97	111
149	4	23	1	2	75		65	67	89
150	4	43	1	0	0				
151	4	23	1	2	63	72		81	99
152	4	21	1	1	35	72	111	113	123
153	4	21	1	2	56	72	91	93	103
154	4	23	1	2	70	72		97	111
155	4	21	2	3	77		69	77	105
156	4	21	2	3	114		69	73	91
157	4	21	2	2	97	72	77	79	103
158	4	23	2	2	42	72	105	109	123
159	4	21	2	2	64	72		81	111
160	4	21	2	3	95	72	85	87	105
161	4	35	2	3	83	72	81	85	103
162	4	32	3	4	152	72	77	79	95
163	4	32	3	2	80	72		97	117
164	4	43	3	1	25			119	132
165	4	23	3	3	110			67	89
166	4	21	3	3	135	72		81	93
167	4	23	3	5	150		63	67	81
168	4	43	3	1	35	72	120	123	130

169	5	27	1	2	67			57	75
170	5	27	1	2	96	72	83	85	97
171	5	27	1	2	50	72		99	107
172	5	27	1	3	86	72		97	105
173	5	27	1	2	43	72		79	97
174	5	27	1	2	70	72	85	87	97
175	5	27	1	2	41	72	113	116	126
176	5	27	2	2	85			61	77
177	5	27	2	0	0				
178	5	27	2	2	63	72		95	117
179	5	27	2	2	85		57	61	81
180	5	27	2	2	85	72	77	79	95
181	5	27	2	2	88		61	63	87
182	5	27	2	die	.				
183	5	27	3	0	0	72	123	130	
184	5	27	3	0	0	119	125	130	
185	5	27	3	3	145		67	69	87
186	5	27	3	3	122	72	99	105	113
187	5	27	3	3	130			57	75
188	5	27	3	3	142			63	81
189	5	43	3	0	0				
190	5	27	1	2	75	72	87	91	101
191	5	27	1	none	.				
192	5	33	1	3	77	72		81	96
193	5	43	1	1	25	72	111	113	124
194	5	27	1	2	68	72		87	101
195	5	43	1	2	90	72		77	93
196	5	35	1	die	.				
197	5	27	2	2	85		57	61	77
198	5	27	2	4	155		61	63	85
199	5	27	2	3	135		61	63	85
200	5	43	2	2	70	72		77	101
201	5	27	2	0	0				
202	5	27	2	2	75		61	63	97
203	5	27	2	3	85		61	63	87
204	5	27	3	3	112		59	61	79
205	5	27	3	3	143			61	83
206	5	27	3	3	103	72		95	107
207	5	27	3	3	147			63	85
208	5	27	3	4	162			57	68
209	5	27	3	3	102			57	74
210	5	27	3	3	137		69	73	91
211	6	35	1	0	0				
212	6	43	1	2	77	72		87	99
213	6	35	1	2	75			63	85
214	6	35	1	2	85		59	61	81
215	6	43	1	1	15	72	115	118	128
216	6	43	1	0	0				

217	6	35	1	3	87		63	67	83
218	6	35	2	2	90	72		75	95
219	6	37	2	3	92	72	75	79	96
220	6	35	2	2	64			111	119
221	6	35	2	1	15	72	113	115	131
222	6	35	2	3	53	72	81	87	115
223	6	35	2	2	75			63	87
224	6	35	2	3	110	72		81	101
225	6	37	3	0	0	130	138		
226	6	35	3	4	150			63	85
227	6	35	3	0	0	72	130		
228	6	35	3	none	.				
229	6	35	3	3	130	72	99	101	111
230	6	35	3	3	143		71	75	87
231	6	35	3	3	144	72		97	103
232	6	35	1	2	61		61	63	77
233	6	35	1	2	67			63	77
234	6	35	1	2	80			75	93
235	6	43	1	2	76	72	107	109	116
236	6	43	1	2	37	72	77	81	95
237	6	43	1	1	5	72	125	130	138
238	6	43	1	2	90	72	100	102	110
239	6	35	2	2	102	72	85	87	105
240	6	35	2	3	100	72		75	101
241	6	35	2	3	90		57	61	81
242	6	39	2	0	0	133			
243	6	43	2	2	80	72		75	103
244	6	43	2	2	88	72	81	83	97
245	6	35	2	2	91		59	61	82
246	6	35	3	3	31	72	111	113	121
247	6	35	3	3	122			95	105
248	6	35	3	3	130	72	99	101	107
249	6	35	3	3	172	69	77	79	96
250	6	41	3	none	.				
251	6	43	3	sick	.				
252	6	43	3	3	105	72	97	99	109
253	7	41	1	2	67		69	71	95
254	7	41	1	2	65		59	61	81
255	7	41	1	none	.				
256	7	41	1	die	.				
257	7	41	1	2	73			67	93
258	7	41	1	2	80	72		83	85
259	7	41	1	2	50	72		91	104
260	7	41	2	sick	.				
261	7	41	2	3	95		67	69	91
262	7	41	2	3	110	72		81	96
263	7	41	2	2	67			87	105
264	7	41	2	0	0				

265	7	41	2	die	.	die			
266	7	41	2	2	85	72	89	91	103
267	7	43	3	3	99	72		87	99
268	7	41	3	3	122	72	87	91	99
269	7	41	3	sick	.				
270	7	41	3	3	122	72		92	102
271	7	41	3	3	131		65	69	82
272	7	41	3	3	95	72	83	85	97
273	7	41	3	4	139		63	67	82
274	7	41	1	2	49	72	103	105	115
275	7	41	1	2	37		59	61	75
276	7	43	1	2	54	72		95	113
277	7	41	1	2	71	72	81	83	97
278	7	41	1	2	82			63	87
279	7	41	1	sick	.				
280	7	41	1	2	79	72		91	105
281	7	41	2	3	91	72		94	111
282	7	41	2	3	78	72	89	91	111
283	7	41	2	sick	.				
284	7	41	2	3	109	72	89	91	101
285	7	41	2	0	0	72		125	138
286	7	41	2	3	113			91	101
287	7	41	2	0	0	72	123	138	
288	7	41	3	3	119		63	67	87
289	7	41	3	3	105	72		93	95
290	7	41	3	3	93	72	79	81	97
291	7	43	3	none	.				
292	7	41	3	2	89	72	93	95	103
293	7	41	3	3	114	72	79	81	96
294	7	41	3	3	106	72	95	97	109
295	8	43	1	2	61			67	87
296	8	43	1	2	68	72	87	89	103
297	8	43	1	2	64			61	92
298	8	43	1	2	68		61	63	87
299	8	43	1	2	87	72	75	77	87
300	8	43	1	2	70	72	75	77	95
301	8	43	1	sick	.				
302	8	43	2	2	96	72		75	97
303	8	43	2	2	82	72		77	97
304	8	43	2	2	73		63	67	93
305	8	43	2	2	80	72		75	99
306	8	43	2	2	66			63	87
307	8	43	2	3	95			63	85
308	8	43	2	3	114	72		87	103
309	8	43	3	3	124	72	81	83	95
310	8	43	3	2	36	72		113	123
311	8	43	3	2	93	72	93	95	105
312	8	43	3	3	101	72	77	81	105

313	8	43	3	4	128		69	73	91
314	8	43	3	3	118	72		97	105
315	8	43	3	3	131	72		95	103
316	8	43	1	2	40			63	93
317	8	43	1	2	48	72	77	79	95
318	8	43	1	2	50		69	73	95
319	8	43	1	2	61	72		109	116
320	8	43	1	2	70	72	81	83	97
321	8	43	1	2	75		69	73	81
322	8	43	1	sick	.				
323	8	43	2	2	90	72		81	105
324	8	43	2	3	101		59	61	81
325	8	43	2	2	93		63	67	93
326	8	43	2	2	104	72		87	105
327	8	43	2	2	80	72	99	103	115
328	8	43	2	3	96		69	73	99
329	8	43	2	3	105	72		95	105
330	8	43	3	0	0				
331	8	43	3	0	0				
332	8	43	3	2	72	72		83	97
333	8	43	3	2	100	72	95	97	107
334	8	43	3	die	.				
335	8	43	3	sick	.				
336	8	43	3	3	122	72	85	87	95
337	9	43	1	2	74	72		75	93
338	9	43	1	0	0	69			
339	9	43	1	2	58	72	75	79	93
340	9	43	1	2	66	72		75	93
341	9	43	1	2	50			105	117
342	9	43	1	2	45	72	75	77	96
343	9	43	1	2	71		67	69	85
344	9	43	2	2	61		71	73	97
345	9	43	2	3	102		69	73	93
346	9	43	2	2	75		69	73	95
347	9	43	2	2	97	72		87	103
348	9	43	2	2	70	72		87	104
349	9	43	2	2	68	72	79	81	97
350	9	43	2	2	62		71	75	93
351	9	43	3	2	87	72	73	75	91
352	9	43	3	3	82		69	73	87
353	9	43	3	3	94	72	77	79	93
354	9	43	3	3	91			81	95
355	9	43	3	none	.				
356	9	43	3	3	86	72	75	77	93
357	9	43	3	3	107	72	81	83	95
358	9	43	1	2	67			81	97
359	9	43	1	none	.				
360	9	43	1	0	0	72		116	130

361	9	43	1	2	44	72	81	83	103
362	9	43	1	1	22	72	105	111	125
363	9	43	1	0	0	72	138		
364	9	43	1	2	50	72	79	81	93
365	9	43	2	3	105		69	73	87
366	9	43	2	2	64	72	77	79	97
367	9	43	2	3	85	72		97	111
368	9	43	2	3	63	72		81	97
369	9	43	2	0	0	72	133		
370	9	43	2	2	50	72	111	113	125
371	9	43	2	0	0				
372	9	43	3	2	57	72	75	77	97
373	9	43	3	3	118		71	73	93
374	9	43	3	3	105	72	75	77	87
375	9	43	3	3	104	72	79	81	95
376	9	43	3	2	105	72	97	99	111
377	9	43	3	3	76	72		83	96
378	9	43	3	3	126	72	89	92	99
379	10	43	1	2	44	72	81	83	101
380	10	43	1	2	72	72	91	93	107
381	10	43	1	2	68	72	83	85	97
382	10	43	1	2	52	72	89	91	105
383	10	43	1	2	85	72		87	101
384	10	43	1	2	67	72	87	89	103
385	10	43	1	none	.				
386	10	43	2	3	82	72		87	105
387	10	43	2	3	101	72	89	91	99
388	10	43	2	3	70	72		95	105
389	10	43	2	3	99	72	101	103	109
390	10	43	2	2	67	72	85	87	103
391	10	43	2	2	65	72	87	91	97
392	10	43	2	2	50	72	109	111	125
393	10	43	3	3	107	72	101	103	111
394	10	43	3	2	97	72		87	103
395	10	43	3	3	110	72	91	93	101
396	10	43	3	3	82	72	89	91	105
397	10	43	3	3	93	72		89	101
398	10	43	3	3	111	72		87	97
399	10	43	3	3	118	72		87	97
400	10	43	1	3	65	72		105	117
401	10	43	1	none	.				
402	10	43	1	2	72	72		85	104
403	10	43	1	3	87	72		81	97
404	10	43	1	none	.				
405	10	43	1	2	52	72	81	85	95
406	10	43	1	2	47	72	85	87	111
407	10	43	2	3	114	72		81	97
408	10	43	2	2	98	72	89	91	111

409	10	43	2	3	86	72	93	95	105
410	10	43	2	2	75	72		87	99
411	10	43	2	2	62	72	109	111	121
412	10	43	2	0	0	125			
413	10	43	2	none	.				
414	10	43	3	2	70	72		81	97
415	10	43	3	3	105	72		89	105
416	10	43	3	3	95	72	85	89	97
417	10	43	3	3	102	72	85	87	97
418	10	43	3	3	127	72		87	103
419	10	43	3	3	85	72		87	99
420	10	43	3	3	85	72	97	99	116
421	11	43	1	1	10	72		117	133
422	11	43	1	3	78	72	91	93	97
423	11	43	1	2	62	72		87	103
424	11	43	1	2	85	72		93	101
425	11	43	1	2	67	72		101	111
426	11	43	1	1	35	72		119	130
427	11	43	1	none	.				
428	11	43	2	0	0				
429	11	43	2	2	77	72		96	111
430	11	43	2	2	86	72		93	105
431	11	43	2	2	90	72	89	91	105
432	11	43	2	2	83	72		93	105
433	11	43	2	3	78	72	89	91	105
434	11	43	2	2	87	72		107	111
435	11	43	3	3	67	72		97	105
436	11	43	3	2	80	72		97	107
437	11	43	3	2	95	72	89	91	103
438	11	43	3	3	125	72		93	105
439	11	43	3	3	85	72		97	105
440	11	43	3	3	127	72		93	105
441	11	43	3	2	90	72	97	99	111
442	11	43	1	none	.				
443	11	43	1	2	87	72		87	101
444	11	43	1	2	66	72		109	111
445	11	43	1	2	72	72	103	105	113
446	11	43	1	0	0				
447	11	43	1	none	.				
448	11	43	1	0	0				
449	11	43	2	die	.	121			
450	11	43	2	3	95	72	93	95	105
451	11	43	2	3	83	72		93	101
452	11	43	2	2	70	72		87	105
453	11	43	2	0	0				
454	11	43	2	3	72	72	105	109	115
455	11	43	2	2	42	72		99	125
456	11	43	3	3	99	72		87	101

457	11	43	3	2	91	72	93	95	103
458	11	43	3	3	103	72		97	111
459	11	43	3	2	97	72		87	101
460	11	43	3	2	98	72		105	117
461	11	43	3	1	45	72		111	125
462	11	43	3	2	75	72		97	109

Survival rate of floating time and size class from Microsoft Excel

Anova: Two-Factor Without Replication

SUMMARY	*Count*	*Sum*	*Average*	*Variance*
Row 1	3	35	11.66667	1.333333
Row 2	3	37	12.33333	4.333333
Row 3	3	33	11	3
Row 4	3	39	13	1
Row 5	3	36	12	1
Row 6	3	36	12	1
Row 7	3	33	11	1
Row 8	3	36	12	4
Row 9	3	38	12.66667	0.333333
Row 10	3	37	12.33333	2.333333
Row 11	3	34	11.33333	6.333333
Column 1	11	122	11.09091	1.090909
Column 2	11	137	12.45455	1.672727
Column 3	11	135	12.27273	2.418182

ANOVA

Source of Variation	*SS*	*df*	*MS*	*F*	*P-value*	*F crit*
Rows	12.54545	10	1.254545	0.638889	0.764332	2.347878
Columns	12.06061	2	6.030303	3.070988	0.068694	3.492828
Error	39.27273	20	1.963636			
Total	63.87879	32				

Results from SAS analysis (some important statistical points)

The GLM Procedure

Class Level Information

Class	Levels	Values
size	3	1 2 3
float_time	11	1 2 3 4 5 6 7 8 9 10 11

Number of Observations Read	394
Number of Observations Used	357

The GLM Procedure

Dependent Variable: rhrad_grow Rank for Variable hrad_grow

Source	DF	Sum of Squares	Mean Square	F Value	Pr > F
Model	32	3421953.518	106936.047	35.24	<.0001
Error	324	983297.756	3034.870		
Corrected Total	356	4405251.275			

R-Square	Coeff Var	Root MSE	rhrad_grow Mean
0.776790	27.86583	55.08965	197.6961

Source	DF	Type I SS	Mean Square	F Value	Pr > F
size	2	53046.800	26523.400	8.74	0.0002
float_time	10	3227600.264	322760.026	106.35	<.0001
size*float_time	20	141306.454	7065.323	2.33	0.0012

Source	DF	Type III SS	Mean Square	F Value	Pr > F
size	2	59570.343	29785.171	9.81	<.0001
float_time	10	3119960.435	311996.043	102.80	<.0001
size*float_time	20	141306.454	7065.323	2.33	0.0012

The GLM Procedure

Dependent Variable: rnnodes Rank for Variable nnodes

Source	DF	Sum of Squares	Mean Square	F Value	Pr > F
Model	32	1098346.107	34323.316	4.17	<.0001
Error	324	2668306.666	8235.514		
Corrected Total	356	3766652.773			

R-Square	Coeff Var	Root MSE	rnnodes Mean
0.291597	45.77783	90.74973	198.2395

Source	DF	Type I SS	Mean Square	F Value	Pr > F
size	2	919293.6778	459646.8389	55.81	<.0001
float_time	10	95138.7886	9513.8789	1.16	0.3206
size*float_time	20	83913.6405	4195.6820	0.51	0.9622

Source	DF	Type III SS	Mean Square	F Value	Pr > F
size	2	910411.5688	455205.7844	55.27	<.0001
float_time	10	87523.6737	8752.3674	1.06	0.3907
size*float_time	20	83913.6405	4195.6820	0.51	0.9622

The GLM Procedure

Dependent Variable: rsum_nodes Rank for Variable sum_nodes

Source	DF	Sum of Squares	Mean Square	F Value	Pr > F
Model	32	1881999.164	58812.474	7.38	<.0001
Error	324	2581975.942	7969.062		
Corrected Total	356	4463975.106			

R-Square	Coeff Var	Root MSE	rsum_nodes Mean
0.421597	45.34708	89.26960	196.8585

Source	DF	Type I SS	Mean Square	F Value	Pr > F
size	2	1552114.106	776057.053	97.38	<.0001
float_time	10	226929.548	22692.955	2.85	0.0021
size*float_time	20	102955.511	5147.776	0.65	0.8766

Source	DF	Type III SS	Mean Square	F Value	Pr > F
size	2	1517656.929	758828.464	95.22	<.0001
float_time	10	213637.370	21363.737	2.68	0.0036
size*float_time	20	102955.511	5147.776	0.65	0.8766

The GLM Procedure

Dependent Variable: rroot_day Rank for Variable root_day

Source	DF	Sum of Squares	Mean Square	F Value	Pr > F
Model	32	582719.927	18209.998	3.41	<.0001
Error	324	1729832.266	5338.988		
Corrected Total	356	2312552.193			

R-Square	Coeff Var	Root MSE	rroot_day Mean
0.251981	40.56419	73.06838	180.1303

Source	DF	Type I SS	Mean Square	F Value	Pr > F
size	2	49539.1921	24769.5960	4.64	0.0103
float_time	10	333095.2378	33309.5238	6.24	<.0001
size*float_time	20	200085.4974	10004.2749	1.87	0.0137

Source	DF	Type III SS	Mean Square	F Value	Pr > F
size	2	37734.6074	18867.3037	3.53	0.0303
float_time	10	336193.2776	33619.3278	6.30	<.0001
size*float_time	20	200085.4974	10004.2749	1.87	0.0137

The GLM Procedure

Dependent Variable: rlift_day Rank for Variable lift_day

Source	DF	Sum of Squares	Mean Square	F Value	Pr > F
Model	32	803136.603	25098.019	2.73	<.0001
Error	324	2983763.397	9209.146		
Corrected Total	356	3786900.000			

R-Square	Coeff Var	Root MSE	rlift_day Mean
0.212083	53.61134	95.96430	179.0000

Source	DF	Type I SS	Mean Square	F Value	Pr > F
size	2	37346.8084	18673.4042	2.03	0.1333
float_time	10	374028.6512	37402.8651	4.06	<.0001
size*float_time	20	391761.1434	19588.0572	2.13	0.0037

Source	DF	Type III SS	Mean Square	F Value	Pr > F
size	2	34084.6369	17042.3185	1.85	0.1588
float_time	10	369017.9674	36901.7967	4.01	<.0001
size*float_time	20	391761.1434	19588.0572	2.13	0.0037

The GLM Procedure

Dependent Variable: rstand_day Rank for Variable stand_day

Source	DF	Sum of Squares	Mean Square	F Value	Pr > F
Model	32	923622.883	28863.215	2.87	<.0001
Error	324	3258080.449	10055.804		
Corrected Total	356	4181703.332			

R-Square	Coeff Var	Root MSE	rstand_day Mean
0.220872	49.17138	100.2786	203.9370

Source	DF	Type I SS	Mean Square	F Value	Pr > F
size	2	51552.4426	25776.2213	2.56	0.0786
float_time	10	462930.0751	46293.0075	4.60	<.0001
size*float_time	20	409140.3648	20457.0182	2.03	0.0060

Source	DF	Type III SS	Mean Square	F Value	Pr > F
size	2	48034.1489	24017.0744	2.39	0.0934
float_time	10	454212.0878	45421.2088	4.52	<.0001
size*float_time	20	409140.3648	20457.0182	2.03	0.0060

The GLM Procedure

Dependent Variable: rTL_day Rank for Variable TL_day

Source	DF	Sum of Squares	Mean Square	F Value	Pr > F
Model	32	764737.723	23898.054	2.23	0.0003
Error	324	3473505.203	10720.695		
Corrected Total	356	4238242.926			

R-Square	Coeff Var	Root MSE	rTL_day Mean
0.180437	50.83311	103.5408	203.6877

Source	DF	Type I SS	Mean Square	F Value	Pr > F
size	2	27788.5699	13894.2850	1.30	0.2750
float_time	10	435055.4917	43505.5492	4.06	<.0001
size*float_time	20	301893.6612	15094.6831	1.41	0.1156

Source	DF	Type III SS	Mean Square	F Value	Pr > F
size	2	20321.8840	10160.9420	0.95	0.3887
float_time	10	407182.4394	40718.2439	3.80	<.0001
size*float_time	20	301893.6612	15094.6831	1.41	0.1156

The GLM Procedure
Multivariate Analysis of Variance

Characteristic Roots and Vectors of: E Inverse * H, where
H = Type III SSCP Matrix for size
E = Error SSCP Matrix

		Characteristic Vector V'EV=1						
Characteristic Root	Percent	rhrad_grow	rnnodes	rsum_nodes	rroot_day	rlift_day	rstand_day	rTL_day
0.87662033	79.19	-0.00020043	0.00018958	0.00059778	-0.00006273	-0.00011489	0.00027437	0.00022710
0.23040060	20.81	0.00032379	0.00000703	-0.00007919	0.00028069	-0.00013282	0.00128894	-0.00129456
0.00000000	0.00	-0.00003114	-0.00012304	0.00007994	-0.00016436	-0.00150573	0.00149035	0.00010658
0.00000000	0.00	0.00001027	0.00004384	-0.00004381	-0.00075873	0.00081072	-0.00001391	0.00001675
0.00000000	0.00	-0.00022607	0.00014839	-0.00010176	0.00071297	-0.00000566	-0.00031318	0.00037689
0.00000000	0.00	0.00092638	0.00004630	0.00015762	-0.00002141	-0.00000771	-0.00042622	0.00051292
0.00000000	0.00	-0.00000830	-0.00079261	0.00061013	0.00000101	0.00000036	0.00002010	-0.00002419

MANOVA Test Criteria and F Approximations for the Hypothesis of No Overall size Effect
H = Type III SSCP Matrix for size
E = Error SSCP Matrix

S=2 M=2 N=158

Statistic	Value	F Value	Num DF	Den DF	Pr > F
Wilks' Lambda	0.43308890	23.60	14	636	<.0001
Pillai's Trace	0.65438374	22.16	14	638	<.0001
Hotelling-Lawley Trace	1.10702093	25.09	14	505.45	<.0001
Roy's Greatest Root	0.87662033	39.95	7	319	<.0001

NOTE: F Statistic for Roy's Greatest Root is an upper bound.

NOTE: F Statistic for Wilks' Lambda is exact.

The GLM Procedure
Multivariate Analysis of Variance

Characteristic Roots and Vectors of: E Inverse * H, where
H = Type III SSCP Matrix for float_time
E = Error SSCP Matrix

Characteristic Root	Percent	Characteristic Vector V'EV=1						
		rhrad_grow	rnnodes	rsum_nodes	rroot_day	rlift_day	rstand_day	rTL_day
3.36893487	86.60	0.00100284	-0.00004551	0.00001643	0.00013031	-0.00003760	0.00009907	-0.00023147
0.22221030	5.71	-0.00005358	0.00016082	0.00041526	0.00024595	0.00025563	-0.00001067	0.00025832
0.14743021	3.79	0.00009278	-0.00016976	0.00014589	-0.00060634	-0.00091597	0.00135462	0.00002599
0.09118603	2.34	-0.00000350	-0.00057916	0.00076255	-0.00013670	-0.00028063	0.00006898	0.00011106
0.03580785	0.92	0.00015806	0.00032822	0.00002443	-0.00079493	0.00093209	-0.00047432	0.00003560
0.02074072	0.53	0.00011501	0.00003580	0.00005753	-0.00012231	0.00008065	-0.00133939	0.00140808
0.00374664	0.10	-0.00000780	0.00045195	-0.00000021	0.00028900	-0.00104672	0.00060787	0.00016590

MANOVA Test Criteria and F Approximations for the Hypothesis of No Overall float_time Effect
H = Type III SSCP Matrix for float_time
E = Error SSCP Matrix

S=7 M=1 N=158

Statistic	Value	F Value	Num DF	Den DF	Pr > F
Wilks' Lambda	0.14094013	10.62	70	1861.1	<.0001
Pillai's Trace	1.22359666	6.86	70	2268	<.0001
Hotelling-Lawley Trace	3.89005662	17.59	70	1248.2	<.0001
Roy's Greatest Root	3.36893487	109.15	10	324	<.0001

NOTE: F Statistic for Roy's Greatest Root is an upper bound.

The GLM Procedure
Multivariate Analysis of Variance

Characteristic Roots and Vectors of: E Inverse * H, where
H = Type III SSCP Matrix for size*float_time
E = Error SSCP Matrix

Characteristic Root	Percent	Characteristic Vector V'EV=1						
		rhrad_grow	rnnodes	rsum_nodes	rroot_day	rlift_day	rstand_day	rTL_day
0.24613830	37.19	-0.00053519	0.00031375	-0.00011025	-0.00000345	0.00035679	0.00060273	-0.00048363
0.14366001	21.70	0.00074625	-0.00001413	-0.00001577	-0.00046708	0.00056268	0.00041615	-0.00071112
0.12086468	18.26	0.00031386	0.00012196	-0.00000552	0.00095187	0.00004301	-0.00022145	-0.00021959
0.07091326	10.71	0.00028569	0.00006802	0.00027391	-0.00017277	-0.00029219	-0.00013725	0.00098780
0.04291323	6.48	0.00000145	-0.00002977	0.00056625	-0.00002001	-0.00092875	0.00114644	-0.00022636
0.02718789	4.11	-0.00003860	0.00035147	0.00013438	-0.00019137	0.00115415	-0.00149236	0.00057414
0.01021957	1.54	-0.00017468	-0.00068036	0.00059432	-0.00005563	0.00047924	-0.00030384	-0.00001936

MANOVA Test Criteria and F Approximations for the Hypothesis of No Overall size*float_time Effect
H = Type III SSCP Matrix for size*float_time
E = Error SSCP Matrix

S=7 M=6 N=158

Statistic	Value	F Value	Num DF	Den DF	Pr > F
Wilks' Lambda	0.54015139	1.47	140	2123.3	0.0004
Pillai's Trace	0.57491623	1.45	140	2268	0.0006
Hotelling-Lawley Trace	0.66189693	1.50	140	1576.2	0.0003
Roy's Greatest Root	0.24613830	3.99	20	324	<.0001

NOTE: F Statistic for Roy's Greatest Root is an upper bound.

Elevated CO_2 regeneration results

Obs	Elevco	hdradgrow	Liftday	Standday	TLday
1	a	39	79	85	91
2	a	39	71	75	85
3	a	7	65	71	85
4	a	39	63	69	78
5	a	39	54	64	75
6	a	39	72	78	89
7	a	39	57	64	73
8	a	39	58	64	78
9	a	9	48	54	71
10	a	21	39	43	66
11	a	21	66	69	78
12	a	31	41	45	69
13	a	8	54	64	75
14	a	7	54	59	73
15	a	7	71	75	82
16	a	27	78	80	85
17	a	29	63	69	75
18	a	39	63	69	85
19	a	21	64	66	78
20	a	39	63	69	73

Obs	Elevco	hdradgrow	Liftday	Standday	TLday
21	a	7	.	.	.
22	a	39	64	69	75
23	a	39	59	61	75
24	a	39	63	69	78
25	b	39	48	54	73
26	b	7	45	59	78
27	b	39	73	78	82
28	b	39	33	37	54
29	b	39	51	61	78
30	b	9	48	54	71
31	b	27	33	37	61
32	b	39	85	91	105
33	b	7	51	59	78
34	b	39	64	66	75
35	b	7	51	64	80
36	b	27	63	69	80
37	b	7	69	71	78
38	b	21	65	71	85
39	b	7	63	69	78
40	b	9	69	71	85
41	b	39	78	80	85
42	b	9	58	64	71
43	b	39	63	69	78
44	b	7	64	66	75
45	b	13	66	69	78
46	b	13	27	33	69
47	b	27	27	33	69
48	b	39	58	64	78

Dependent Variable: hdradgrow

Source	DF	Sum of Squares	Mean Square	F Value	Pr > F
Model	1	275.520833	275.520833	1.44	0.2365
Error	46	8810.958333	191.542572		
Corrected Total	47	9086.479167			

Dependent Variable: Liftday

Source	DF	Sum of Squares	Mean Square	F Value	Pr > F
Model	1	285.168054	285.168054	1.66	0.2038
Error	45	7717.768116	171.505958		
Corrected Total	46	8002.936170			

Dependent Variable: Standday

Source	DF	Sum of Squares	Mean Square	F Value	Pr > F
Model	1	240.325663	240.325663	1.52	0.2245
Error	45	7130.610507	158.458011		
Corrected Total	46	7370.936170			

Dependent Variable: TLday

Source	DF	Sum of Squares	Mean Square	F Value	Pr > F
Model	1	13.691644	13.691644	0.21	0.6488
Error	45	2931.159420	65.136876		
Corrected Total	46	2944.851064			

Sunlight regeneration results

The SAS System

Obs	light	Liftday	Standday	TLday
1	Control	32	36	56
2	Control	25	36	56
3	Control	25	36	63
4	Control	51	58	68
5	Open	47	58	66
6	Open	66	77	90
7	Open	66	70	81
8	Open	26	32	47
9	Open	47	58	89
10	Open	63	66	72
11	Open	57	68	85
12	Open	60	65	80
13	Shaded	61	63	79
14	Shaded	36	47	68
15	Shaded	56	58	74
16	Shaded	47	58	70
17	Shaded	49	54	68
18	Shaded	61	74	79
19	Shaded	22	32	49
20	Shaded	63	74	91
21	Shaded	70	81	95
22	Shaded	63	66	89
23	Shaded	36	47	58

The SAS System

The GLM Procedure

Class Level Information		
Class	**Levels**	**Values**
light	3	Control Open Shaded

Number of Observations Read	23
Number of Observations Used	23

The SAS System

The GLM Procedure

Dependent Variable: Standday

Source	DF	Sum of Squares	Mean Square	F Value	Pr > F
Model	2	1207.381423	603.690711	3.28	0.0588
Error	20	3685.227273	184.261364		
Corrected Total	22	4892.608696			

R-Square	Coeff Var	Root MSE	Standday Mean
0.246777	23.76017	13.57429	57.13043

Source	DF	Type I SS	Mean Square	F Value	Pr > F
light	2	1207.381423	603.690711	3.28	0.0588

Source	DF	Type III SS	Mean Square	F Value	Pr > F
light	2	1207.381423	603.690711	3.28	0.0588

The SAS System

The GLM Procedure

t Tests (LSD) for Standday

Note: This test controls the Type I comparisonwise error rate, not the experimentwise error rate.

Alpha	0.05
Error Degrees of Freedom	20
Error Mean Square	184.2614
Critical Value of t	2.08596

Comparisons significant at the 0.05 level are indicated by *.**

light Comparison	Difference Between Means	95% Confidence Limits		
Open - Shaded	2.295	-10.862	15.453	
Open - Control	20.250	2.910	37.590	***
Shaded - Open	-2.295	-15.453	10.862	
Shaded - Control	17.955	1.422	34.487	***
Control - Open	-20.250	-37.590	-2.910	***
Control - Shaded	-17.955	-34.487	-1.422	***

The SAS System

Obs	light	Liftday	Standday	TLday
1	Control	32	36	56
2	Control	25	36	56
3	Control	25	36	63
4	Control	51	58	68
5	Open	47	58	66
6	Open	66	77	90
7	Open	66	70	81
8	Open	26	32	47
9	Open	47	58	89
10	Open	63	66	72
11	Open	57	68	85
12	Open	60	65	80
13	Shaded	61	63	79
14	Shaded	36	47	68
15	Shaded	56	58	74
16	Shaded	47	58	70
17	Shaded	49	54	68
18	Shaded	61	74	79
19	Shaded	22	32	49
20	Shaded	63	74	91
21	Shaded	70	81	95
22	Shaded	63	66	89
23	Shaded	36	47	58

The SAS System

The GLM Procedure

Class Level Information		
Class	**Levels**	**Values**
light	3	Control Open Shaded

Number of Observations Read	23
Number of Observations Used	23

The SAS System

The GLM Procedure

Dependent Variable: Liftday

Source	DF	Sum of Squares	Mean Square	F Value	Pr > F
Model	2	1248.894269	624.447134	3.18	0.0634
Error	20	3932.931818	196.646591		
Corrected Total	22	5181.826087			

R-Square	Coeff Var	Root MSE	Liftday Mean
0.241014	28.56782	14.02307	49.08696

Source	DF	Type I SS	Mean Square	F Value	Pr > F
light	2	1248.894269	624.447134	3.18	0.0634

Source	DF	Type III SS	Mean Square	F Value	Pr > F
light	2	1248.894269	624.447134	3.18	0.0634

The SAS System

The GLM Procedure

t Tests (LSD) for Liftday

Note: This test controls the Type I comparisonwise error rate, not the experimentwise error rate.

Alpha	0.05
Error Degrees of Freedom	20
Error Mean Square	196.6466
Critical Value of t	2.08596

Comparisons significant at the 0.05 level are indicated by *.**

light Comparison	Difference Between Means	95% Confidence Limits		
Open - Shaded	2.727	-10.865	16.319	
Open - Control	20.750	2.837	38.663	***
Shaded - Open	-2.727	-16.319	10.865	
Shaded - Control	18.023	0.943	35.102	***
Control - Open	-20.750	-38.663	-2.837	***
Control - Shaded	-18.023	-35.102	-0.943	***

The SAS System

Obs	light	Liftday	Standday	TLday
1	Control	32	36	56
2	Control	25	36	56
3	Control	25	36	63
4	Control	51	58	68
5	Open	47	58	66
6	Open	66	77	90
7	Open	66	70	81
8	Open	26	32	47
9	Open	47	58	89
10	Open	63	66	72
11	Open	57	68	85
12	Open	60	65	80
13	Shaded	61	63	79
14	Shaded	36	47	68
15	Shaded	56	58	74
16	Shaded	47	58	70
17	Shaded	49	54	68
18	Shaded	61	74	79
19	Shaded	22	32	49
20	Shaded	63	74	91
21	Shaded	70	81	95
22	Shaded	63	66	89
23	Shaded	36	47	58

The SAS System

The GLM Procedure

Class Level Information		
Class	**Levels**	**Values**
light	3	Control Open Shaded

Number of Observations Read	23
Number of Observations Used	23

The SAS System

The GLM Procedure

Dependent Variable: TLday

Source	DF	Sum of Squares	Mean Square	F Value	Pr > F
Model	2	709.457510	354.728755	2.02	0.1592
Error	20	3516.977273	175.848864		
Corrected Total	22	4226.434783			

R-Square	Coeff Var	Root MSE	TLday Mean
0.167862	18.23063	13.26080	72.73913

Source	DF	Type I SS	Mean Square	F Value	Pr > F
light	2	709.4575099	354.7287549	2.02	0.1592

Source	DF	Type III SS	Mean Square	F Value	Pr > F
light	2	709.4575099	354.7287549	2.02	0.1592

The SAS System

The GLM Procedure

t Tests (LSD) for TLday

Note: This test controls the Type I comparisonwise error rate, not the experimentwise error rate.

Alpha	0.05
Error Degrees of Freedom	20
Error Mean Square	175.8489
Critical Value of t	2.08596

Comparisons significant at the 0.05 level are indicated by *.**

light Comparison	Difference Between Means	95% Confidence Limits	
Open - Shaded	1.705	-11.149	14.558
Open - Control	15.500	-1.439	32.439
Shaded - Open	-1.705	-14.558	11.149
Shaded - Control	13.795	-2.355	29.946
Control - Open	-15.500	-32.439	1.439
Control - Shaded	-13.795	-29.946	2.355

Appendix B

^{137}Cs and Organic Matter Results for Transect 1

FC a Detector: Aug-13	Mangrove Ge6					Energy: Efficiency: B. Ratio	1468 keV 0.0174 0.107		661.7 keV 0.024 0.846			
Depth (cm)	Mean Depth (cm)	Mass +cup (g)	Mass (g)	Bulk Den. (g/cm3)	counting time (s)	K-40 net cts	K-40 spec act (Bq/kg)	Cs-137 net cts	Cs-137 +/-	Cs-137 spec act (Bq/kg)	Cs-137 +/- (Bq/kg)	POM(%)
0-2	-1	121.05	68.4	0.435	47143	2056	342.7	61	88.0	0.9	1.4	12.09
2-4	-3	129.27	76.6	0.487	41374	1409	238.9	74	84.0	1.2	1.3	10.31
4-6	-5	123.39	70.7	0.450	43849	1592	275.9	76	86.0	1.2	1.4	9.95
6-8	-7	137.34	84.6	0.538	42111	2140	322.5	142	83.0	2.0	1.2	9.67
8-10	-9	151.18	98.5	0.626	41652	3458	452.8	223	83.0	2.7	1.0	9.58
10-12	-11	148.45	95.8	0.609	36501	3342	513.6	142	81.0	2.0	1.1	8.83
12-14	-13	144.29	91.6	0.583	49907	4607	541.3	215	93.0	2.3	1.0	9.04
14-16	-15	151.86	99.2	0.631	37177	3399	495.2	287	78.0	3.9	1.0	9.36
16-18	-17	143.5	90.8	0.578	46628	4463	566.2	229	91.0	2.7	1.1	8.55
18-20	-19	143.96	91.3	0.581	36239	3476	564.5	221	78.0	3.3	1.2	9.12
20-22	-21	144.79	92.1	0.586	46469	4322	542.5	246	89.0	2.8	1.0	9.28
22-24	-23	136.71	84.0	0.534	37743	3226	546.5	234	78.0	3.6	1.2	9.68
24-26	-25	139.24	86.5	0.551	49917	4348	540.6	339	90.0	3.9	1.0	10.47
26-28	-27	148.29	95.6	0.608	38014	3277	484.4	338	78.0	4.6	1.1	8.70
28-30	-29	148.61	95.9	0.610	45235	4135	511.9	374	86.0	4.3	1.0	9.16
30-32	-31	141.76	89.1	0.567	41281	3814	557.2	321	81.0	4.3	1.1	8.00
32-34	-33	155.26	102.6	0.652	45742	4307	493.1	237	92.0	2.5	1.0	7.76
34-36	-35	146.66	94.0	0.598	40811	3352	469.5	119	88.0	1.5	1.1	7.31
36-38	-37	144.93	92.2	0.587	46268	3951	497.3	139	94.0	1.6	1.1	7.61
38-40	-39	143.15	90.5	0.575	41740	3392	482.6	207	88.0	2.7	1.2	7.67
40-42	-41	139.28	86.6	0.551	42619	3639	529.7	305	87.0	4.1	1.2	7.57
42-44	-43	144.95	92.3	0.587	81950	7366	523.3	554	122.0	3.6	0.8	6.69
44-46	-45	164.85	112.2	0.713	38888	3843	473.3	354	99.0	4.0	1.1	6.52
46-48	-47	160.03	107.3	0.683	50288	4904	488.0	779	114.0	7.1	1.0	6.53

48-50	-49	155.38	102.7	0.653	35136	3181	473.6	505	81.0	6.9	1.1	6.52
50-52	-51	151.29	98.6	0.627	50144	4569	496.4	371	92.0	3.7	0.9	7.06
52-54	-53	157.87	105.2	0.669	36468	3584	501.9	273	78.0	3.5	1.0	6.84
54-56	-55	160.13	107.4	0.683	43488	4363	501.6	259	85.0	2.7	0.9	6.12
56-58	-57	154.67	102.0	0.649	40878	3722	479.6	231	83.0	2.7	1.0	6.08
58-60	-59	159.36	106.7	0.678	41223	3821	466.8	92	85.0	1.0	1.0	6.12
60-62	-61	169.73	117.0	0.744	38854	3689	435.8	3	84.0	0.0	0.9	6.26
62-64	-63	162.47	109.8	0.698	45545	3997	429.4	1	91.0	0.0	0.9	6.02
			Volume of segment			157.2	cm^3					

FC c	Short	mangrove (transition)			Energy:	1468 keV		661.7 keV				
Detector:	Ge7				Efficiency:	0.0174		0.0252				
13-Aug					B. Ratio	0.107		0.846				
Depth	Mean Depth	Mass + cup (g)	Mass	Bulk Den.	counting time	K-40 net cts	K-40 spec act	Cs-137 net cts	Cs-137 +/-	Cs-137 spec act	Cs-137 +/-	
(cm)	(cm)		(g)	(g/cm3)	(s)		(Bq/kg)			(Bq/kg)	(Bq/kg)	POM (%)
0-2	-1	95.21	42.5	0.270	41700	2331	706.3	186	36.0	4.9	1.0	14.17
2-4	-3	133.07	80.4	0.511	36487	3702	678.1	63	44.0	1.0	0.7	10.91
4-6	-5	133.17	80.5	0.512	49913	4601	615.3	226	47	2.6	0.6	11.20
6-8	-7	131.96	79.3	0.504	37182	3462	631.0	177	41.0	2.8	0.7	12.29
8-10	-9	141.67	89.0	0.566	46624	4757	616.0	139	50.0	1.6	0.6	10.89
10-12	-11	152.29	99.6	0.634	36192	3795	565.5	105	45.0	1.4	0.6	10.83
12-14	-13	137.26	84.6	0.538	46606	4691	639.3	243	50.0	2.9	0.6	11.50
14-16	-15	137.69	85.0	0.541	37793	3616	604.7	286	40.0	4.2	0.6	11.70
16-18	-17	131.5	78.8	0.501	49935	4605	628.6	174	54.0	2.1	0.6	12.06
18-20	-19	126.78	74.1	0.471	38044	3341	636.7	213	42.0	3.5	0.7	13.27
20-22	-21	133.22	80.5	0.512	45227	3957	583.6	267	49.0	3.4	0.6	13.24
22-24	-23	133.91	81.2	0.517	41293	3712	594.6	337	43.0	4.7	0.6	12.20
24-26	-25	123.11	70.4	0.448	45762	3683	613.9	259	47.0	3.8	0.7	10.76
26-28	-27	127.63	74.9	0.477	40793	3605	633.5	284	45.0	4.4	0.7	11.24
28-30	-29	132.2	79.5	0.506	46265	4290	626.5	372	50.0	4.7	0.6	11.37
30-32	-31	127.22	74.5	0.474	41725	3758	649.2	398	44.0	6.0	0.7	10.64
32-34	-33	125.3	72.6	0.462	42608	3512	609.8	249	48.0	3.8	0.7	10.18
34-36	-35	135.08	82.4	0.524	81917	7508	597.6	669	68.0	4.7	0.5	9.44
36-38	-37	141.81	89.1	0.567	38800	3923	609.4	574	47.0	7.8	0.6	8.57

38-40	-39	147.23	94.5	0.601	50321	5267	594.7	817	51.0	8.1	0.5	7.98
40-42	-41	144.11	91.4	0.581	35151	3751	627.0	526	44.0	7.7	0.6	8.25
42-44	-43	143.69	91.0	0.579	50156	5281	621.5	587	53.0	6.0	0.5	7.95
44-46	-45	150.78	98.1	0.624	36479	3955	593.7	444	45.0	5.8	0.6	7.62
46-48	-47	156.01	103.3	0.657	43497	4919	588.0	491	48.0	5.1	0.5	7.51
48-50	-49	150.96	98.3	0.625	40886	4513	603.4	313	48.0	3.7	0.6	7.43
50-52	-51	150.55	97.9	0.622	41234	4474	595.6	310	46.0	3.6	0.5	7.33
52-54	-53	150.66	98.0	0.623	38873	4280	603.7	232	42.0	2.9	0.5	7.87
54-56	-55	146.66	94.0	0.598	45533	4953	621.8	140	46.0	1.5	0.5	7.61
56-58	-57	153.29	100.6	0.640	53765	5899	585.9	153	50.0	1.3	0.4	7.36
58-60	-59	146.6	93.9	0.597	35816	3875	618.9	111	40.0	1.5	0.6	8.12
60-62	-61	170.26	117.6	0.748	44537	5225	536.0	113	44.0	1.0	0.4	7.54
				Volume of segment		157.2	cm^3					

FC Marsh 1

Detector: Ge4

Aug-13

					Energy:	1468 keV		661.7 keV				
					Efficiency:	0.0174		0.0321				
					B. Ratio	0.107		0.846				
Depth (cm)	Mean Depth (cm)	Mass+cup (g)	Mass (g)	Bulk Den. (g/cm3)	counting time (s)	K-40 net cts	K-40 spec act (Bq/kg)	Cs-137 net cts	Cs-137 +/-	Cs-137 spec act (Bq/kg)	Cs-137 +/- (Bq/kg)	POM (%)
0-2	-1	140.06	87.36	0.556	42224	4537	660.6	407	101.0	4.1	1.0	9.38
2-4	-3	135.26	82.56	0.525	43684	4746	706.8	335	108.0	3.4	1.1	9.22
4-6	-5	129.1	76.40	0.486	41315	4072	692.9	216	104.0	2.5	1.2	8.14
6-8	-7	142.45	89.75	0.571	46480	4928	634.5	180	116.0	1.6	1.0	8.33
8-10	-9	141.33	88.63	0.564	38110	4174	663.7	295	103.0	3.2	1.1	8.23
10-12	-11	133.43	80.73	0.514	44961	4596	680.1	323	110.0	3.3	1.1	9.18
12-14	-13	130.52	77.82	0.495	84340	8534	698.4	672	148.0	3.8	0.8	8.83
14-16	-15	120.12	67.42	0.429	43675	3947	720.0	353	104.0	4.4	1.3	8.61
16-18	-17	127.3	74.60	0.475	41266	4039	704.7	253	103.0	3.0	1.2	9.20
18-20	-19	128.03	75.33	0.479	39800	3899	698.5	508	93.0	6.2	1.1	10.43
20-22	-21	119.09	66.39	0.422	42298	3964	758.2	354	107.0	4.6	1.4	10.34
22-24	-23	124.47	71.77	0.457	42859	4675	816.3	559	105.0	6.7	1.3	8.41

24-26	-25	134.34	81.64	0.519	50145	5270	691.4	459	138.0	4.1	1.2	8.29
26-28	-27	139.07	86.37	0.549	35056	3787	671.8	472	106.0	5.7	1.3	8.13
28-30	-29	135.21	82.51	0.525	49974	5126	667.7	850	116.0	7.6	1.0	7.43
30-32	-31	153.26	100.56	0.640	36338	4709	692.2	837	105.0	8.4	1.1	6.84
32-34	-33	154.62	101.92	0.648	43335	5229	635.9	778	122.0	6.5	1.0	6.57
34-36	-35	157.82	105.12	0.669	40734	4996	626.7	651	117.0	5.6	1.0	6.93
36-38	-37	146.83	94.13	0.599	41075	4601	639.2	500	116.0	4.8	1.1	8.00
38-40	-39	122.2	69.50	0.442	38727	3705	739.4	348	104.0	4.8	1.4	9.41
40-42	-41	131.54	78.84	0.502	45403	4291	643.9	199	116.0	2.0	1.2	9.37
42-44	-43	133.33	80.63	0.513	53672	5211	646.8	428	119.0	3.6	1.0	9.33
44-46	-45	124.29	71.59	0.455	35679	3284	690.6	120	100.0	1.7	1.4	9.79
46-48	-47	126.36	73.66	0.469	44374	4446	730.6	50	117.0	0.6	1.3	9.61
48-50	-49	133.08	80.38	0.511	88756	8746	658.5	227	158.0	1.2	0.8	9.21
50-52	-51	140.12	87.42	0.556	82644	8807	654.7	207	156.0	1.1	0.8	8.60
52-54	-53	141.27	88.57	0.563	37687	4172	671.3	189	103.0	2.1	1.1	8.10
54-56	-55	148.15	95.45	0.607	44106	4793	611.5	84	114.0	0.7	1.0	7.68
56-58	-57	90.33	37.63	0.239	43092	2793	925.1	171	101.0	3.9	2.3	7.95
				Volume of segment		157.2	cm^3					

FC b Mangrove + Marsh
Detector: Ge6
Aug-13

						Energy:	1468 keV		661.7 keV			
						Efficiency:	0.0174		0.024			
						B. Ratio	0.107		0.846			
Depth (cm)	Mean Depth (cm)	Mass +cup (g)	Mass (g)	Bulk Den. (g/cm3)	counting time (s)	K-40 net cts	K-40 spec act (Bq/kg)	Cs-137 net cts	Cs-137 +/-	Cs-137 spec act (Bq/kg)	Cs-137 +/- (Bq/kg)	POM (%)
0-2	-1	130.78	78.1	0.497	53805	3345	427.7	180	94.0	2.1	1.1	10.77
2-4	-3	137.1	84.4	0.537	35801	2242	398.5	108	77.0	1.8	1.3	9.93
4-6	-5	123.75	71.1	0.452	44523	2823	479.3	95	85	1.5	0.9	10.43
6-8	-7	119.38	66.7	0.424	89052	6583	595.5	240	121.0	2.0	1.0	10.61
8-10	-9	122.65	70.0	0.445	82877	6378	590.9	342	112.0	2.9	1.0	10.79
10-12	-11	113.57	60.9	0.387	37825	2707	631.5	119	76.0	2.6	1.6	12.46
12-14	-13	112.5	59.8	0.380	44233	2896	588.1	190	79.0	3.6	1.5	13.34
14-16	-15	104.43	51.7	0.329	37056	2245	629.0	162	74.0	4.2	1.9	12.76
16-18	-17	106.58	53.9	0.343	52971	3331	626.9	208	90.0	3.6	1.6	11.51

18-20	-19	109.67	57.0	0.362	39422	2723	651.2	110	80.0	2.4	1.8	11.90
20-22	-21	105.84	53.1	0.338	45429	2820	627.4	247	82.0	5.1	1.7	13.75
22-24	-23	108.01	55.3	0.352	39222	2645	654.9	309	78.0	7.0	1.8	13.00
24-26	-25	110.96	58.3	0.371	46886	3230	635.1	328	87.0	5.9	1.6	11.97
26-28	-27	112.78	60.1	0.382	36273	2570	633.4	271	74.0	6.2	1.7	11.16
28-30	-29	111.27	58.6	0.373	48697	3602	678.3	539	87.0	9.3	1.5	10.21
30-32	-31	116.76	64.1	0.408	37627	2854	636.0	381	78.0	7.8	1.6	9.75
32-34	-33	110.67	58.0	0.369	47485	3603	703.0	450	89.0	8.1	1.6	9.54
34-36	-35	125.48	72.8	0.463	38166	3083	596.1	541	79.0	9.6	1.4	8.96
36-38	-37	133.74	81.0	0.516	53657	4542	561.0	931	94.0	10.6	1.1	7.46
38-40	-39	146.65	94.0	0.598	81092	7635	538.3	2623	120.0	17.0	0.8	6.97
40-42	-41	125.75	73.1	0.465	39412	3155	588.6	933	83.0	16.0	1.4	9.04
42-44	-43	121.8	69.1	0.440	45285	3579	614.3	684	85.0	10.8	1.3	10.01
44-46	-45	120.67	68.0	0.432	39809	3013	598.1	217	82.0	4.0	1.5	9.88
46-48	-47	126.27	73.6	0.468	45472	3715	596.5	166	86.0	2.5	1.3	9.15
48-50	-49	132.46	79.8	0.507	42560	3592	568.4	275	78.0	4.0	1.1	9.10
50-52	-51	128.41	75.7	0.482	43673	3469	563.5	182	82.0	2.7	1.2	9.61
52-54	-53	126.41	73.7	0.469	37009	2922	575.3	138	75.0	2.5	1.4	10.79
54-56	-55	120.29	67.6	0.430	48091	3711	613.2	104	85.0	1.6	1.3	11.97
56-58	-57	116.27	63.6	0.404	40948	2789	575.5	47	80.0	0.9	1.5	13.34
58-60	-59	117.7	65.0	0.413	43305	2967	566.2	129	80.0	2.3	1.4	13.31
60-62	-61	116.14	63.4	0.404	84705	5813	581.0	246	110.0	2.3	1.0	13.88
62-64	-63	125.65	73.0	0.464	41542	3010	533.5	2	83.0	0.0	1.4	13.70
64-66	-65	140.31	87.6	0.557	44090	3766	523.7	132	81.0	1.7	1.0	14.29
				Volume of segment		157.2	cm^3					

^{137}Cs and organic matter results for transect 2

FC a - tall mangrove		1			Energy:	1468 keV		661.7 keV				
Detector:	Ge4				Efficiency:	0.0174		0.0324				
Feb-14					B. Ratio	0.107		0.846				
Depth	Mean Depth	Mass+cup	Mass	Bulk Den.	counting time	K-40 net cts	K-40 spec act	Cs-137 net cts	Cs-137 +/-	Cs-137 spec act	Cs-137 +/-	POM
(cm)	(cm)	(g)	(g)	(g/cm3)	(s)		(Bq/kg)			(Bq/kg)	(Bq/kg)	(%)
0-2	-1	135.06	82.36	0.524	49400	5371	709.1	147	120.0	1.3	1.1	8.88
2-4	-3	140.62	87.92	0.559	41644	4824	707.7	247	104.0	2.5	1.0	9.00
4-6	-5	143.45	90.75	0.577	47320	5596	699.9	226	113.0	1.9	1.0	8.78
6-8	-7	138.03	85.33	0.543	50101	5882	739.0	190	123.0	1.6	1.0	8.45
8-10	-9	161.04	108.34	0.689	47675	6017	625.7	313	116.0	2.2	0.8	7.54
10-12	-11	165.11	112.41	0.715	43127	5618	622.4	88	123.0	0.7	0.9	7.48
12-14	-13	147.72	95.02	0.604	36015	4169	654.3	139	108.0	1.5	1.2	8.34
14-16	-15	135.69	82.99	0.528	53163	5782	703.9	305	124.0	2.5	1.0	8.77
16-18	-17	145.32	92.62	0.589	66542	8159	711.1	126	149.0	0.7	0.9	7.97
18-20	-19	154.17	101.47	0.645	36490	4266	618.8	224	105.0	2.2	1.0	7.37
20-22	-21	162.24	109.54	0.697	47673	6191	636.8	431	119.0	3.0	0.8	7.58
22-24	-23	145.42	92.72	0.590	36181	4453	713.0	150	109.0	1.6	1.2	7.78
24-26	-25	151.67	98.97	0.630	45556	5793	690.1	470	120.0	3.8	1.0	7.41
26-28	-27	136.52	83.82	0.533	37656	4235	720.7	381	103.0	4.4	1.2	8.27
28-30	-29	142.35	89.65	0.570	37143	4492	724.6	301	107.0	3.3	1.2	8.21
30-32	-31	142.51	89.81	0.571	36706	4261	694.3	406	104.0	4.5	1.2	7.80
32-34	-33	139.29	86.59	0.551	46170	5242	704.3	353	123.0	3.2	1.1	8.02
34-36	-35	137.95	85.25	0.542	61250	6927	712.5	738	127.0	5.2	0.9	8.35
36-38	-37	136.9	84.20	0.536	35993	3906	692.3	540	93.0	6.5	1.1	8.27
38-40	-39	143	90.30	0.574	36408	4447	726.5	187	109.0	2.1	1.2	7.57
40-42	-41	143.98	91.28	0.581	36855	4005	639.4	247	106.0	2.7	1.1	7.37
42-44	-43	150.88	98.18	0.625	46765	5452	637.8	505	111.0	4.0	0.9	7.39
44-46	-45	143.28	90.58	0.576	38837	4375	668.0	269	104.0	2.8	1.1	7.33
46-48	-47	146.25	93.55	0.595	44033	5365	699.5	213	119.0	1.9	1.1	6.95
48-50	-49	147.34	94.64	0.602	39668	4807	687.7	181	113.0	1.8	1.1	6.88
50-52	-51	152.88	100.18	0.637	48492	5699	630.1	188	126.0	1.4	0.9	6.96

52-54	-53	145.85	93.15	0.593	40154	4721	677.9	189	109.0	1.8	1.1	6.79
54-56	-55	166.64	113.94	0.725	42069	5330	597.2	243	111.0	1.8	0.8	6.37
56-58	-57	151.62	98.92	0.629	36006	4545	685.4	124	106.0	1.3	1.1	6.16
58-60	-59	163.02	110.32	0.702	38548	5098	643.9	136	115.0	1.2	1.0	5.85
60-62	-61	158.72	106.02	0.674	47479	6336	676.1	301	120.0	2.2	0.9	6.09
62-64	-63	148.04	95.34	0.606	47102	5827	696.9	325	114.0	2.6	0.9	6.15
				Volume of segment		157.2	cm^3					

FC c	short mangrove					Energy:	1468 keV		661.7 keV			
Detector:	Ge6					Efficiency:	0.0174		0.024			
Feb-14						B. Ratio	0.107		0.846			
Depth (cm)	Mean Depth (cm)	Mass +cup (g)	Mass (g)	Bulk Den. (g/cm3)	counting time (s)	K-40 net cts	K-40 spec act (Bq/kg)	Cs-137 net cts	Cs-137 +/-	Cs-137 spec act (Bq/kg)	Cs-137 +/- (Bq/kg)	POM (%)
0-2	-1	142.11	89.4	0.569	49513	2805	340.3	13	91.0	0.1	1.0	7.85
2-4	-3	129.71	77.0	0.490	47221	3685	544.3	183	87.0	2.5	1.2	10.90
4-6	-5	162.05	109.4	0.696	36177	2012	273.2	20	78	0.2	1.0	8.16
6-8	-7	131.87	79.2	0.504	47725	2280	324.1	58	91.0	0.7	1.1	11.25
8-10	-9	125.78	73.1	0.465	48708	3612	545.0	237	90.0	3.3	1.2	13.09
10-12	-11	111.58	58.9	0.375	53184	1958	335.8	204	91.0	3.2	1.4	13.68
12-14	-13	129.91	77.2	0.491	39792	3107	543.2	267	80.0	4.2	1.3	12.34
14-16	-15	132.7	80.0	0.509	46259	2818	409.0	305	87.0	4.0	1.1	11.40
16-18	-17	131.68	79.0	0.502	66746	3189	324.9	499	106.0	4.6	1.0	10.98
18-20	-19	127.15	74.5	0.474	41830	2867	494.5	487	81.0	7.6	1.3	11.28
20-22	-21	129.72	77.0	0.490	36185	2202	424.4	263	77.0	4.6	1.3	10.86
22-24	-23	134.54	81.8	0.521	36860	2791	496.9	382	77.0	6.2	1.2	10.38
24-26	-25	139.17	86.5	0.550	43372	2952	422.8	453	88.0	5.9	1.1	10.11
26-28	-27	161.01	108.3	0.689	39030	1877	238.5	656	83.0	7.6	1.0	8.73
28-30	-29	146.07	93.4	0.594	36336	3316	525.0	834	78.0	12.0	1.1	8.60
30-32	-31	129.08	76.4	0.486	61370	3268	374.5	1072	102.0	11.2	1.1	9.42
32-34	-33	132.25	79.6	0.506	37354	2523	456.0	492	80.0	8.1	1.3	9.31
34-36	-35	129.39	76.7	0.488	36625	2475	473.3	192	78.0	3.3	1.4	10.88
36-38	-37	114.22	61.5	0.391	45633	3274	626.4	203	82.0	3.5	1.4	12.84
38-40	-39	112.48	59.8	0.380	47406	3239	613.9	50	87.0	0.9	1.5	12.53

40-42	-41	119.23	66.5	0.423	37742	2707	579.0	32	77.0	0.6	1.5	12.35
42-44	-43	119.67	67.0	0.426	50259	2624	418.7	55	90.0	0.8	1.3	12.17
44-46	-45	121.55	68.9	0.438	36058	1950	421.9	54	76.0	1.1	1.5	11.78
46-48	-47	121.76	69.1	0.439	44094	1788	315.4	229	82.0	3.7	1.3	11.28
48-50	-49	119.85	67.2	0.427	36553	2785	609.4	36	77.0	0.7	1.5	10.38
50-52	-51	135.72	83.0	0.528	47900	3777	510.1	273	82.0	3.4	1.0	9.21
52-54	-53	133.8	81.1	0.516	47680	3829	531.9	201	84.0	2.5	1.1	9.23
54-56	-55	133.07	80.4	0.511	42107	3266	518.4	46	80.0	0.7	1.2	9.95
56-58	-57	129.75	77.1	0.490	40241	2381	412.5	43	82.0	0.7	1.3	11.10
58-60	-59	131.1	78.4	0.499	38847	2866	505.4	24	79.0	0.4	1.3	9.58
			Volume of segment			157.2	cm^3					

FC b	Marsh				Energy:	1468 keV		661.7 keV				
Detector:	Ge7				Efficiency:	0.0174		0.0249				
20-Feb					B. Ratio	0.107		0.846				
Depth	Mean Depth	Mass + cup (g)	Mass	Bulk Den.	counting time	K-40 net cts	K-40 spec act	Cs-137 net cts	Cs-137 +/-	Cs-137 spec act	Cs-137 +/-	
(cm)	(cm)		(g)	(g/cm3)	(s)		(Bq/kg)			(Bq/kg)	(Bq/kg)	POM (%)
0-2	-1	120.66	68.0	0.432	49541	2931	467.6	183	41.0	2.6	0.6	8.48
2-4	-3	102.02	49.3	0.314	38075	2112	604.1	79	36.0	2.0	0.9	10.51
4-6	-5	121.17	68.5	0.436	46288	2711	459.4	244	39	3.7	0.6	11.31
6-8	-7	123.32	70.6	0.449	47431	3295	528.4	214	42.0	3.0	0.6	10.77
8-10	-9	114.86	62.2	0.395	47753	3033	548.8	176	45.0	2.8	0.7	9.38
10-12	-11	120.6	67.9	0.432	37789	1997	418.0	228	37.0	4.2	0.7	11.02
12-14	-13	106.2	53.5	0.340	36311	2000	553.0	211	34.0	5.2	0.8	11.12
14-16	-15	122.34	69.6	0.443	36153	2116	451.4	206	39.0	3.9	0.7	10.8
16-18	-17	111.15	58.5	0.372	36087	2335	594.6	369	40.0	8.3	0.9	10.75
18-20	-19	109.67	57.0	0.362	36039	2223	581.6	311	42.0	7.2	1.0	9.83
20-22	-21	115.86	63.2	0.402	37236	2569	586.7	422	46.0	8.5	0.9	10.18
22-24	-23	116.64	63.9	0.407	61346	3810	521.7	965	58.0	11.7	0.7	9.69
24-26	-25	124.85	72.2	0.459	36877	2203	444.7	887	44.0	15.8	0.8	9.56
26-28	-27	116.74	64.0	0.407	41808	2468	495.1	572	45.0	10.1	0.8	10.42
28-30	-29	119.56	66.9	0.425	53246	3586	541.0	443	47.0	5.9	0.6	11.08

30-32	-31	110.49	57.8	0.368	66728	3815	531.4	450	53.0	5.5	0.7	11.45
32-34	-33	116.95	64.3	0.409	39761	2343	492.6	221	39.0	4.1	0.7	10.83
34-36	-35	120.63	67.9	0.432	36581	2036	440.1	2	39.0	0.0	0.7	11.64
36-38	-37	112.06	59.4	0.378	43320	2452	512.2	77	37.0	1.4	0.7	13.21
38-40	-39	104.93	52.2	0.332	36128	1362	387.7	4	34.0	0.1	0.9	12.76
40-42	-41	111.09	58.4	0.371	47874	2638	506.9	8	45.0	0.1	0.8	12.45
42-44	-43	108.21	55.5	0.353	47644	2538	515.4	58	40.0	1.0	0.7	14.04
44-46	-45	103.96	51.3	0.326	50229	2358	491.9	25	39.0	0.5	0.7	13.55
46-48	-47	104.37	51.7	0.329	42232	2488	612.4	70	36.0	1.5	0.8	13.26
48-50	-49	118.06	65.4	0.416	45668	2453	441.4	51	41.0	0.8	0.7	13.42
50-52	-51	116.47	63.8	0.406	48693	2880	498.2	24	45.0	0.4	0.7	11.34
52-54	-53	109.89	57.2	0.364	40268	2273	530.1	44	37.0	0.9	0.8	10.28
54-56	-55	116.69	64.0	0.407	37531	2544	569.0	16	38.0	0.3	0.8	9.26
56-58	-57	119.02	66.3	0.422	39002	2281	473.7	18	37.0	0.3	0.7	9.48
58-60	-59	123.32	70.6	0.449	47209	3382	544.9	89	38.0	1.3	0.5	9.62
60-62	-61	161.22	108.5	0.690	44117	3387	380.0	22	42.0	0.2	0.4	7.25
				Volume of segment		157.2	cm^3					

FC d Mix
Detector: Ge6
Aug-14

						Energy:	1468 keV		661.7 keV			
						Efficiency:	0.0174		0.024			
						B. Ratio	0.107		0.846			
Depth (cm)	Mean Depth (cm)	Mass +cup (g)	Mass (g)	Bulk Den. (g/cm3)	counting time (s)	K-40 net cts	K-40 spec act (Bq/kg)	Cs-137 net cts	Cs-137 +/-	Cs-137 spec act (Bq/kg)	Cs-137 +/- (Bq/kg)	POM (%)
0-2	-1	77.9	25.2	0.160	37812	1156	651.6	82	74.0	4.2	3.8	9.747
2-4	-3	91.72	39.0	0.248	41436	2187	726.5	120	76.0	3.6	2.3	10.916
4-6	-5	104.56	51.9	0.330	47569	914	199.0	98	86	1.9	1.7	12.582
6-8	-7	116.64	63.9	0.407	39373	2718	579.9	250	76.0	4.9	1.4	10.863
8-10	-9	119.57	66.9	0.425	45113	3550	632.1	431	80.0	7.0	1.3	10.649
10-12	-11	116.45	63.8	0.406	46884	2504	450.0	127	89.0	2.1	1.5	10.232
12-14	-13	110.68	58.0	0.369	39179	2771	655.2	289	77.0	6.2	1.7	10.869
14-16	-15	113	60.3	0.384	36028	1098	271.5	28	79.0	0.6	1.8	11.512
16-18	-17	109.79	57.1	0.363	37542	2576	645.6	251	77.0	5.7	1.8	11.915

18-20	-19	109.91	57.2	0.364	51474	646	117.8	471	91.0	7.8	1.5	10.476
20-22	-21	110.04	57.3	0.365	42437	2839	626.7	732	85.0	14.7	1.7	11.748
22-24	-23	117.37	64.7	0.411	47339	1449	254.2	919	89.0	14.7	1.4	10.871
24-26	-25	107.75	55.1	0.350	38040	1478	379.1	731	75.0	17.1	1.7	11.989
26-28	-27	108.34	55.6	0.354	45481	3084	654.6	633	86.0	12.2	1.7	12.034
28-30	-29	104.12	51.4	0.327	45570	929	212.9	482	84.0	10.0	1.8	11.684
30-32	-31	107.66	55.0	0.350	41633	1897	445.3	319	79.0	6.8	1.7	12.144
32-34	-33	111.2	58.5	0.372	38524	2725	649.5	93	78.0	2.0	1.7	12.337
34-36	-35	113.11	60.4	0.384	44763	2963	588.5	110	85.0	2.0	1.5	11.747
36-38	-37	106	53.3	0.339	37361	560	560.9	82	76	1.7	1.9	13.465
38-40	-39	107.5	54.8	0.349	46882	1899	397.0	224	81.0	4.3	1.5	13.883
40-42	-41	104.72	52.0	0.331	37310	2446	676.9	256	70.0	6.4	1.8	13.019
42-44	-43	110.81	58.1	0.370	45640	1740	352.4	107	85.0	2.0	1.6	12.832
44-46	-45	110.98	58.3	0.371	37826	1196	291.4	136	73.0	3.0	1.6	13.342
46-48	-47	111.43	58.7	0.374	36543	2034	509.0	68	76.0	1.5	1.7	12.965
48-50	-49	111.61	58.9	0.375	46967	3280	636.7	21	84.0	0.4	1.5	11.677
50-52	-51	116.62	63.9	0.407	44646	3266	614.7	314	77.0	5.4	1.3	10.952
52-54	-53	111.33	58.6	0.373	46895	1472	287.6	139	84.0	2.5	1.5	11.339
			Volume of segment			157.2 cm^3						

Appendix C

^{137}Cs Profiles and Transect 1's organic matter profiles

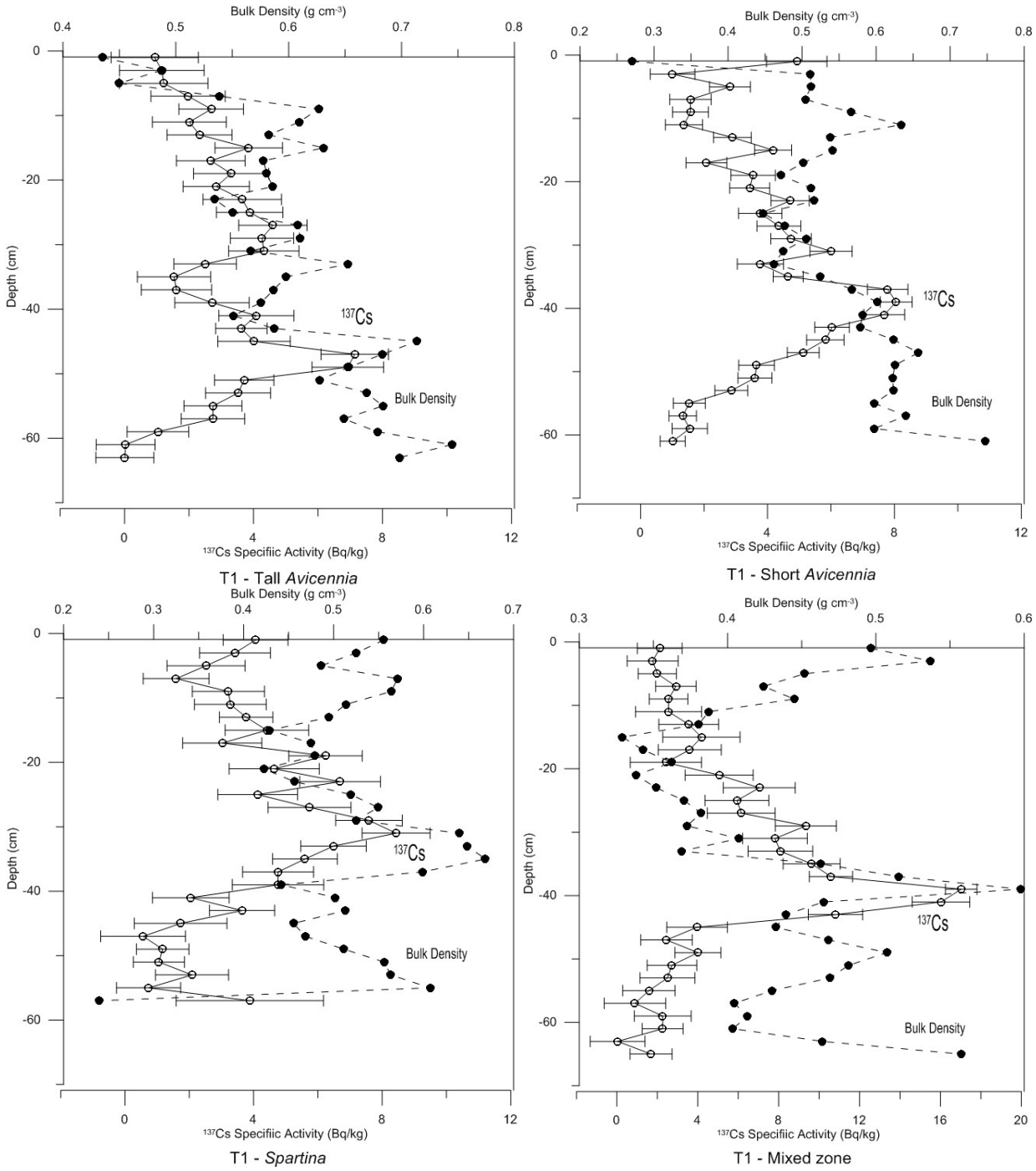

Figure C-1. ^{137}Cs profiles from tall *Avicennia*, short *Avicennia*, *Spartina*, and mixed zone from transect 1.

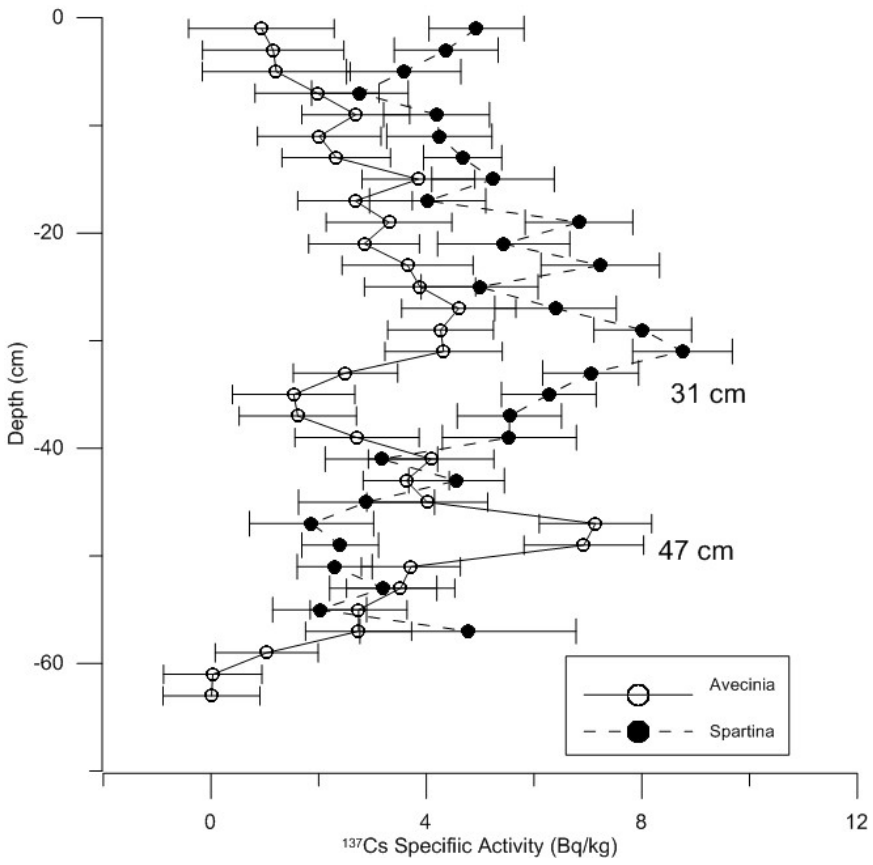

Figure C-2. ^{137}Cs profiles from tall *Avicennia* and *Spartina* from transect 1.

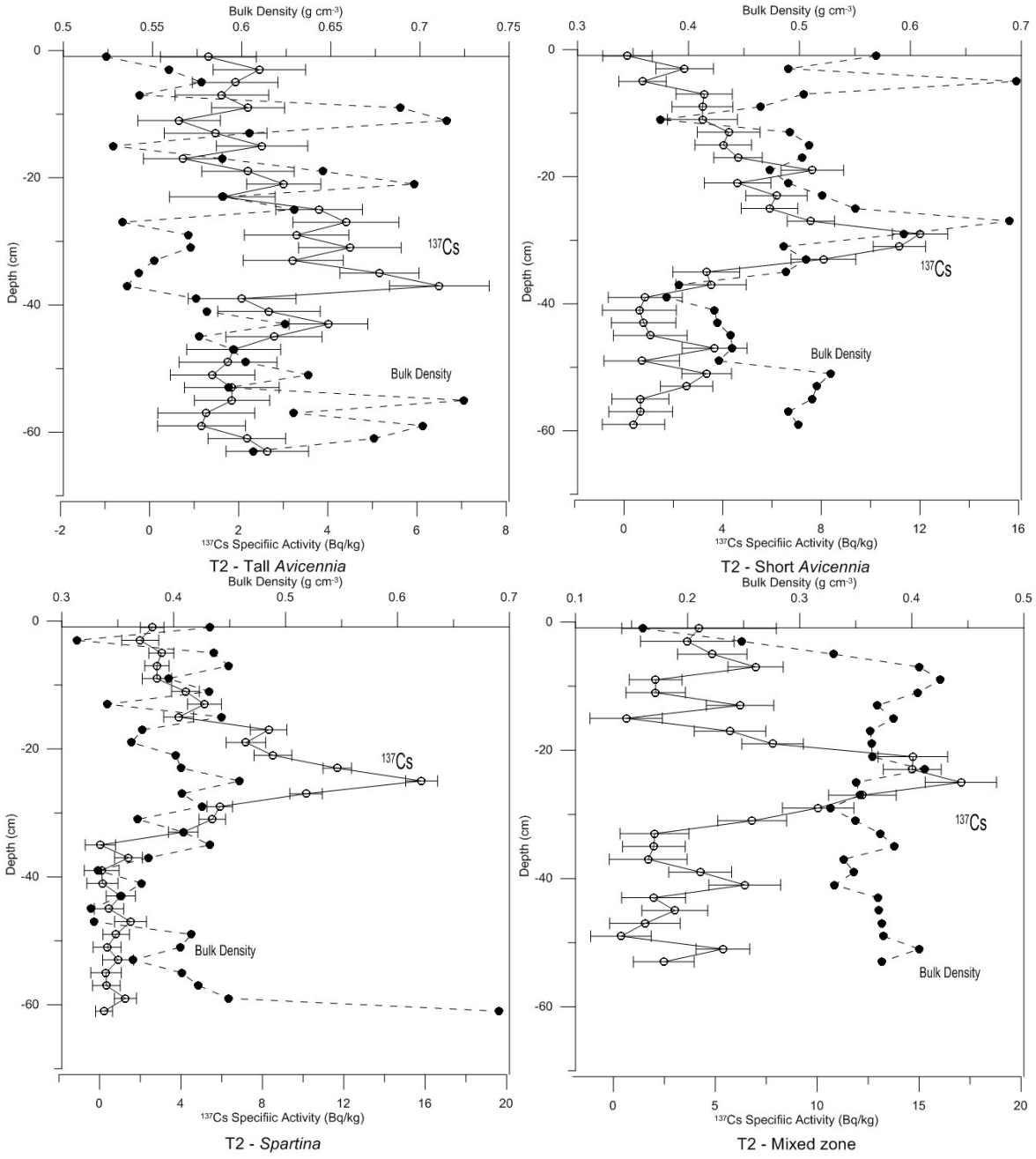

Figure C-3. ^{137}Cs profiles from tall *Avicennia*, short *Avicennia*, *Spartina*, and mixed zone from transect 2.

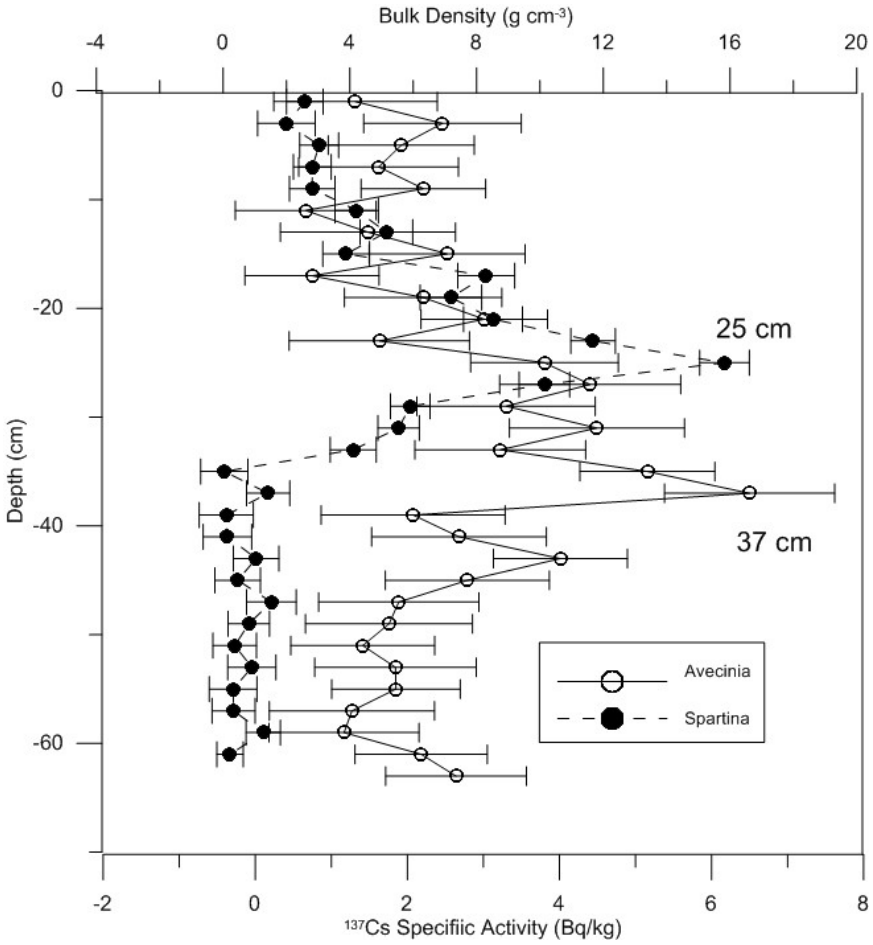

Figure C-4. ^{137}Cs profiles from tall *Avicennia* and *Spartina* from transect 2.

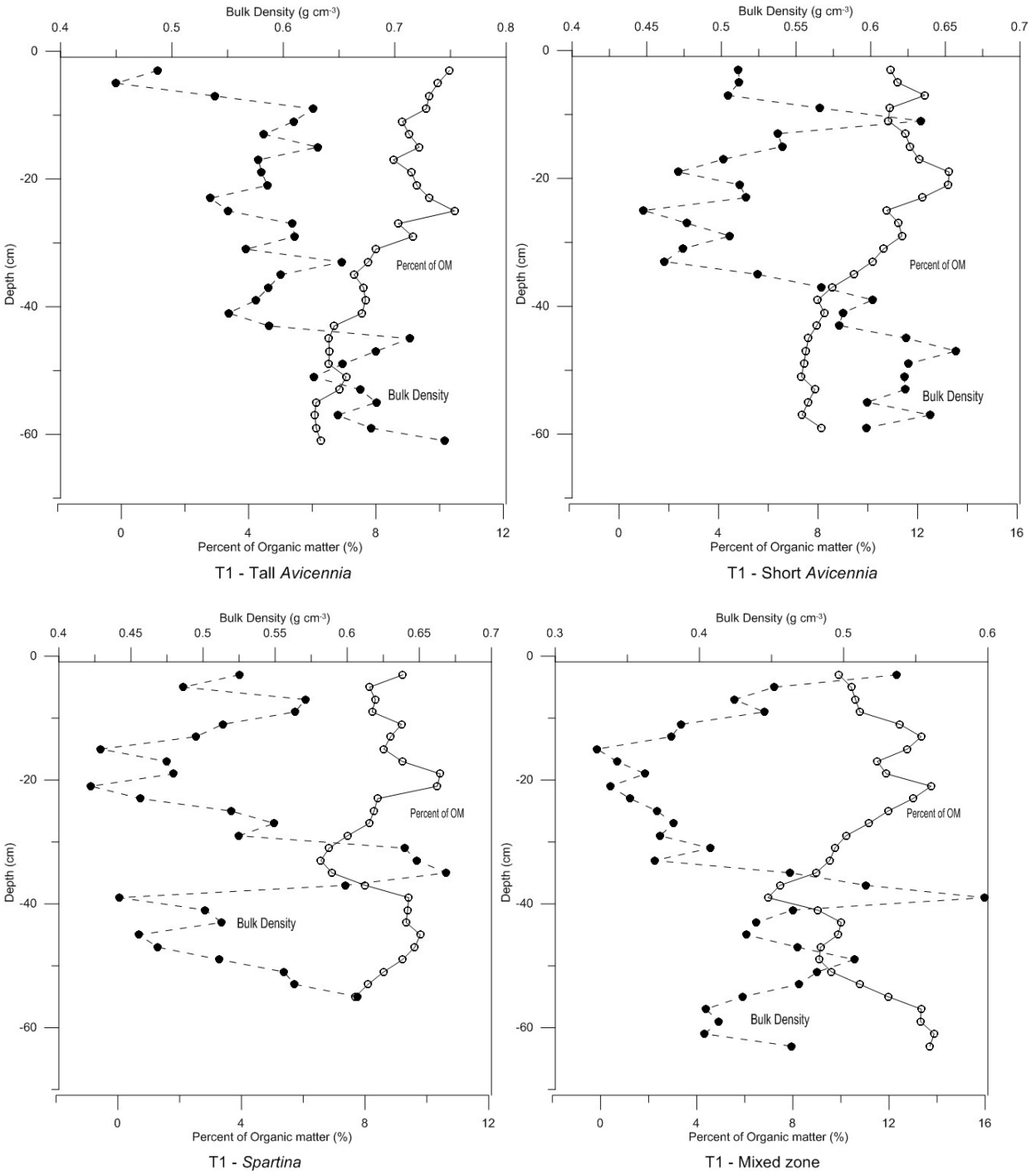

Figure C-5. Organic matter profile of tall Avicennia, short Avicennia, Spartina, and mixed zone from transect 1.

Appendix D

Soil cores location

Figure D-1. Soil core locations near Fourchon.

Figure D-2. Soil core sites (transect 1).

Figure D-3. Soil core sites (transect 2).